PEOPLE'S DEMOCRATIC REPUBLIC OF ALGERIA
MINISTRY OF HIGHER EDUCATION AND RESEARCHSCIENTIST

LARBI BEN MHIDI-OUM EL BOUAGHI UNIVERSITY
FACULTY OF EXACT SCIENCES AND SCIENCES OF NATURE AND LIFE
DEPARTMENT OF MATERIAL SCIENCES

Order N° :

Serie:

Thesis

In order to obtain the

LMD DOCTORATE in PHYSICS

SPECIALTY: PHYSICS OF SEMICONDUCTORS AND MATERIALS

Title:

Fabrication and characerization of semiconductor materials doped polymer

Presented by :

Miss Rouabah Nouhad

In front of the jury

Pr.Kamel Guergouri	**President**	Univ. Larbi Ben Mhidi Oum El Bouaghie
Pr.Boudine Boubekeur	**Reporter**	Univ. MentouriConstantine
Pr.Zaabat Mourad	**Co-reporter**	Univ. Larbi Ben Mhidi Oum El Bouaghie
Pr.Chettah Abdelhak	**Examiner**	Univ. 20 août 1955 Skikda
Pr.Aissani Linda	**Examiner**	Univ. Abbes Laghrour Khenchela

Defended on

Acknowledgement

I would like to thank the power in whose hands is my life, supreme power of universe, almighty Allah for his unparallel grace ....

I owe it to the University of Oum El Bouaghui for accepting me to enroll as a research scholar, specifically the relevant authorities. I consider it a personal blessing and privilege to have been able to do my research in this extraordinary abode of learning.

I would like to express my sincere and everlasting gratitude to my supervisor **Pr. Boudine Boubekeur** for his excellence guidance throughout my research. He inculcated in me the knowledge and motivation to learn more about research. I am highly grateful to my supervisor **Pr. Zaabat Mourad** for his kind guidance and support during my research.

I am deeply grateful to all members of the jury for agreeing to examine and to read my thesis.

I would also like to thank **Mr. Baghou Mourad** God bless his soul for all help maintaining and the facilities in the university . I also would like to thank to all members of the department of physics and respectable engeneering members, our research collaborators, library staff, my dear colleagues, and my friends for their generous help and support.

I also would like to thank to all respectable lab members , our research collaborators, my dear colleagues, and my friends for their generous help and support.

Words are inadequate to express gratitude towards my family. My Parents **Rouabah Mohamed**, **Hadji Nouara** and my brothers **Abir,Acheraf,Wassim,Wiaam** and **Duaa** are the source of inspiration and courage in every ups and down of my life.I feel proud to say that they are finest people on the face of earth.Every achievement of this thesis is the result of their prayers, encouragement and love.

My in-depth gratitude and wishes to all my Teachers, professors, friends and relatives.....

To all of you,

thank you.

Rouabah Nouhad

Index

Chapter II : Preparation and Characterization Techniques

Chapter III :Synthesis and characterization of CdS/PVC nanocomposites

ChapterIV : Preparation and characterization of Ag :MgO/PVC nanocomposites

List of abbreviations

AFM : Atomic Force Microscope

Ag : Silver

CB : Conduction band

CdS : Cadmium sulfide

cfu : macfarland

eV : Electron volt

FTIR : Fourier-transform infrared spectroscopy

ml : Millilitre

µl : Microlitre

MB : Methylene blue

MgO : Magnesium oxide

Nm : Nanometer

NP : Nanoparticle

$\boldsymbol{O_2^{\bullet -}}$: superoxide radicals anions

$\boldsymbol{^{\bullet}OH}$: hydroxyl radicals

PL : Photoluminescence

PVC : Polyvinyle chloride

QS : Quantum size

SEM : Scanning electron microscopy

UV : Ultra violet

VB : Valence band

XRD : X-ray diffraction

List of figures

List of Tables

General Introduction

Composite polymer-inorganic nanoparticles are of great importance of today's scientific world due to their biological, optical, electronic and magnetic applications. The size of the nanoparticles, the spatial organization and the interaction with the polymer chain are essential to determine the behavior of the nanocomposite [1].

Nanocomposites based on thermoplastic polymers like PVC have attracted increasing attention, which is produced from ethylene and anhydrous hydrochloric acid. Polyvinyl chloride is the most representative commodity plastics thanks to their cost-efficient manufacturing processes, excellent thermomechanical properties, and their good environmental compatibility, including eas of recycling. PVC as a commodity plastic has been widely used in industrial fields for many years, due to its easy modification, low cost due to, nonflammability [2,3].

Cadmium sulfide (CdS) is a well known semiconductor with bandgap energy of 2.4 eV, which can be used in various applications such as photocatalyst, optoelectronic devices, and solar cell panel .This semiconductor have been mostly synthesized by high temperature pyrolysis of organometallic precursors, ion exchange, microemulsion route, microwave, hydrothermal, photochemical, and electrochemical [4] .The researchers are finding the performance of polymer-CdS nanocomposites for their surface modifixation of the host materials possibility be an approach to mediate the structure and properties of the resultant nanocomposite photocatalyst [5].

Magnesium oxide (MgO) is one of the foremost important functional metal oxides which have been widely used in numerous areas.Even though, wide band gap insulator (~ 4.2 eV). MgO nanoparticles have various numerous prospects in applications, such as catalysis, poisonous waste remediation, material industry, paints and superconductors due to their abundant source of raw materials, high thermal stability, low biological toxicity and biodegradability due to their high surface-to-volume ratio and small size, penetrating microorganisms [6,7].

The aim of this thesis was the preparation of polymer nanocomposite films made of PVC (matrix) of polyvinyl chloride doped with cadmium sulphide and magnesium oxide. This thesis also contains well full details about the structural, morphological, optical and photocatalytic properties of the synthetized nanocomposite.Their applicability was tested using methylene

blue in the range of UV light.The present thesis consists of four chapters and the contents of the thesis are as follows:

Chapter 1 provides an insight in the world of nanomaterials, nanocomposites and semiconductor-polymer nanocomposites. Further it includes a brief review on cadmium sulfide and magnesium oxide nanoparticles along with their properties and applications, as well as polymer-based nano-composites and their various applications based on Polyvinyl Chloride and its uses in different fields.The motivation for the study of CdS/PVC and MgO/PVC nanocomposites at the end of this chapter.

Chapter2 describes the experimental methods used for the preparation of nanomaterials and nanocomposites reported in this thesis ,and also the different techniques of structural, optical, morphological and photocatalytic characterization of nanocomposite materials which will allow us to study their properties and determine their performances.

Chapter3 covers in the first part, the synthesis of CdS nanoparticles and CdS/PVC nanocomposites have been described.. The second part of this chapter presents the results of the characterization by (XRD,FTIR ,RAMAN,UV,PL,SEM) and the test photocatalytic ofnanocompositesfor methylene blue dye degradation under the UV visible light.

Chapter4 delineates the synthesis of MgO/PVC, Ag :MgO/PVC nanocomposites using a sol gel methodwith deposition by Spin-coating. We will present the results of the characterization (XRD,FTIR,UV,AFM) of the different samples. Preliminary results on the photocatalytic and antimicrobial activit of nanocomposites functionalized by Ag doped MgO nanoparticles will also be presented.

Chapter I

Introduction and Literature Review

I.1 Introduction

Nanomaterials are the fundamental materials of research today and they have great use in our everyday life. These materials have dimensions in submicron scale contrasted.The first study of nanoparticles took place in 1857 when Michael Faraday synthesized the ruby red colloids of gold and concluded that the color was due to the small size of the metallic particles. Gold and silver nanoparticles have been found efficient colorants for glasses. Until 1959, no one had thought of using atoms and molecules to make devices. Nobel laureate physicist Richard Feynman delivered a visionary speech called “There's a lot of room at the bottom” before the American Physical Society meeting, where he talked about making things happen small. His talk on nanoscience became a classic milestone in the field of nanotechnology, although he never changed the word "nano" or "nanotechnology". This conference can be defined as the beginning of nanotechnology. Nanotechnology reduces the bulk of material to nano-regime increasing their surface/volume ratio, sprightly and cheap. The nanometer unit derives its prefix "nano" from a Greek word which means extremely small. Scientists use this prefix to indicate 10-9 or a billionth. A nanometer means 10-9 meters, it is roughly the length occupied by five silicon atoms or ten hydrogen atoms aligned in a line[8,9].

There are two main reasons why nanoscale materials have different characteristics. It is an increase in the relative surface area and quantum effects. At the nanoscale, the quantum effects have become more important. These effects can determine the properties of nanomaterials, leading to new optical, electrical and magnetic behaviors. These emerging characteristics have had a huge impact in electronics, medicine and other fields. Nanomaterials have a higher aspect ratio (higher surface /volume ratio) than their traditional forms. Therefore, they have a high chemical reactivity, which can affect their resistance [10].

Nanoscience and nanotechnology are a vast field of interdisciplinary research and development, which has exploded globally in recent years. Nanotechnology combines solid state physics, chemistry, electrical engineering, chemical engineering, biochemistry, biophysics and materials science. It is a highly interdisciplinary field, involving ideas integrated from many traditional disciplines, such as chemistry to biology, materials science to electrical engineering. Scientists use tools and develop expertise to sell commercial nanotechnology products. This includes polymer science and technology and covers research in a wide range of fields [11].

Nanostructured composite materials are composed of organic polymers and inorganic fillers. They represent the fusion of traditional organic materials and inorganic materials, thus forming a true hybrid composition . This concept is very attractive because it consists of mixing several ingredients to create materials with synergistic properties. The polymer nanocomposite is a multiphase system that contains one billionth of a nano, It is in dispersed phase in continuous polymer phase called a matrix [12]. Nanocomposites are commonly used in the manufacture of automobiles, flame retardants, packaging materials, systems administration of drugs, medical devices, coatings, adhesives, sensors, films and consumer products.The mixture of nanoparticles and polymers has led to significant improvements in the performance of polymer composites [13].The chapter 1 focuses on the general introduction of the nanocomposites, their classification and the synthetic routes of nanoparticles and polymer nanocomposites. . Specifically the recent literature on CdS ,MgO and Poly (vinyl chloride) . The properties and applications of the nanocomposites are covered in the next section . Also the objectives of the present study are given in the end.

I.2 Nanoparticles

Nanoparticles are in fact bridges between bulk materials and atomic or molecular structures. Nanoparticles are microscopic particles with a size of 1 nm to 100 nm, surrounded by an interface layer. This layer is an indispensable part of materials at the nanometric scale and fundamentally affects all properties. The usual interface layer is made up of ions, inorganic and organic molecules[14].

Nanoparticles can be synthesized by physical, chemical, biological, or hybrid methods through the growth, shaping, or assembly of materials. Generally, the synthesis of nanomaterials can be divided into two categories. Top-down and bottom-up methods. In the "top-down" method, macroscopic particles can be reduced to nanometric size by physically breaking the material. The method involves mechanical grinding, high-energy grinding, and mechanical processing. However, as nanocomposites generally consist of a continuous phase/matrix containing a second nanophase/charge and their particle size is less than 100 nm, this method is not effective because particle sizes less than 500 nm cannot be generated. On the other hand, the "bottom-up" approach involves the aggregation of atoms to form particles of a certain size, shape or structure. Bottom-up methods include physical and chemical methods. In this method, the

materials and phases are produced by physical or chemical methods from precursor compounds that form nanometric or nanocomposite materials. The advantages of chemical methods over physical methods are that they are relatively simple technologies, inexpensive and low-temperature technologies, and do not require complicated equipment. Materials can be synthesized into different shapes, sizes, and structures. Nanoparticles have a high aspect ratio and are therefore unique and beneficial for today's emerging applications. This special property helps them to interact more effectively with their environment, especially when they need to have adsorption and interaction characteristics in a gaseous environment. Currently, due to various potential applications in the fields of biomedical, optics, and electronics fields, research on nanomaterials is a broad area of research[15].

I.2.1 Classification of nanoparticules

In general, nanomaterials can be divided into three different morphologies or nanostructures [16, 17, 18]:

a) Zero- dimensional

b) One-dimensional

c) Two-dimensional nanostructure.

(A) Zero-dimensional nanostructure (0D): In zero dimensional nanomaterials quantization occurs in three dimensions. Some other terms for zero-dimensional nanoparticles are: If the nanoparticles are single crystals, they are often called nanocrystals. When the characteristic size of the nanoparticles is sufficiently small and quantum effects are observed, quantum dots are a general term used to describe these nanoparticles.

(B) One-dimensional nanostructure (1D): In one-dimensional nanostructure, quantization occurs in two dimensions. Size nanostructures have different names, including nanorods, nanosheets, nanofibers, nanoribbons, etc.Nanowires generally refer to linear structures with specific growth directions, but their lateral and cross-sectional shapes may not be well defined or uniform (Figure I.1 (a)). Nanowires are shorter length nanowires (Figure I.1 (b)). Nanotubes are one-dimensional nanostructures with hollow internal channels (Figure I.1 (c)). Nanoribbons are one-dimensional nanostructures with well-defined sides (Figure I.1 (d)), and they have a tighter shape and uniformity than nanowires.

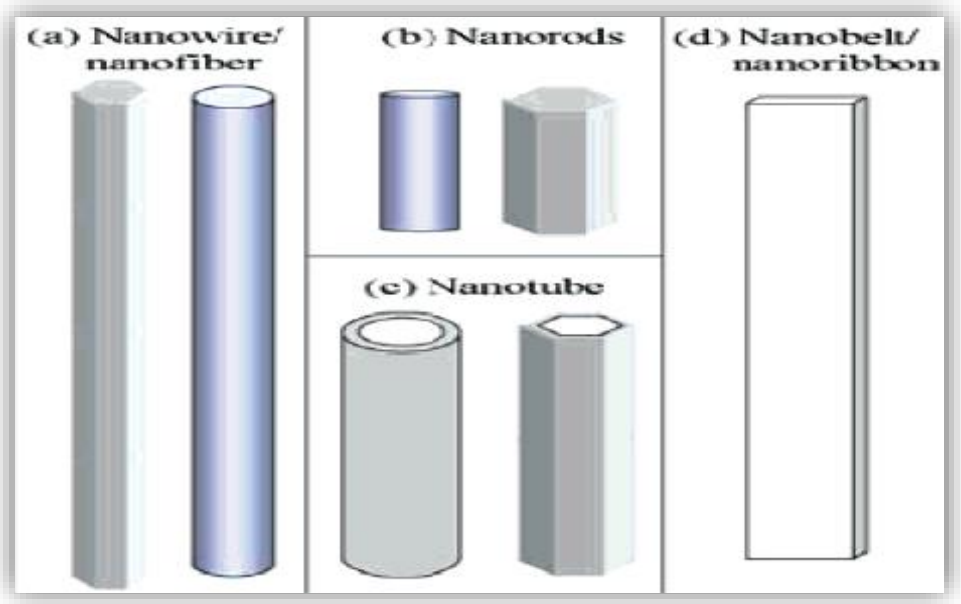

Fig. I.1 Typical morphologies of one-dimensional nanostructures: (a) nanowires, (b) nanorods, (c) nanotubes and (d) nanobelts.

(C) Two-dimensional nanostructure (2D): In two-dimensional nanostructures, quantization occurs in one dimension. If the width / thickness ratio of the nanostrip reaches a thousand, that is to say the aspect ratio of writing paper, the ultra-wide band can be classified as a 2D nanostructure (nanosheet). It should be noted that in terms of the above nanostructures, the surface / volume ratio and the quantum confinement effects are significantly different. For a given mass, the 0D nanomaterials have the largest exposed surface, followed by the 1D, and finally the 2D nanomaterials have the smallest exposed surface. As Figure I.2 shows, for different types of nanostructures, the density of states (DOS) (the number of electronic states per unit of volume and energy) has changed considerably. For bulk materials, DOS has a square root dependence on energy, and this dependence varies with the dimension of the quantum structure, as shown in Figure I.2. Changes in DOS dimensions have led to extraordinary optical and electrical performance in the production of advanced nanodevices.

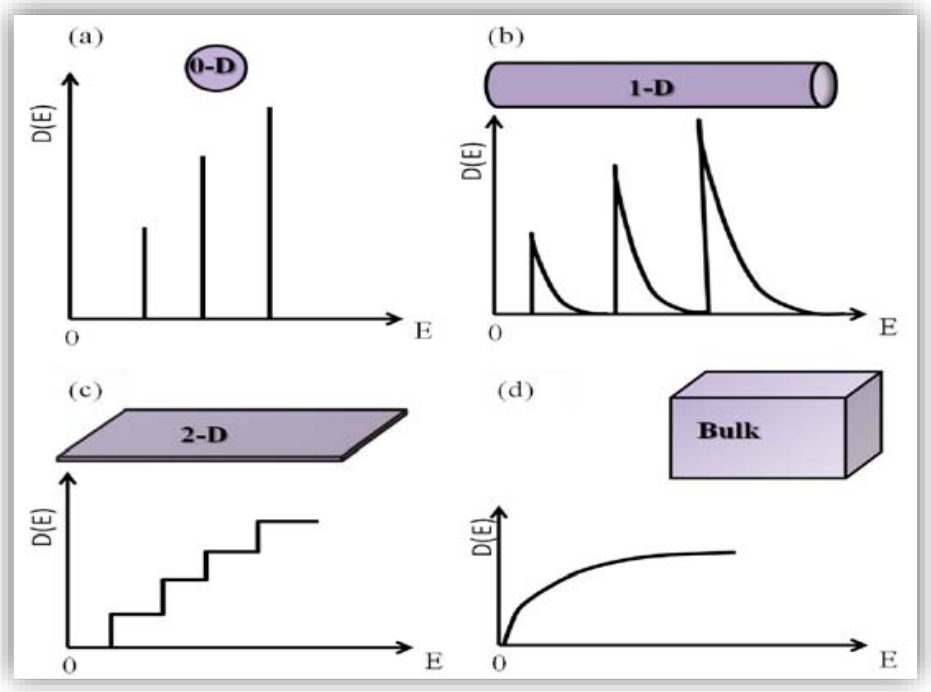

Fig. I.2 Density of states (DOS) plots for: (a) 0-dimensional (0-D), (b) 1-dimensional (1-D) and (c) 2-dimensional (2-D) nanostructrues; (d) Bulk material.

I.2.2 Methods of manufacturing nanoparticles

The functional nanomaterials have been manufactured by the following two methods:

(i) The top-down approach and (ii) the bottom-up approach. In the top-down technique, for the synthesis of nanomaterials, the macro crystalline structures are broken down into nanocrystalline structures, but the original integrity of the material is retained. Examples of top-down techniques are lithography, etching, ion implantation, ball-milling and chemical reaction between two constituents.In the bottom-up technique, small molecular building blocks are joined to produce nanostructures with defined geometries and specific functions. Examples of bottom-up techniquesare sol-gel technology, electrodeposition, physical and chemical vapour deposition, epitaxialgrowth,laser ablation,etc [22].

Cracking of the solid material generated can be achieved by dry grinding and wet grinding. In the dry grinding method, various equipment used are jet mills, hammer mills, ball mills, etc., to crush solid materials by impact, compression, or friction. On the other hand, the wet grinding of the solid base material is carried out using a drum ball mill or a vibrating ball mill. Bottom-up methods are roughly divided into gas and liquid phase methods [19]. For the former, the chemical vapor deposition method involves a chemical reaction, while the physical vapor

deposition method uses the cooling of the evaporated material. Although the gas phase method can minimize the presence of organic impurities in the particles compared to the liquid phase method, they require the use of complicated vacuum equipment, which has the disadvantages of high cost and low productivity. For many years, the liquid phase method has been the main method of preparing nanoparticles. The chemical reduction of metal ions is a typical example of the liquid / liquid method, and its main advantage is the ease of manufacturing particles of various shapes, such as nanowires, nanowires, nanoprisms, nanoplates, and hollow nanoparticles [19]. Using chemical reduction methods, the shape and size of nanoparticles can be refined by changing the reducing agent, dispersing agent, reaction time and temperature [20]. The process uses simple equipment or instruments and a large number of nanoparticles can be produced at low cost in a short time. Due to the use of non-degradable polymers, toxic substances, and dangerous chemicals, some of these methods are very expensive and not very environmentally friendly. Other reduction methods used to synthesize nanoparticles include photo-reduction using gamma rays, ultrasound, and liquid plasma [21]. These methods do not use chemically reducing substances and therefore have the advantage that no foreign impurities are added to the nanoparticles. In addition to these methods, spray drying, spray pyrolysis, solvothermal synthesis, and supercritical methods are also known. The general technique of the sedimentation method is the sol-gel method, which has been widely used in the manufacture of metal oxide nanoparticles [22].

I.2.3 General applications of nanoparticles

Nanoparticles have made it possible to considerably improve the performance of applications in all industries, in particular in aerospace, automotive, electronics, medical, glass, optics and consumer products. The potential benefits of nanotechnology are everywhere, as described below[23,24,25]:

Optics: Nanoparticles can be designed and used to coat anti-reflective products to produce refractive indices for various surfaces. Light-based Biosensor for the detection of cancer can also be extended.

Magnetic: Nanoparticles have the potential to augmente the density of various storage media, and when magnetized, they can improve the contrast of MRI images. They can also develop the cooling systems currently used by transformers in these type of processes.

Mechanical: nanoparticles can improve the wear resistance of almost all mechanical equipment. They can also provide these devices with unprecedented corrosion resistance and create new composites and structural materials that are lighter and stronger than the composites and structural materials we use today.

Electronic products: The small size of nanoparticles help to produce sophisticated and efficient electronic products. They cannot only provide high conductivity materials, but also provide more exquisite parts for small consumer electronics devices (such as mobile phones). In terms of advertising, electronic nanoparticle products can create digital displays that are more economical in terms of electricity consumption, lower production costs and more vivid colors.

Energy: Nanoparticle batteries will be more durable and have a higher energy density than the batteries we use today. Clusters of metallic nanoparticles can also have revolutionary applications in the storage of hydrogen. They can also produce extremely efficient fuel cells by acting as electrocatalysts for these devices. Nanoparticles can also pave the way for practical and renewable energy. They have demonstrated the ability to improve the efficiency of solar panels on several occasions. Not only that, when nanoparticles are used as catalysts in internal combustion engines, they also have characteristics that make the engines more efficient and therefore more economical.

Apart from the above uses of nanoparticles, nanoparticles seem to be useful in the detection of diseases. Also, the taste and qualitity of foods and drinks can be improved with the help of nanoparticles.

Biology: Nanocrystalline materials can be used in many fields, but the environmental applications of these materials are particularly important. Air and water pollution remains a challenge in all regions of the world. In many cases, pollution control technology is limited by the poor performance and /or high cost of existing absorbent materials;

A large number of research activities are aimed at developing new adsorbents. The following list provides some examples of this situation:

• **Controlling chemical leaks and accidental release of hazardous chemicals in different locations and environments:** accidental releases of chemicals are common in laboratories, industrial sites and all locations where chemicals are used. Accidental spills and leaks often cause environmental pollution. Nanoscale has developed a specialized and safe adsorbent

formulation, FAST-ACT_ (the first application of an absorbent treatment resistant to chemical threats), a powder that can safely manage spills and eliminate the environment.

• **Prevention of chemical risks:** Nanocrystalline metal oxides can be incorporated into protective textiles or skin creams to provide additional protection against chemical and biological risks. Toxic substances on nanoparticles are destroyed, eliminating the threat of gas leakage and secondary pollution.

• **Indoor air quality control in buildings and vehicles:** currently, various air filtration technologies are commercially available; including particulate filters, electrostatic precipitators and activated carbon filters. There remains a large group of high volatility chemicals that cannot be effectively controlled by these approaches. Attempts to develop more effective sorbents or catalysts for these pollutants are underway.

• Elimination of elemental and oxidized mercury from combustion gases generated by electric utilities using coal as an energy source:Recent regulations promulgated by the U.S.E.

The presence of arsenic, perchlorate and methyl-t-butyl ether (MTBE) in drinking water causes serious health problems and has resulted in mandatory maximum levels of contaminants (MCL) for arsenic and may trigger new EPA regulations.

I.3 Importance of II-VI nanostructures

The advancement made in physics and technology of semiconductors depends mostly on three families of materials: the group elemental, III–V, and II–VI compound semiconductors. These semiconductors II–VI crystallize either in the wurtzite crystalor zincblende lattice structure. The first research papers on II–VI compound semiconductors goes back to the middle of the nineteenth century. Currently, the compound semiconductors II–VI are widely used as photodetectors, x-ray sensors and scintillators, phosphors in lighting, displays, etc. Thus, it seems to timely bring together the most up-to-date information about material and semiconducting properties of II–VI compound [26].

II–VI semiconductors (zinc chalcogenides: ZnO, ZnS, ZnSe, ZnTe; cadmium chalcogenides: CdS, CdSe, CdTe) are a class of materials that has been intensively studied in the field of nanostructures. Additionally, the range of their wide direct band gap offers a flexibility to fabricate optoelectronic devices to work on various wavelengths of choice. Now the continuous research on II-VI semiconductors is of the greatest importance[27].

I.3.1 Cadmium sulfide nanoparticles (CdS): Introduction and general properties

Cadmium sulfide (CdS) is one of the extensively studied semiconductor material belonging to II-VI group in the periodic table. Further, Cadmium sulfide has rapidly developed in recent years because of its structure richness and novel properties. It is one of the dominant nanomaterials in nanotechnology as the same time as carbon nanotubes and Si nanowires. Due to its wider bandwidth (2.42 eV) and non-linear optical properties. Also known, cadmium sulfide has the closest physical properties with zinc oxide, including crystal structures, lattice constants, etc. In spite of these, surprisingly research on CdS nanostructures has come to the forefront only recently and no extensive reports on CdS nanostructures are available [28,29]. CdS nanomaterials has already shown vital applications influorescence probe, sensors, solar battery, photo electrocatalysis and laser light-emitting diodes, etc

(a) Crystallographic structures of CdS

Cadmium sulfide can crystallize in four different structures; the hexagonal structure (wurtzite), the cubic structure (zinc-blende), the cubic rock salt structure and the distorted rock salt structure. Among these four crystalline structures, the wurtzite,which can be found in nature as rare Greenockite mineral is thermodynamically moststable and thus the most common. CdS with zinc-blende modification is a metastable structure, however it can be still found in nature as rare mineral Hawleyite [29].

Crystal structure	Space group		Lattice parameters (Å)
	(Hermann-Mauguin)	(Schönflies)	
Wurtzite	$P6_3mc$	C_{6v}^4	a = 4.1348, c = 6.7490
Zinc-blende	$F\bar{4}3m$	T_d^2	a = 5.818
Rock salt	$Fm\bar{3}m$	O_h^5	a = 5.32
Dist. rock salt	$Pmmn$	D_{2h}^1	a = 3.471, b = 4.873, c = 3. 399

Table I.1: The lattice parameters and space groups of all the above crystalline structures of CdS.

Hexagonal and cubic structures are twins to each other; only a change in symmetry is demanded to transform the cubic to hexagonal lattice. For the zinc-blende structure,the stacking sequenceof {111} planesis ABCABCABC repeating pattern, wherease forwurtzite structure , the stacking sequence of (0001) planes is ABABAB repeating pattern.For rotation of 60°of second plane around the (111) direction, where the Cd atoms move to the hexagonal sites. The transformation of crystal structure from the cubic to hexagonal due to the displacement of Cd atoms was clearly shown in Fig. I.3 [29,30].

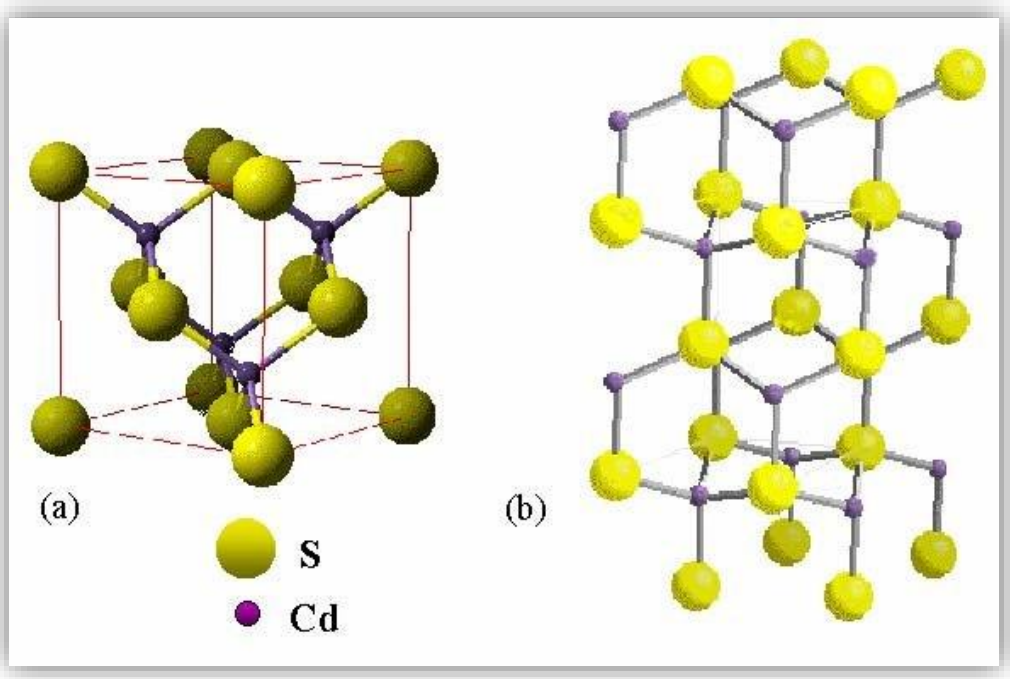

Fig. I.3 :The crystal structure of CdS (a) cubic zinc-blend (b) hexagonal **.**

I.3.2 Magnesium oxide (MgO): Introduction and General properties

Oxide (MgO) has become one of the most interesting oxides in recent years for for both fundamental and applicational research areas,because it is a very important metal oxide for used in catalysis and toxic waste remediation, and it is also frequently utilized such as additives for refractory, paint and semiconductor products ,due to their unique physical-chemical properties.

Magnesium oxide (MgO) is a wide band-gap insulator (7.8 eV) with rock-salt crystal structure (fee) at ambient pressure [28], the Mg ions occupying octahedral sites within the anion closed packed structure.MgO is white powder, odorless and nontoxic which possesses a high melting pointand and hardness [30].

(a) Crystallographic structures of MgO

This compound crystallizes in face-centered cubic structure with symmetry space group F m3met, it has 2 atoms per elementary cell. The Mg atom occupies the Wyckoff4a site (0,0,0) and the O atom occupies the 4b site (12,12,12) , so the Mg atom resides in the center of an octahedron r Regular formed by O atoms. The lattice parameter of MgO at room temperature is 4.21˚A and it is the only structural variable in MgO. Thus, the crystallographic simplicity of this material makes it the ideal candidate for observing the effect of thermal fluctuations in nuclei over wide temperature ranges. Magnesium Oxide MgO has the crystallographic structure of NaCl, i.e. a face-centered cubic Bravais lattice comprising a magnesium atom and an oxygen atom, the two sub-lattices being shifted by (121212). MgO mesh is 4.211 Å [32].

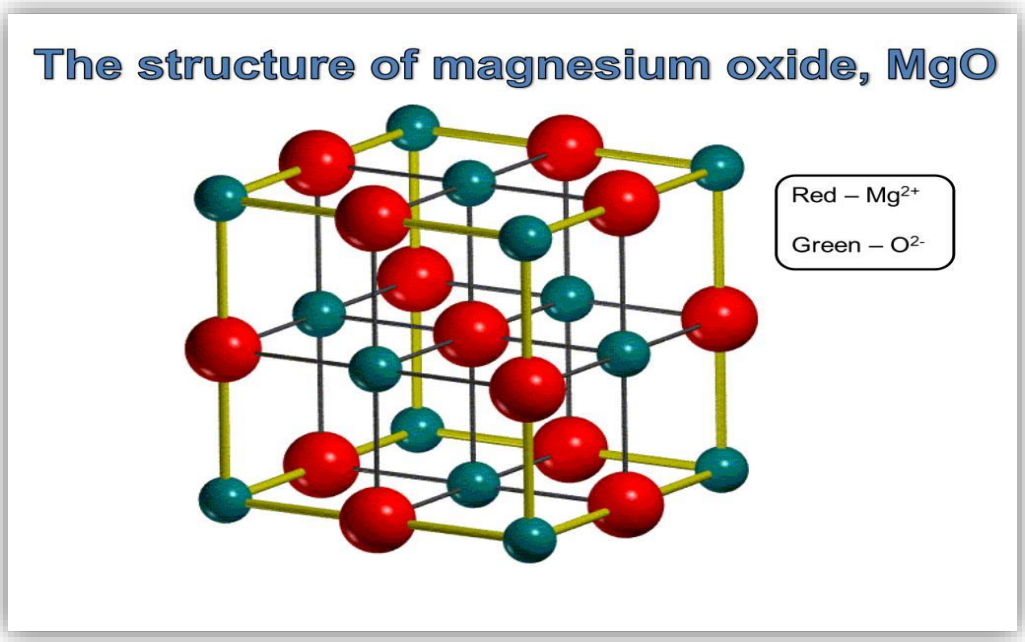

Fig. I.4: Magnesium oxide (MgO) crystalline structure.

1.4 Polymers and their classification

Polymers are the particular class of materials, consisting of a set of regularly repeated chemical units (monomer) of the same type or different type, joined end to end or sometime in a more complicated way. These extremely large chain macro molecules are very essential in today life as food, clothes, house builds, body parts, starch protein, polyester, nylon, wood, cellulose, paints, nucleic acids etc. are the examples for some polymers (natural and synthetic polymers). Polymers were formed due to different polymerization reactions.When the monomers just add on to form polymer, without changing its structural identity is known as addition polymerization. Here the molecular weight of the polymer roughly equals the sum of monomer units present in the polymer and the monomer unit should be unsaturated (example: formation of polyethylene from ethylene).A polymer is chain of repeated units, called monomers. If the polymers are formed by joining monomers and elimination of smaller molecules like water, ammonia, carbon di oxide etc.are called condensation polymerization [32-33].

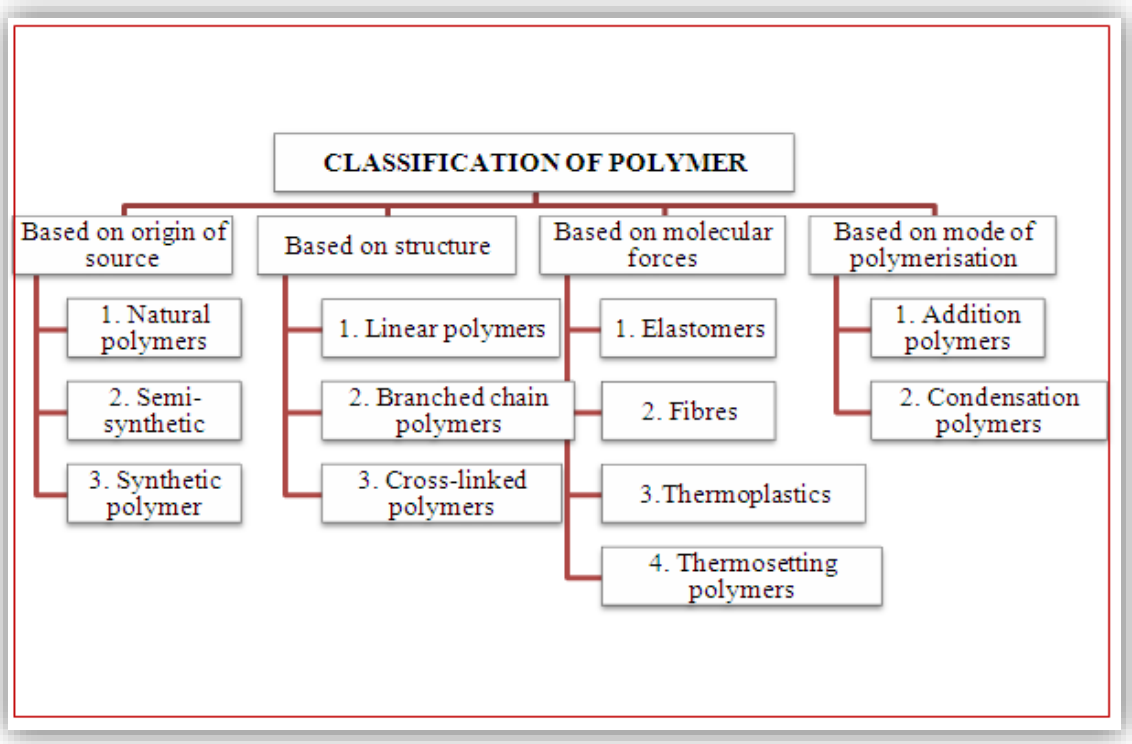

Fig I.5: Polymer Classification.

I.4.1 Poly (vinyl chloride) (PVC)

The advanced manufacturing of PVC via vinyl chloride polymerization technology has developed primarily in USA and Germany. In the early 1930s, commercial manufacturing of PVC through emulsion polymerization was ongoing at Germany. PVC was accidentally synthesized in 1872 by German chemist Eugen Baumann [33].Now PVC is one of the worlds's chief products that are produced on a massive scale with its demand increasing day by day. After poly (ethylene) and poly (propylene), poly (vinyl chloride) is the third major synthetic thermoplastic polymer. It is a brittle, glassy, light-weight material that is resistant to acids and bases. Low cost, mechanical, corrosion resistance andanti-chemical properties of PVC make it much attractive.

Suspension technique is the consignment route for PVC production made from using vinyl chloride monomer (VCM) as a raw material. PVC consists of 42% hydrocarbon and 58% chlorine. The PVC production accounts for 35% of chlorine formed industrially and only 0.3% of world's supply of gas and oil compared to other polymers (mostly hydrocarbons that is manufactured from petroleum) . The PVC production is less dependent on oil and gas and hence it is cost effective. PVC alone is difficult to process and for making products due to its brittle nature.

PVC has linear structure but some short branches are formed sometimes in the structure, chlorine atom in each repeating unit. Because of the presence of chlorine atoms,the intermolecular attraction among the chain is very high, which makes the polymer horny rigid, stiff and hard.However, because of random polymerization the polymer is amorphous in nature with all possible tacticity in the structure with 55% syndiotactic (5% crystalline) and hence T, is approximately 80 OC. Mechanically it is good and properties vary with plasticizer content. It is soluble in THF, cyclohexanone, methyl ethyl ketone (MEK), etc. It exhibits self-extinguishing characteristic due to presence of large amount of chlorine atom (56.8%) in its structure.PVC has low thermal stability which can be made to take on various colors [35].

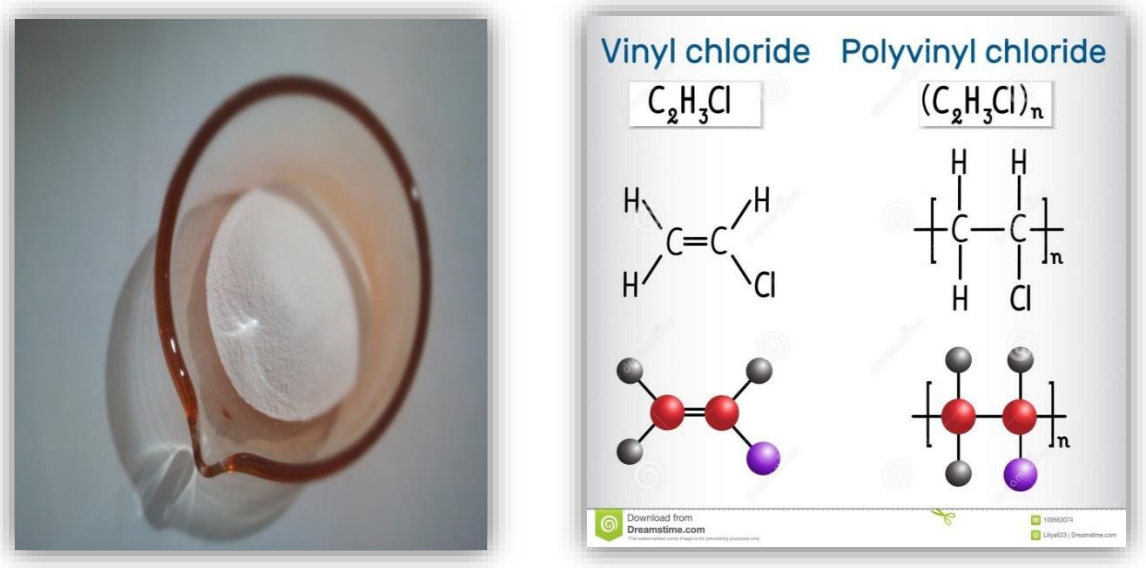

Fig.I.6:Structure chemical formula and molecule model of PVC .

I.4.2 Applications of Poly (vinyl chloride)

The least thermal stability of PVC has limited its application in several fields which require working at high temperature. Poor thermal stability of PVC can lead to the formation of conjugated polyene sequences. Flexible forms of PVC is produced by adding plasticizers and it varies depending on the applications which include hoses, tubing, electrical insulation, coats, jackets and upholstery. It is also used for making inflatable products such as water beds and pool toys .By varying the amount of plasticizer and other ingredients, it can be used for a wide range of applications from hard building materials to soft baby pants. It is also used as electrical insulation material for cable application especially sheathing (cover over the insulator of electrical wire) material. The unplasticized PVC is used in chemical plants and equipments, storage tank, building items like pipes, sheets, door, frame, containers, roof sheet, floor tiles, wall lining, etc. Semirigid and flexible application includes packaging, tubes, flexible pipes, hoses, sheets, films, footwear, belting, cables, baby pants,toys, etc.PVC based wood composites are widely used in building construction applications,such as windowldoor profiles, decking, railing and siding because they offer goodmechanical properties, chemical and water resistance,

rot-proof ability, stain and paintability,as well as a long lifetime (UV resistance, free from maintenance)[35,36].

I.5 Additives

The incorporation of fillers or adding salts in the polymer matrix helps polymer to get new properties. It is the kind of interest due to occurrence of multifunctionality in the polymer composite therefore doping or adding external material in the polymer having been extensively studied. The prepared polymer composites exhibit enhanced optical properties, electrical properties, mechanical properties and electrochemical properties depending on selection of polymer matrix and doped element [37].

Intrinsic charge carriers were absent in most of the polymers. Doping process provides required charge carriers. Different types of doping molecules provide different types of properties. The doping molecules may be metal oxide nano particles, lithium salts, sodium salts, ammonium salts, chalcone derivatives etc. After addition of these salts, it may interact with active groups of polymer and forms polymer doped complexes via hydrogen bonding, coulomb interactions, hydrophilic interactions etc. These interactions enhance basic polymeric properties and also add doping material dependent properties.This complex formation is also dependent on factors like temperature,concentration of the additives, electro negativity, ionic radius of the cations of the additive etc. These factors are being the reason for modification of physicochemical properties of the polymer matrix[38].

Doping salts in the polymer matrix results in the loss of mechanical strength of the matrix, in order to overcome from this limitation, the matrix was filled with nano/micro particle as we discussed in above sections. Nowadays,addition of nanoparticles makes polymer multifunctional i.e. nanoparticles not only enhances mechanical properties it but also enhances optical, electrical as well as other physicochemical properties [38].

I.6 Polymer-matrix Nanocomposite

Introducing nanoparticles into the polymer matrix yields a multifunctional,nhighly performing new class of material known as polymer nanocomposites (PNCs). Polymer nanocomposites are considered the materials of the 21st century. They combine the use of a nanostructured inorganic or organic filler with size typically of 1–100 Å in at least one dimension, and a polymeric continuous matrix. Nanoparticles in the polymer matrix develop a new polymer nanocomposites with extraordinary properties. As size of the particle reduces,

surface area to volume ratio increases which increases impact of behavior of atoms on a surface area of the particle due to increase in interaction with the polymer matrix. This influences on properties of a composite when they interact with a polymer matrix.This makes the polymer composite, a multifunctional material by enhancing thermal properties, mechanical properties, electrical and dielectric properties, microstructural properties, electrochemical properties which in turn affects their optical, catalytic and other chemical properties, thus suggesting applications in the field of functional materials, such as, temperature sensors, linear polarizers, optoelectronic and chemiresistor devices.

Among the polymeric matrices used in the preparation of nanocomposites, thermoplastic polymers represent a class of interest both for scientific research and application at industrial level. Polymers such as polyvinyl chloride polyolefins, polyesters, polyamides, homopolymers and copolymers of styrene, are known for their good mechanical properties, durability and versatility in processing that allow their use in many of the different forms used in the sensing devices of interest in this review.Along with this, two more factors need an attention during preparation, they are interfacial interaction compatibility of nanoparticle with polymer matrix and proper processing technique to get uniform nanoparticle dispersion in the polymer matrix.

I.6.1 Properties of polymer nanocomposites

Nanocomposites consisting of a polymer and nanofiller frequently exhibit remarkably improved mechanical and materials properties when compared to those of pristine polymers.The overall properties of polymer nanocomposites are controlled by the properties of the nanoparticles area ,as they presented below [41,42]:

I.6.1.1 Mechanical Properties Tensile and flexuralMechanical:

The tensile modulus of a polymeric material has been shown to be remarkably improved when nanocomposites are formed.The Young's modulus tends to increase with the volume fraction of inclusions in every case. In some systems, there is a critical volume fraction at which aggregation occurs and the modulus goes down .

Interaction between polymer matrix and filler may play an important role in the effects of the polymer nanocomposites properties . For polymer nanocomposite with good interaction between load and matrix, the yield strength tends to increase with increasing volume fraction and decreasing particle size, and modulus is increased similarly. Under the same conditions,

when there is a bad interaction between the matrix and the particles, the pattern will change. [44].

I.6.1.2. Dynamic mechanical analysis

DMA has been used to study the temperature dependence of storage modulus and loss modulus upon nanocomposites formation under different experimental procedures. The nanocomposites showed remarkable improvement in storage modulus. This behavior is explained on the basis of good interaction between the polymer and the filler particles [46]. In general, the viscoelastic properties of nanocomposites tend to be superior to those of pure polymer systems. When the nanoparticles-polymer matrix interaction is good, the storage modulus increases with the increase in the volume fraction. Storage modulus also tends to increase with decreasing particle size.

1.6.1.3 Optical transparency

Mostly, the nanoparticles employed have size between 1-100 nm, when nanoparticles are dispersed in a polymer matrix, the resulting nanocomposite is optically clear in visible light. So studies of optical transparency of nanocomposites are very important [47].

I.6.1.4 Electrical:

Dielectric spectroscopy (DS) is a very powerful technique that can be used to study various dielectric processes in both electrical and non-electrical applications. DS describes the dielectric properties of materials, which play an essential role in the description of physical phenomena in modern science and engineering.

Dielectric spectroscopy provides information on the dynamics molecular motion of the individual constituents of a complex material and the characterization of its bulk properties[].

With low concentrations of nanofiller into polymer , It has indicated that the presence of a small quantity of inorganic nanofillers can affect the real and imaginary parts of the complex permittivity[ ].The effect of nanofillers is unique as the incorporation of nanofillers into polymers can reduce the relativepermitivity compared to the value of the neat polymer materials.

I.6.1.5 Thermal

Polymer materials have good insulating properties and processability but the thermal conductivity is rather weak. The microparticles, which have been used for more than 50 years as filler, change the property of a polymer considerably. The study of nanostructured materials

might help in developing a new branch of polymer-based nanocomposites, which can be used in special applications. It has been found that filler size, geometry, concentration, dispersion, orientation, crystal structure, and interface between the polymer matrix and filler affect the thermal conductivity of the host polymer.

In case of nanodielectrics, the surface modified nanoparticles reorganize the polymer matrix in such a way that the interface polymer layer in the proximity of the particles changes its properties signif icantly. The interface polymer layer, which is created by surface modified nanoparticles, has semicrystalline properties. It means that polymer chains are not chaotically distributed.

Generally, the incorporation of filler into the polymer matrix was found to enhance thermal stability by acting as a superior insulator and mass transport barrier to the volatile products generated during decomposition.

The role of nanofiller in the nanocomposite structure may be the main reason for the difference in TGA results of these systems compared to the previously reported systems.

I.6.1.6 Gas barrier properties

Nanoparticles are thought to increase the barrier properties by creating a maze or 'tortuous path' that retards the progress of the gas molecules toward the matrix resin. beside ,The filler (inorganic) acts as a heat barrier, which enhances the overall thermal stability of the system, In the early stages of thermal decomposition, the filler would shift the decomposition to higher temperature. After that, this heat barrier effect would result in a reverse thermal stability.

I.6.1.7 Rheology

In order to understand the processibility of these materials, i.e. the final stage of any polymeric material, it is necessary to understand the detailed rheological behavior of these materials in the molten state. Understanding the rheological properties of molten nanocomposites is not only important for gaining basic knowledge about processability, but also for understanding the structure-property relationship of these materials.

I.6.1.8 Others properties

Polymer nanocomposites also show improvement in most general polymeric properties. For example, in addition to the decreased permeability of liquids and gases, nanocomposites also show significant improvement in solvent uptake for specific applications. Scratch resistance is

another property that is strongly enhanced by the incorporation of layered silicates. Finally, polymer nanocomposites have been used in highly technical areas such as in the improvement of ablative properties in aeronautics [48] .

I.6.2 Preparation of polymer nanocomposites

Many reviews have been focused onto the preparation of nanocomposites from thermoplastic polymers often addressed to highlight their improved thermal and mechanical features when compared to polymer matrix or traditional composites Methods for preparation polymer nanocomposites generally involves the dispersion of nanomaterials into the polymer matrix. Researchers have tried a variety of processing techniques to make polymer matrix nanocomposites. Broadly all these techniques can be divided into two parts : ex-situ and in-situ. In ex-situ both the polymer and the nanofiller are taken separately and mixed together.The blending can be carried out either in a polymer melt, if the components tolerate the blending temperature above the melting temperature of the polymer, or in a polymer solution, if a suitable solvent is available.

In situ polymerization in the presence of the nanoparticle is possible in all different polymerizationsbut only if the nanoparticle does not inhibit the polymerization reaction. Regardless of the preparation method of the polymer nanocomposite, a good compatibility between the components is essential in order to produce a homogenous polymer nanocomposite. Thus, the synthesis of polymeric nanocomposites can be classified under two major categories: as physical and chemical methods.These methods are discussed below [43,44,45,46,47] .

I.6.2.1 Physical methods (Melt Intercalation Method)

Physical preparation methods for polymeric nanocomposites are based on dispersion of liquid particles, but differ in the type of the continuous phase. ,. During solvent molding , a polymer, a solvent and nanoparticle are combined and thoroughly mixed by ultrasonication and the solvent is allowed to evaporate leaving behind the nanocomposite typically as a thin film. The solvent chosen must completely dissolve the polymer as well as disperse the nanoparticle.

- **Direct Mixing of Polymer and Nanofillers**

This process is a approach for fabrication of polymer nanocomposite ,which is based on the decomposition of the aggregated nanofillers during mixing process. This technique includes

two general ways of mixing the polymer and nanofillers. The first way is mixing a polymer, with nanofillers above the glass transition temperature of the polymer without using any solvents,, generally called melt compounding method. The second way involves mixing of polymer and nanofillers in solution using solvents, generally called solvent method/solution mixing [53].

- **Melt Compounding**

This method involves the melting of polymer powder or pellets to form a viscus solution and nanofillers are added into polymer solution by high shear rate combined with high temperature diffusion above the glass transition temperature with intensive mixing for some time and nanocomposite comes out from the die.From this type of method, the shear stress (hydrodynamics force) is induced in the polymer melt by viscus drag, and this shear stress is used to breakdown the nanofiller aggregates and thereby promotes homogeneous and uniform nanofiller dispersion in the polymer matrix[54]. The final shape of components can be fabricated by compression molding, injection molding or fiber production technique[50].

- **Solvent Method**

In this method, the shear stresses induced in the polymer matrix are lowered compared to that in melt compounding. The nanofillers are pre-dispersed in the solvent by sonication in order to breakdown the nanofiller aggregates and polymer is dissolved in a co-solvent. The resulting nanocomposites are recovered from solvent through solvent evaporation or by the solvent coagulation method. The polymer nanocomposites fabricated by one of the above methods a re finally processed by conventional manufacturing methods like injection molding, calendaring, casting, compression molding, blow molding, rotational molding, extrusion molding, thermoforming, etc [55]

I.6.2.2 Chemical methods

The process of direct mixing and melting of particles with polymers generally lead gradients of fillers introduced into the matrix, which results in the turbidity / translucency of the composite material due to agglomeration of the nanoparticles. To overcome these problems, in situ polymerization and in situ nanoparticle formation methods have been developed [48,49,50].

- **In Situ Polymerization Method**

The in situ polymerization process is to disperse inorganic nanoparticles directly into the monomer solution before the polymerization process. Inorganic particles tend to separate quickly and settle out of the organic polymer. Because the low molecular weight monomer solution easily penetrates between the layers, causing swelling.Radiation, heat and diffusion from the initiator are used to polymerize the resulting mixture. The monomers are then polymerized between the charges to form a nanocomposite of exfoliated polymers. The only disadvantage of this method is that the synthesis at high temperature can cause the decomposition of the polymer [51,52].

- **In-situ particle formation**

This chemical process based on the sol-gel polymerization process makes it possible to synthesize polymer nanocomposites in the presence of polymers or monomers. It is possible to manipulate the organic / inorganic interface interactions at different scales of molecular and nanometric length . Subsequently generating a homogeneous polymer nanocomposite structure, thus overcoming the problem of agglomeration of nanoparticles .

- **Sol- gel Method**

The term sol-gel is associated to two relations steps, sol and gel.In this process, solid nanoparticles are dispersed in a monomer solution to form a colloidal suspension of solid nanoparticles (sol). They form an interconnected network between phases (gel) by polymerization reactions followed by the hydrolysis procedure. The 3D network of polymer nanoparticles is distributed throughout the liquid. The polymer acts as a nucleating agent and promotes the growth of layered crystals. As the crystal grows, the polymer penetrates between the layers to form polymer nanocomposites [52].

I.6.3 Applications of polymer nanocomposites

Polymer nanocomposite materials have potential applications in wide range of fields which includes information and communication technologies, medical care, water decontamination, polymer electrolyte, agriculture and packaging etc .Various applications of polymer nanocomposites are given below: [53,54]

- **Automotive industry**

The use of polymer nanocomposites in automotive industries has tremendously reduced the weight and processing cost. Clay incorporated tires have excellent mechanical strength compared to ordinary tires, as well as improved gas barrier performance and flame retardance

for tubeless tire applications. Nanocomposites are also used in the manufacturing of car parts such as handles, rear view mirror, timing belt, components of the gas tank, engine cover, bumper, etc.

- **Packaging industry**

By making nanocomposites barrier properties (towards Oxygen and CO_2) of the polymers used in the packaging industry have been improved. Further, the polymer nanocomposite formation increases the thermal stability and flexibility and hence is extensively used in food and beverage packaging industries. Due to excellent solvent barrier properties polymer nanocomposites have been used in chemical protective and surgical gloves in order to protect against chemical warfare agents and for avoiding contamination from medicine.

- **Catalysis**

The high surface area of the nanocomposites is finding applications in catalysis fields, to enhance efficiency of catalyst. Due to their high surface area and synergetic properties, nanocomposites enhances the rate of reaction and also show significant advantages such as activity, selectivity, recyclability and lifetime in chemical transformations and electrocatalysis (fuel cells).

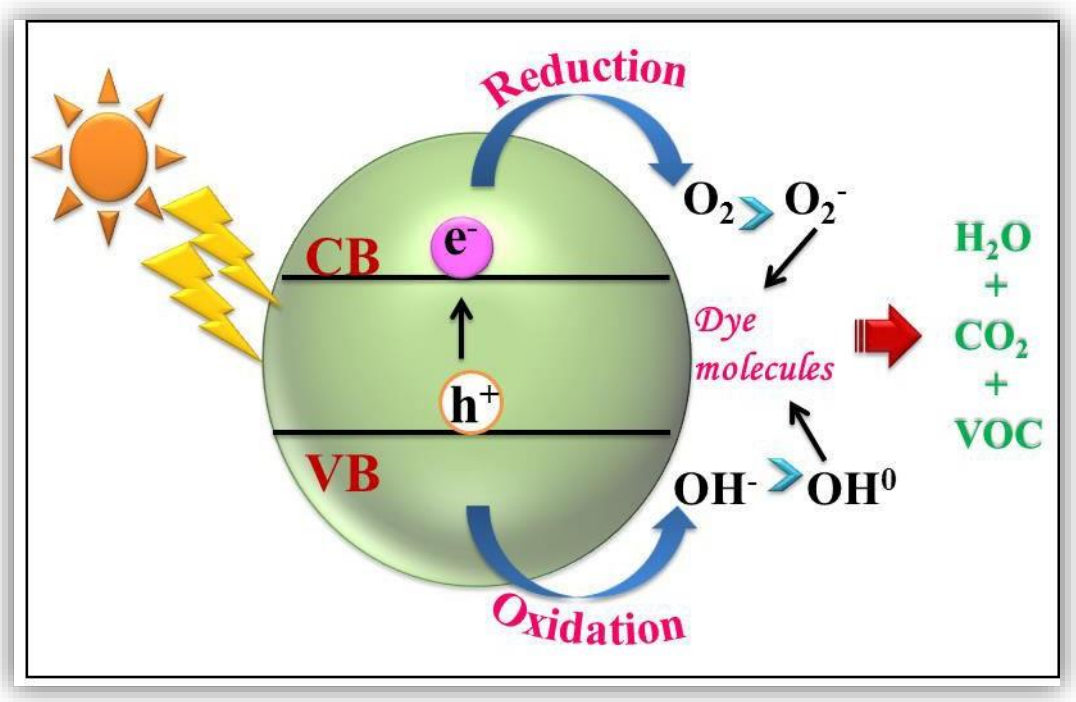

Fig. I.7: Mechanism of photocatalysis.

❖ **Solid Polymer Electrolyte**

Polymer nanocomposites are having immense applications in polymer electrolytes. Incorporation of nanomaterials in polymers improves the conductivity of the polymer electrolyte by reducing the crystallinity of polymer and by improving the mechanical and interfacial properties, which are essential for electrolyte applications such us flexible displays, solar cells, electronic paper, and a gas sensor .

❖ **Water treatment applications**

Nanocompositeshave been used in the degradation of pollutants, dyes and other organic contaminants discharged into the water by industries such as rubber vulcanization and textile industries. Further, these are also used in the killing of microorganisms present in the contaminated water. Consequently photocatalysis can be applied in such diverse areas (Figutre I.8) as water purification, Air purification, Anti fogging, Anti-bacterial and surface cleaning.

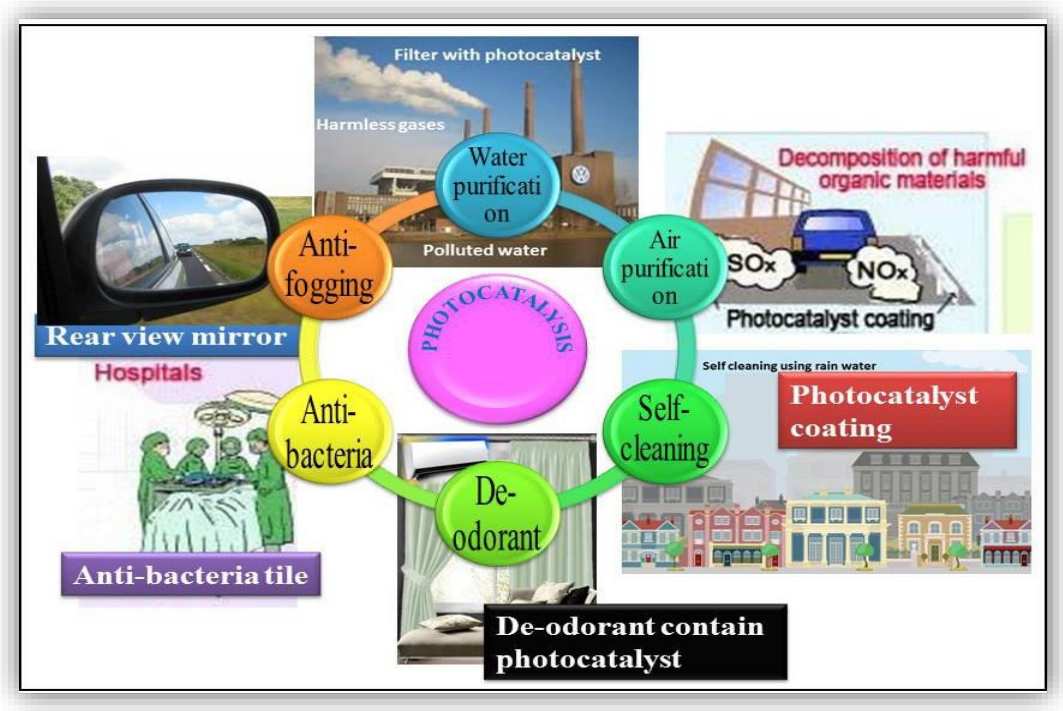

Fig. I.8: Applications of photocatalysis.

Out of all these applications, this thesis focuses mainly on the use of polymer nanocomposites for photocatalytic and antibacterial activities.

I.7Motivation for the present study

I.7.1 Why the choice of PVC as polymer matrix ?

PVC is a versatile polymer, chemically resistant, low cost dielectric polymer. It is miscible with several additives due to its chemical structure and is appropriate to mold into several products based on applications.Poly(vinyl chloride) can be considered as one of the common medical polymers .Hence, in order to control undesirable microorganisms on food surfaces, it is beneficial to coat antimicrobial agents onto the surface of the plastic film and incorporate antimicrobial agents into the polymeric matrix . In addition, it is utilized in other industrial applications with antibacterial products as water hoses and flooring. .Particulary the photocatalytic degradation of PVC generates no dioxins and the decomposition process is easy to occur under natural environmental conditions.

I.7.2 Why the choice of CdS , MgO as nanoparticles ?

Cadmium sulfide (CdS) is a widely used semiconductor , which is therefore a promising UV light irradiation photocatalyst ,it can be improved obviously. However, these metals are rare and expensive to be applied.MgO is one of the most widely and efficient photocatalysts at present due to its excellent photoactivity, high oxidation potential, physical and chemical stability, nontoxicity, and earth abundancy. Also, Magnesium oxide nanoparticle is a light metal based antimicrobial nanoparticle that can be metabolized and fully resorbed in the body.Despite the great advances made in recent years, the development of the materials based on CdS and MgO is still going on. To this day, work is being carried out to find best modification strategies for optimizing the photochemical properties of CdS,MgO, and the goal is to decrease the band gap and increase the lifetime of photogenerated charge carriers (electron-hole pairs) in order to improve the catalytic activity. Hence, the combination of CdS ,MgO with conjugated polymers has attracted much attention to improving the photocatalytic performance of semiconductor photocatalysts and antibacterial activity.

Chapter II

Preparation and Characterization Techniques

II.1 Introduction :

In the advancement of science and technology, the discovery of novel materials those having varied characteristics and applications have central roles in all fields. Characterization is an important step in the development of exotic materials.They have strong bearing on the properties of materials. It gives information about the crystallinity, surface morphology, structure, nature of active sites, particle size and other characteristic features. This has led to the emergence of a variety of advanced techniques in the field of materials science. Different analytical and instrumental techniques used to acheive a complete characterization of samples are described with relevant principles of their operation and working.

This chapter presents a detailed description of used materials, formulation and procedure for the fabrication of nanocomposites.The nanoparticles prepared by hydrothermal, sol gel method, then all the thin film samples are deposited by spin coating method. This method is relatively cheap, simple and very attractive method for low-cost preparation of large area films. Moreover this technique can be used in good conditions. Description of characterization techniques used for evaluating the structure, morphology, and optical properties of nanocomposites was also included in this chapter.Now photocatalytic technique has emerged as one of the methods for purification of wastewater. A detailed introduction on the concept of photocatalysis,catalyst modification and its utility in the removal of pollutants from wastewater are focused in this chapter.

II.2 Materials used for synthesis

The chemicals were used in this study along with the manufacturers are listed below:

S.No	Name of the Chemicals	Chemical formula
1	Polyvinyl chloride (PVC)	$(C_2H_3Cl)n$
2	Cadmium nitrate	$Cd\ (NO_3)_2$
3	Thiourea	CH_4N_2S
4	Magnesium acetate deahydrate	$Mg(CH_3COO)_2.2H_2O$
5	Magnesium nitrate hexahydrate	$Mg(NO_3)_2{\cdot}6H_2O$
6	silver nitrate	$AgNO_3$
7	Citric acid monohydrate	$C_6H_8O_7{\cdot}H_2O$
8	Tetrahydrofuran (THF)	$(CH_2)_4O$
9	Absolute ethanol	CH_3CH_2OH

Table II**.1 :** list of chemicals.

II.3. Methods

II.3.1 Hydrothermal synthesis

Hydrothermal method is useful for the large scale production of nanosized and micro sized particles. In this method, the chemical precursors are dissolved in suitable solvent and placed in Teflon lined steel vessel also called autoclave. Materials are produced using closed system. Hydrothermal synthesis can be carried out at atmospheric pressures and temperatures from 80°C to 150°C in teflon lined containers or at elevated temperature (up to 550°C) and pressures 93(up to 175 MPa) in platinum or silver lined autoclaves[55] .The method is also particularly suitable for the growth of large good quality crystals with good control over their composition. The particle size and morphology can be tuned by changing the experimental condition like temperature, solvent, etc. The hydrothermal method uses the solubility of almost all inorganic substances in water at high temperature and high pressure, and then crystallizes the dissolved substances from the fluid.

High temperature water plays a vital role in processing the precursor material because the vapor pressure is much higher and the structure of high temperature water is different from that at room temperature. The properties of reagents, including their solubility and reactivity, will also

change at elevated temperatures. These changes provide more parameters to produce different high quality nanoparticles that cannot be obtained at low temperatures.During the synthesis of nanocrystals, parameters such as water pressures, temperature, reaction time, and respective precursor product system can be tuned to maintain high simultaneous nucleation rate, and good size distribution [56]. The components of autoclaves reactor 140 ml are given in Figure II.1.

Fig.II.1 : General-purpose autoclave popularly used for hydrothermal synthesis.

II.3.2 Sol – Gel Method

The sol-gel method allows good chemical homogenization of the cations and the possibility of creating metastable structures at generally lower temperatures than by other methods . In the sol-gel process, a sol (colloidal suspension) formed from metal oxide precursors by hydrolysis and condensation is converted into gel network structure. In fact, a chemical transformation occurs from liquid state to gel state and then converted into metal oxide systems. The sol formed can be converted into a gel and ultimately into different products depending on how the gel is treated. In addition, uniform fibers and powders can also be formed by spinning the soil or precipitated directly into the soil. Evaporation of the solvent from the gel causes a withdrawal accompanied by capillary forces and forms xerogels by collapse of the gel network. Further, when the gel is subjected to supercritical drying, the airgel is formed by

retaining the structure of the gel network. The aerogels appear to be in gel form with large pores[57,58]. The diagram of various sol-gel synthesis processes and their corresponding products is given in Figure II.2 .

Among numerous methods reported for the synthesis of nanomaterials, sol-gel method has got special attention because of the following reasons[56]:

- Different structures of the materials can be prepared using same precursors by slightly changing the experimental conditions
- Low cost and simplicity of the synthesis procedures
- Reliability and repeatability of the materials production because of the involvement of liquid phase synthesis chemistry
- Simple experimental set up and mild temperature conditions
- Precise control on doping is possible

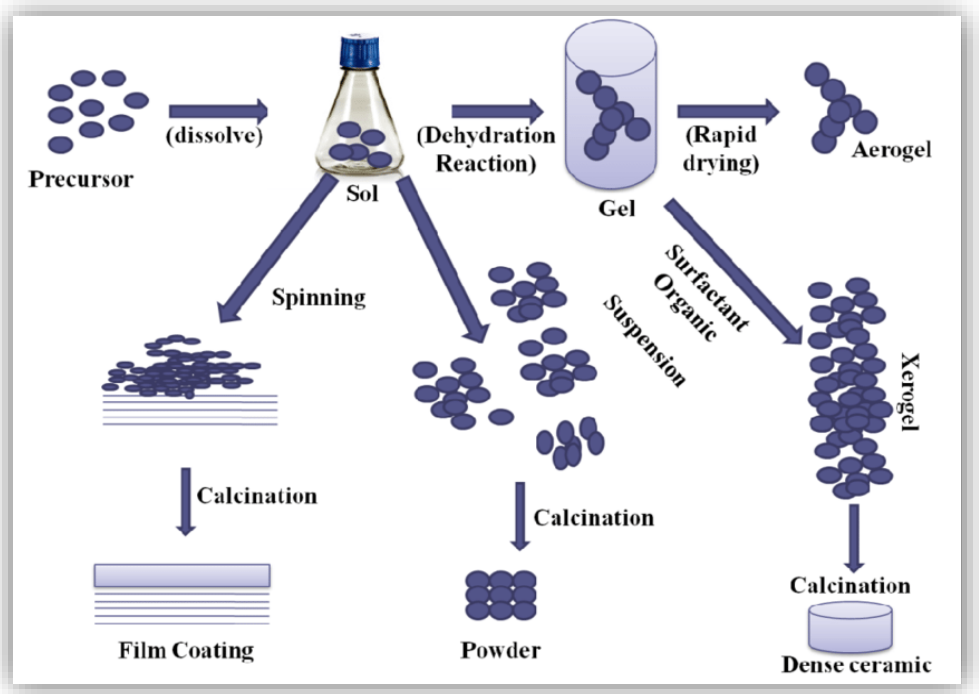

Fig. II.**2 :** Schematic representation of sol-gel process of synthesis of nanomaterials.

II.3.3 Spincoating Technique

Spin coating is a common method of producing uniform thin films of organic materials on flat substrates. This technique can also be used to fabricate organic electronic devices such as organic photovoltaics, organic light emitting diodes , and organic field effect transistors. The typical process consists of depositing a small slurry of fluid resin in the center of the substrate by a pipette, then rotating the substrate at high speed (typically around 3000 rpm). Due to the centripetal acceleration, most of the slurry will be thrown towards the edge of the substrate.

After evaporation of the liquid, a thin film will be left on the surface of the wafer. The rotational speed of the substrate is usually controlled to obtain a film with the desired thickness, as thin as nanometers.Spin coating involves the competition between various forces, such as centrifugal force, viscous force and solvent evaporation rate. The final film thickness and other properties will depend on the nature of the resin (viscosity, drying rate, percentage of solids, surface tension, etc.). One of the most important factors in spin coating is repeatability. Appropriate changes in the parameters that define the spinning process can result dramatic changes in the coating film.

A typical Spinco coating operation involves applying a liquid to the substrate and then accelerating the substrate to a certain speed **(as shown** in Fig. II.3) [59,60].

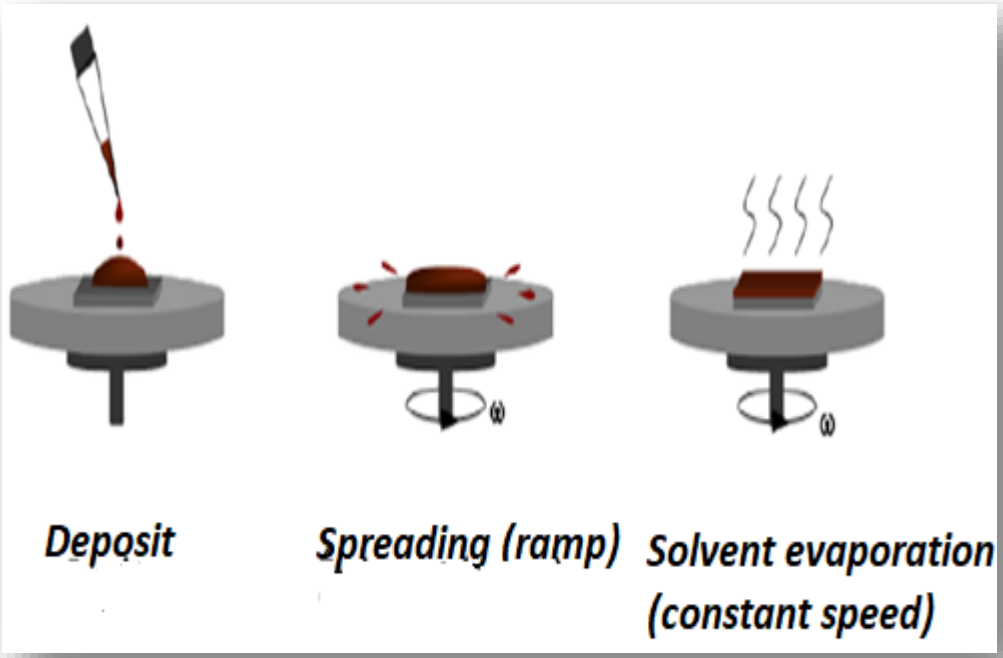

Fig. II.3: Process describing the formation of thin films by spin-coating .

The device is relatively simple, monocrystalline substrate, generally a semiconductor wafer, is placed and maintained by vacuum on a rotating plate at constant high speed, in order to spread the deposited material (in gel form) uniformly by centrifugal force. The speed, acceleration and duration of rotation are controlled by an electric programmer [61].

Fig. II.4: Part of the apparatus specifies the substrate.

II.4 Characterization Techniques

II.4.1 Structural analysis

II.4.1.1 X-ray Diffraction (XRD)

X-ray diffraction is a very important method that has long been used to determine the crystal structure of solids, including lattice constants and geometry, identification of unknown materials, order of monocrystals, defects etc.Diffraction analysis itmainly used for determining the particle size of the nanocrystals[62].A very simple interpretation of the diffraction pattern was given by W.L.Bragg.An X-ray diffraction pattern can be obtained by measuring the angles at which X-rays are diffracted by crystal planes. The Bragg equation describes the relationship between the distance between two planes (d) and the diffraction angle (2 θ) as follows:According to him, the spots were produced due to the reflection of some of the incident X-rays from the various sets of crystal planes, which contain a large number of atoms. Thus for diffraction to occur, Bragg's condition must be satisfied which is

given in equation (II.1). Bragg's equation relates the distance between two hkl planes (d) and the angle of diffraction (2θ) as[63]:

$$2d\ sin\ \theta = n\lambda \qquad \text{(II.1)}$$

Where, λ is the wavelength of of radiation used, n is an integer expressing the order of diffraction(h, k, l)represent Miller indices of the respective planes) , d the inter planar distance of diffracting crystal and θ- the angle of diffraction.

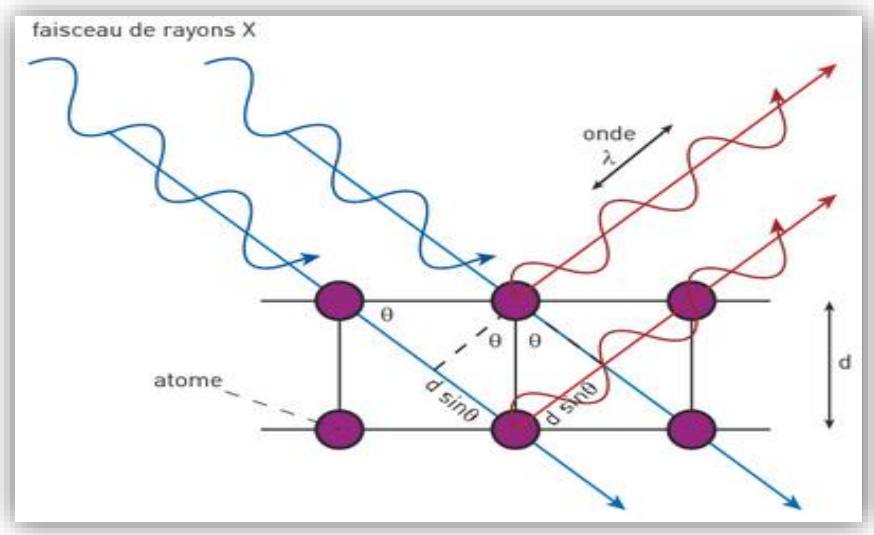

Fig.II.5 : Diagram representing the principale of X-ray diffraction by reticular index planes h, k and l.

The particle size can be estimated using the Debye-Scherrer equationWhen high energy particles falls on matter.When light falls on the crystals, it will be radiated in all directions from the lattice planes and occur constructive or destructive interferences over several ways.X-rays causes a vibration in electrons of materials through elastic or inelastic collisions. Elastic collisions generate coherent scattering (in phase with the incident X-rays) and inelastic collisions leads to Compton scattering of electromagnetic radiations from the vibrating charge of the electrons. The total scattering intensity is measured as the sum of the scattered intensities occurs from each electron. Convergent beam of X-rays always improve the sensitivity and resolution of the diffraction patterns when placing both source and detector at the circumference of same circle.

In Bragg's condition diffraction from one plane occur exactly one wavelength later from the previous plane results constructive interference. Therefore number of planes present in the

crystallites constitutes the width of the diffraction peak. The crystallites sizes are obtained by the Scherrer formula [64] :

$$t = Khkl\frac{\lambda}{\beta}\cos\theta_B \qquad \text{(II.2)}$$

where 't' is the thickness of the crystallite in Å, λ is the wavelength of incident rays, β is the full width at half maximum of the most intense peak in radians and θ is the Bragg's angle37Where, Khkl = is the scherrer's constant whose value depends on the shape of the particle and on the diffraction indices (hkl) .

XRD patterns of the different samples were recorded at ambient conditions using a BRUKER-AXS type D8 diffractometer with monochromatic Cu-Kα1 radiation (λ = 1.5405 Å), 2θ ranging from 10° to 80° in steps of 0.017°/s. The accelerating voltage was set at 40 kV and the current flux was 30 mA.

II.4.1.2 Fourier transform infrared spectroscopy (FTIR)

Infrared spectroscopy detects the vibration characteristics of chemical functional groups of molecules.This technique is useful for only those molecules that are having permanent dipole moment in them. Homo diatomic molecules such as H2, N2, O2cannot produce change in dipole moment

have zero dipole moment and do not detected by IR spectroscopy. When infrared light (400 - 4000 cm-1) interacts with matter, chemical bonds undergo changes in stretching, bending, rotation, twisting or rocking vibration modes. As a result chemical functional groups tend to exhibit changes in the specific wavenumber range. The intensity of IR radiations before and after interactions with materials is measured and the relative intensity is plotted against frequency in an FTIR spectrum [65].

A schematic of FTIR spectrometer is shown in in Figure **II.6**. Spectrometer consists of a source, which is a filament maintained at red or white-hot by passing electric current. Commonly used filaments are Nernst filament (spindle of rare earth oxide) or globar filament (rod of corborundum i. e. SiC).Beam splitter is an optically transparent material (Eg: KBr) coated plate so that it can reflect and transmit 50% of the light. The reflection from two mirrors recombined by beam splitter into a single beam and it is collected by the detector. The detected interferogram signal is interpreted by a mathematical Fourier transformation technique [66].

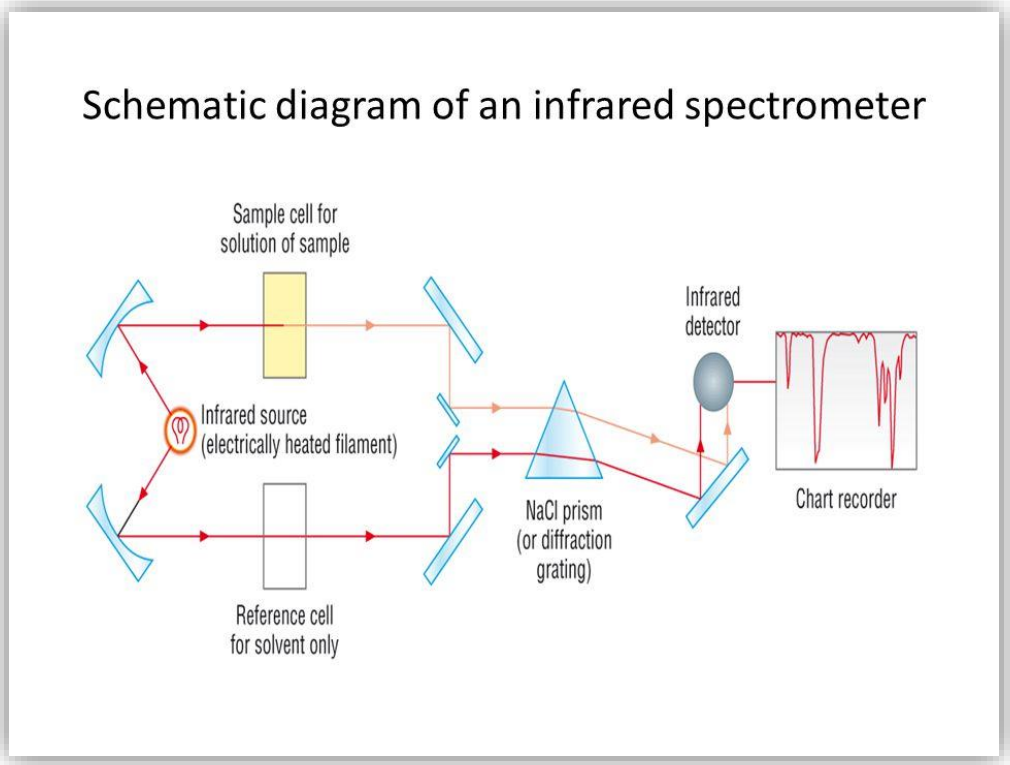

Fig.II.6: Schematic diagram of infrared spectrometer .

The following information obtained from FTIR making it a useful tool for the nanomaterials characterization:

- ✓ Information about : chemical bonding , molecular structure
- ✓ Identification of organic and inorganic nature of materials
- ✓ Information about the degradation of organic compounds

The characteristic vibrational motions of molecules are normally found in the region below 1500 cm^{-1}. In this finger print region, lower frequency bending vibrations are occurring. In 3700-2500 cm^{-1} region, hydrogen stretching vibrations have seen. The region 2500-2000 cm-1 is triple bond region since these bonds have large force constant. 2000-1600 cm^{-1} is the double bond region and 500-1700 cm^{-1} is the single bond stretching and bending region [67]. In the present study, JASCO 4600 FTIR spectrometer is used for the analysis of Infrared spectrum in the wavelength range 400 cm^{-1} – 4000 cm^{-1}.

II.4.1.3 Raman spectroscopy

Raman spectroscopy is based upon the inelastic scattering of monochromatic light within the studied sample, accompanied by the generation or annihilation of elementary excitations. In most experiments the elementary excitations are vibrations, particularly lattice vibrations (phonons). Ramanspectroscopy then provides access to the lattice dynamics of a sample and therewith delivers information on structural properties like chemical composition, orientation, or crystalline quality. In addition, electronic and magnetic properties can be addressed, e.g. by Raman resonance effects and Raman scattering from magnons, respectively. All this information is gathered by the analysis of the Raman signals with regard to their frequency position, frequency width, recorded intensity, and line shape in the Raman spectra. In a typical spectrum, the intensity is plotted versus the so-called Raman shift. The former is proportional to the number of photons of a certain frequency reaching the detector, whereas the Raman shift is given by the frequency difference between the scattered light and the monochromatic excitation source [68,69,70].

Figure **II.7** (a) presents instrumental set up in a Raman spectrometer. Raman spectroscopy analyses the frequency variations in the scattering of visible light radiations when passed through transparent materials. The scattered radiations have either same frequency as that of the incident frequency (Rayleigh scattering) or certain discrete frequencies vary from that of incident radiations (Raman scattering) 41. This altering in frequency corresponds to change in vibrational energy states of the molecules. The intensity of these lines are in the order Rayleigh scattering > Stokes lines > Anti-stokes lines (Figure **II.9** (b)). A Raman shift is observed in the range of 100-4000 cm-1due to the vibrational energy changes. If λ in is the incident wavelength of light and λR is the wavelength of Raman lines [71].

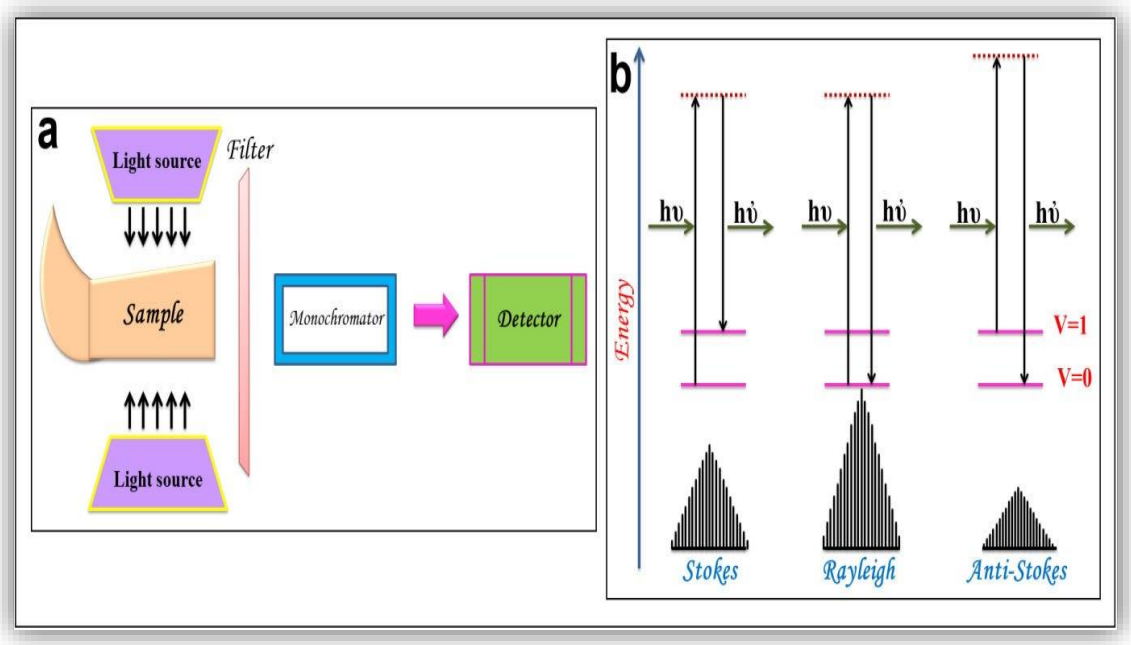

Fig.II.7 : (a) Raman spectroscopy instrumental set up and (b) Raman and Rayleigh scattering

The source used in Raman is coherent monochromatic LASER. To reduce the direct reflections from the source, horn shaped sample holder is used. The detector used is either a photomultiplier or a photographic plate. The importance of Raman spectroscopy is described below:

- ✓ Information of molecular vibrations which are inactive in IR
- ✓ Gives idea about the composition of the materials
- ✓ Detection of impurities
- ✓ Detection of surface bond vibrations
- ✓ Information about crystallinity

The Raman spectra of the samples at room temperature were obtained using a BRUKER Raman SENTERRA R200L System employing a He-Ne Laser (632.8 nm) as the excitation source in the frequency range of 100-800 cm^{-1}.

II.4.2 Optical analysis:

II.4.2.1 UV-Vis Absorption Spectroscopy

Optical absorption spectroscopy is one of the simplest techniques to determine the formation of nanoparticles. UV-Vis spectroscopy is the measurement of wavelength and intensity of absorption of near-ultraviolet and visible light by asample. When a material is exposed to light having an energy that matches the energy band gap of the material, some of the light energy will be absorbed as the electron is promoted from the valence band to the conduction band [72]. The absorption will be observed in the form of a peak, when plotted as a function of wavelength with respect to the intensity of the absorbed radiation. The peak position depends on the particle size. Sharp absorption band also gives the measure of monodispersity in particle size. In case of nanocrystals the bandgap is invariably higher than that of the bulk material. This is due to the fact that, as the size of material goes on decreasing the number of atoms present in the material reduces giving rise to discrete energy levels. Hence, there stands a correlation between the size of nanoparticles andincreasing energy gap, which is reflected in the absorption spectra. The absorption peak shifts towards higher energy with decreasing size of the particle. UV-Vis spectroscopy therefore proves to be one of the important and simplest ways to confirm the formation of nanoparticles. The change in the absorption peak position with respect to bulk gives a clear evidence of nanoparticles formation. Thus, from the absorbance data one can determine the energy bands of the material and the impurity levels within the material. In case of semiconductor or oxide nanoparticles absorption in the UV to visible range can occur with characteristic absorption edge. Thus, from the absorbance data one can determine the energy bands of the material and the impurity levels within the material. The absorbance is directly proportional to the path length and concentration of the absorbing species; the relation is expressed in the form of Beer's Law as [73]:

$$A = \log \frac{I}{I_0} = \alpha\ b\ c \qquad \text{(II.3)}$$

Where, A is the absorption coefficient, α is the molar absorptivity, cconcentration of absorbing species in mole/lit and b is the path length in centimeters (length of the cuvette).

In the present research work, UV-3101 PC-Shimadzu double-beam spectrophotometerin the scan range 190 nm - 800 nm was used to obtain UV spectrum.

II.4.2.2 Photoluminescence spectroscopy (PL)

Photoluminescence (PL) spectroscopy is a non-destructive method used to find the electronic structure of materials. It is also used to find the energy gap;

impurity level and to study the recombination mechanisms. PL is known as a quantum mechanical process in which a photon is absorbed into a material by transferring its energy to an electron in the ground state and exciting it to an excited state within femtosecond timescale[74].

A schematic of a PL system layout is shown in Figure 2.6. Four basic components make up a PL system. A source of radiation, a primary filter or excitation monochromator, secondary filter or emission monochromator and optical detector with appropriate electronics and readout. High-pressure dc Xe arc lamp which emits an intense and relatively stable continuum from 300 nm to 1100nm. Excitation monochromator (primary filter) in the excitation path, which selects the specific wavelengths and transmits them to the sample to be analyzed.The resultant luminescence is isolated by emission monochromator (secondary filter) and then recorded by a detector. Generally, Photomultiplier tube which provides good sensitivity for wavelengths in the visible range is used to detect the resultant luminescence. We have carried out PL studies using a PerkinElmer LS 55 Luminescence spectrometer [75].

In the present work, Perkin-Elmer LS 50B spectrophotometer using He-Cd laser (λ = 325 nm) is used.

II.4.3 Morphological analysis

II.4.3.1 Scanning electron microscopy (SEM)

Scanning Electron Microscope (SEM) is commonly used to study the surfaces, structures, morphologies and forms of materials. SEM can be efficiently used to study the surface structure of the polymer nanocomposites and to view the dispersion of nanoparticles in the bulk matrix . The images are viewed using SEM that are created by detecting secondary electrons ejected from samples as they are bombarded by focusing, high energy electron beams. Unlike optical microscopy, one does not look through the lenses at the actual sample, but one observes the IMAGE of the sample created by the instrument's electronic.SEM can achieve higher magnifications than optical microscopes. When samples are probed with a focused electron beams, a variety of signals can be collected and displayed on the view screen.X-rays characteristic of the elemental composition of the sample can be mapped to sample images and backscattered electrons can also be collected and displayed. When SEM is fitted with

appropriate detectors, one cannot see the images of samples (using secondary and backscattered electron signals), but one can see the images which map the elemental compositions of the samples. SEM analysis was conducted in vacuum environments. Surface morphology and size distribution of particles were examined by scanning electron microscopic images [76,77].

In an electron microscope electrons emitted from a hot filament are usually used. However, sometimes cold cathode (a cathode which emits electrons without heating it) is also used. A narrow beam of electrons is accelerated form the cathode C and is allowed to pass through electro-magnetic lenses. Due to the lenses the beam is converged to a very small diameter. The diameter of the beam at the sample surface can be as small as 10 nm or less. Electrons leaving from the sample (mainly secondary electrons) are given to an amplifier A through a collector plate P. The output of the amplifier determines the potential of the modulating electrode G of the cathode ray tube. Thus the brightness of the spot on the screen is governed by flux of the electrons reaching the plate P. Current from the saw – tooth generator is passed through coils D1 and D2, which cause the initial electron beam and the spot on the screen of the cathode ray tube to deflect. Two such coils are used to produce the deflections in right angles to each other. Thus the electron beam focused on the sample and resulting spot on the screen perform rectangular zigzag roasters in synchronism. As the electron beam scans the surface of the sample, changes in the composition, texture or topography in the sample surface where beam strikes makes the variation in the current collected by the collector. It further changes the brightness in the spot on the screen of the cathode ray tube. Thus one can obtain the image, which is in resemblance with that of the sample [78,79]. By choosing proper parameters for the deflectors, it is possible to have dimensions of the raster scanned on the surface very small than that in the cathode ray tube. Thus one can achieve the image, which is a magnified view of the sample surface.

Morphology of the nanocomposites samples were observed using scanning electron microscope (SEM Tescan Vega3 (JEOL, Japan). (**Fig.II.8**)

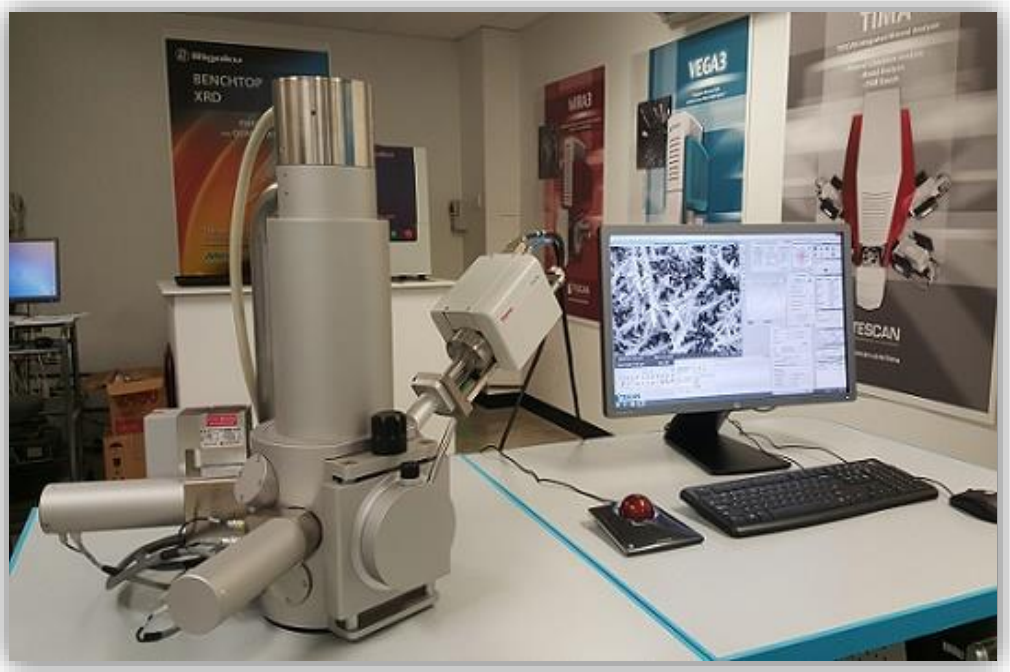

Fig.II.8:The complet SEM.

II.4.3.2 AFM Analysis

Atomic force microscopy (AFM) is an influential surface analysis technique used for micronanostructured coatings. AFM used to study the dispersion of nanofillers in the polymer matrix without any limitation regarding sample preparation. It is used in imaging surface topography on nanoscale. Atomic force microscopes give direct 3-D measurements of the surface structure of the materials[80].

FigureII.13 shows the schematic diagram of Atomic Force Microscope. The main components of atomic force microscope are cantilever with a sharp tip (probes), optical detection system, piezo-scanners andelectronics for a management of scanning procedures and data acquisition. When the tip of the needle is close to the surface of the sample, the force between the tip of the needle and the sample will deflect the cantilever according to Hooke's law. Depending on the situation, the force measured in AFM includes mechanical contact force, van der Waals force, capillary force, chemical bond, electrostatic force, magnetic force. In addition to measuring force, you can also measure more quantities at the same time using a special type of probe.

Typically, a laser spot reflected from the top surface of the cantilever into the photodiode array is used to measure the deflection [81].
A very high resolution surface images, with dimensions on the nanometer scale are obtained. The sensitivity and resolution of the acquired image depends on the properties and dimensions of the cantilever and tip, as well as selected mode of application [82].

There are two main operation modes in AFM: contact mode and tapping or inter-mittent contact mode.

- **Contact mode :**the probe comes into a permanent contact with a sample surface. A product of thecantilever stiffness on its deflection determines the tip-sample force. Imaging with high-resolution was demonstrated with the contact mode AFM on many crystalline surfaces . Besides surface imaging, AFM in its force modulation mode has been effectively usedfor evaluation of sample mechanical properties by modulating the tip-force with anadditional actuator. Lateral tip-sample forces accompany scanning of surfaces with the tip being in contact, and these forces can be recorded for evaluation of surface friction. This limits the contact mode applicability to studies of polymers and biological objects. A drop of the cantilever amplitude when the tip comes into interactionwith a sample is used as a measure of these interactions, and the amplitude drop iskept at a pre-set level during scanning.

- **Tapping mode :** permanent shearing forcesare almost eliminated and the intermittent tip contact with the sample surface occursat a high frequency that also restrict material damage.Such operation is gentler than the contact mode, despite the fact that stiffer probesare used in tapping mode.

Advantage of AFM is that topographic images along with their surface measurement can be obtained without any surface treatment or coating which may damage the surface of the sample [83].

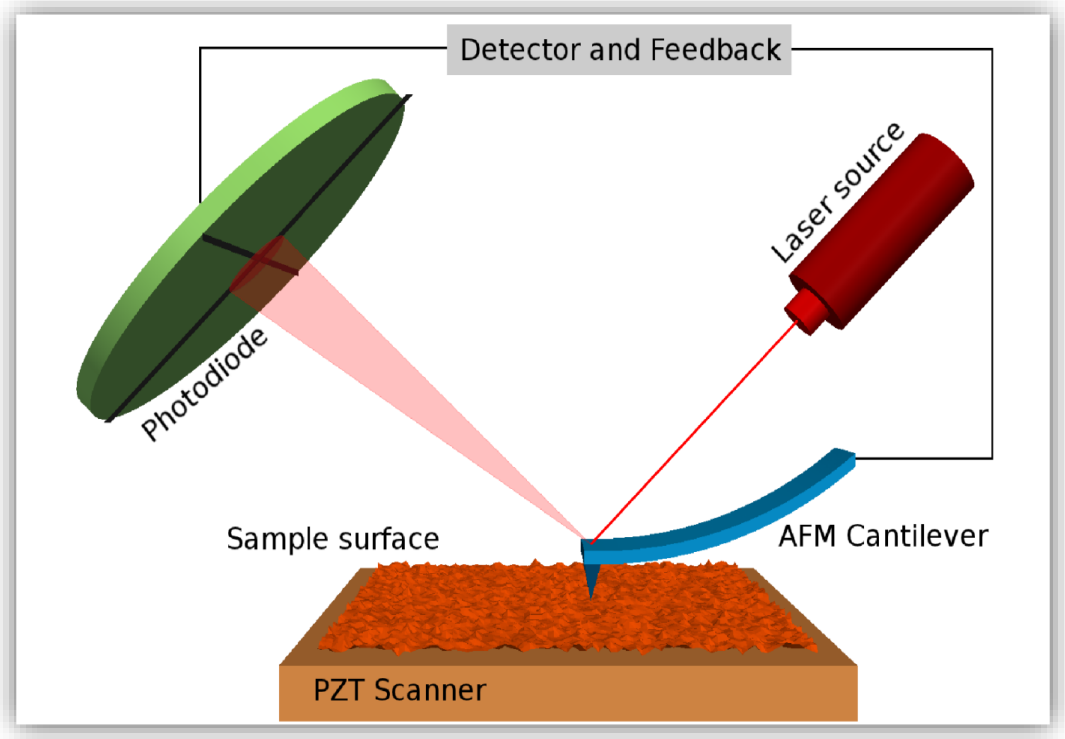

Fig.II.9 : Schematic diagram of Atomic Force Microscope.

II.5 Photocatalytic Processes

Recently, personal care and drugs used in pharmaceuticals, cosmetics, agricultural practices, and veterinarians have been identified as emerging pollutants. The presence of pollutants at low concentration in wastewater streams greatly affects the properties of water, making oxidation or biodegradation difficult. Compared with conventional methods, the photocatalytic process of photodegradation of pollutants in wastewater and water systems has become an efficient method, while traditional methods do not consume much energy and do not form highly toxic products and biodegradable [84,85].Basically, the efficiency of the photocatalysis process depends on the morphology, dimension, or shape of the investigated semiconductor oxides. Therefore, an excellent control and understanding of synthesis conditions are critical for the development of novel and high-performance photocatalysts characterized by efficient separation of charge carriers, increased surface-to-volume ratio, and

light absorption capacity with superior stability/reusability features. Therefore, the incorporation and immobilization of CdS ,MgO nanostructured materials into PVC polymer could represent a strategic approach to benefit from advantages of each component, in order to obtain improved photocatalytic systems.

The significant features targeted are the flexibility of the final architecture, the control over agglomeration/aggregation and the elimination of the post-recovery steps specific to unbounded catalyst particles after the photocatalytic process [86].

The process of photocatalysis uses semiconductors such as metal oxides, nitrides and sulfides. Generally, metal oxides are photoactivated by incident photons from a light source. As a renewable, safe, abundant and clean source of energy, natural sunlight has always been an ideal source of energy for the activation process [97]. When the photo-generated electrons are transferred from the filled valence band (VB) of the metal oxide to the empty conduction band (CB), the photocatalytic reaction begins, leaving positive holes (h^+VB) in the VB. Then, the photogenerated electrons migrate to the surface of the metal oxide, where separation and oxidation-reduction reactions take place. While the reduction and oxidation processes are thermodynamically feasible, they can only occur on the surface of metal oxides excited by light. Then, the photo-induced holes in BV react with the adsorbed water molecules to generate OH radicals. These •OH radicals are having strong oxidative decomposing power and react with organic pollutants and decompose them at the surface and in solution as well into CO2, H2O etc.

On the other hand, if they migrate to the surface of the semiconductor without recombination, they can involve in various oxidation and reduction reactions with adsorbed species on semiconductor surface such as water, oxygen, and organic pollutants. These oxidation and reduction reactions are the fundamental requirements for the photocatalytic reaction. A general mechanism of photocatalytic reaction on a semiconductor is presented in Fig**II.15**.

The incorporation of semi conductor into a polymeric materialwith appropriate energy levels enhances the charge migration between the inorganic semi conductor and polymer to reduce the recombination of the charge carriers [87]. Polymeric nanocomposites are currentlybeen applied in water treatment due to their pore size distribution, perfect mechanical rigidity,tunable, and large surface area [88].

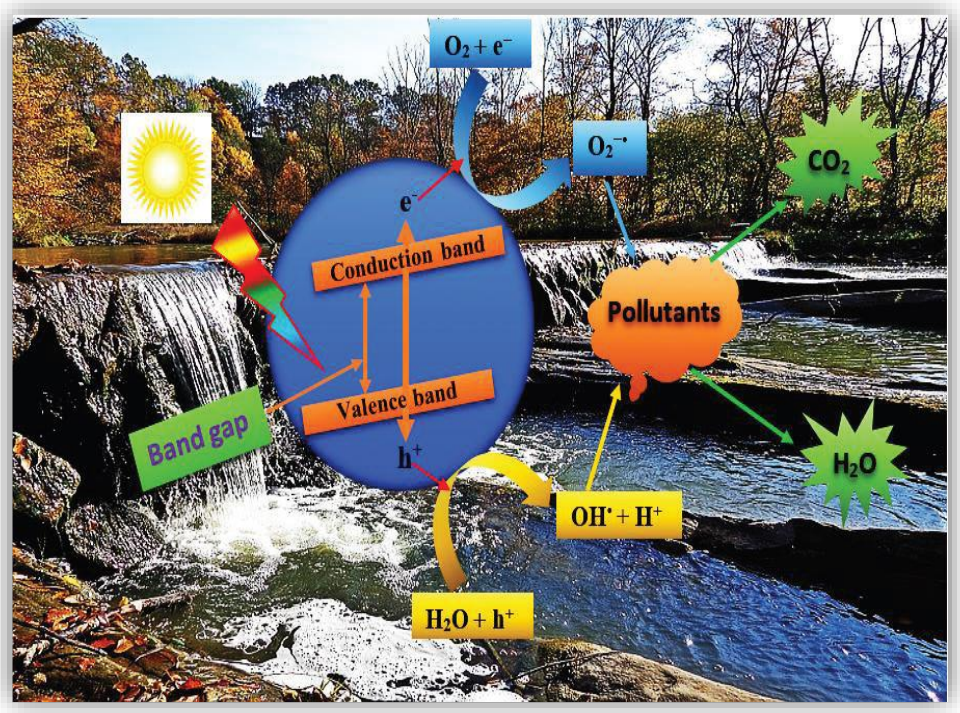

Fig.II.16 : Schematic of photocatalysis process toward the photodegradation of pollutants.

Chapter III

Synthesis and characterization of CdS/PVC nanocomposites

III.1 Introduction

Recently, much attention has been devoted to studies regarding composite polmer-inorganic nanoparticles. The interest in these materials rose due to their biological, optical, electronic and magnetic applications. These potential applications are due to their excellent luminescent and electrical properties [89]. Out of these materials Cadmium Sulfide (CdS) nanocomposites has been focus of interest because it is good photosensitive material with potential application in photo-conducting cells and devices, that makes it important material for the application of solar cells , photo-detectors and biological labeling [90]. Reports have reflected that the devices that contain polymer type nanocomposites of inorganic-organic material can be easily processed to produce new properties materials that are better than single segment polymers [91].Polymer like PVC has attainted tremendous attention in many auspects of life, so it is considered as versatile, beneficial and economical commodity polymers. PVC can be used for indoor construction purposes like sash windows and door shutters due to its easy modification and low cost. PVC can also be used in flooring and water hoses. Besides that PVC can be utilized for different Industrial applications and Anti bacterial properties [92]. Photocatalysis is very important and innovative technique to get rid of hazardous pollutants and also it has been a safe tool for determining the photocatalytic efficiency of different semiconductors [93]. The research has revealed that CdS is efficient UV light irradiation catalyst for photocatalysis[94]. A lot of research has been devoted on embedding photocatalysts in the photodegradable PVC for decomposition of plastics. The interest in PVC arrises due to its easy decomposition and not generating dioxins under natural conditions[95]. Eventually the embedding CdS in the conjugated polymer has been focus of interest for the improvement and performance of photocatalysis[96]. we report a comprehensive study of the effect of dopage of CdS on the PVC of the prepared nanocomposites films synthesized via a Sol-gel procedure. We studied the structural, morphological, optical, photoluminescence properties of PVC/CdS and its application in photocatalytic activity. For the study of the photocatalytic performance, degradation of MB was performed under UV light irradiation.

In this chapter, cadmium sulfide nanoparticles (CdS) embedded in the polymeric polyvinylchloride (PVC) matrixhave been sucessfully preparedvia sol-gel method with deposition by Spin-coating on glass substrates. PVC/CdS nanocomposite films were also

characterised with XRD, FTIR, PL spectroscopy ,UVetc and its application in photocatalytic activity. For the study of the photocatalytic performance, degradation of MB was performed under UV light irradiation.

III.2 Experimental

III.2.1 Synthesis of CdS Nanoparticles

CdS nanoparticles were synthesis via hydrothermal reaction of cadmium nitrate (Cd $(NO_3)_2$) and thioureadissolved in water for 1h. After, the mixture was stirred into the Teflon lined autoclave at 180° C. Then, the obtained products were washed with DI water and ethanol. Finally, the CdS powder were formed by several times and dried at 80°C for 12h.

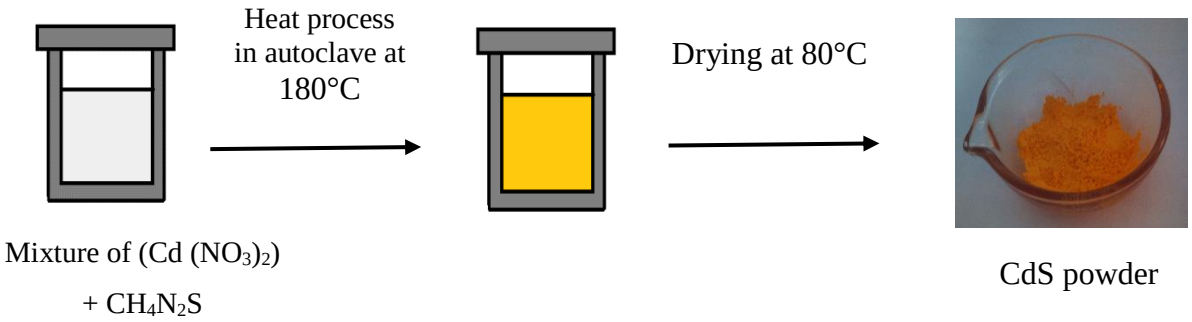

Fig III.1: Hydrothermal synthesis of CdS nanoparticules.

III.2.2 Preparation of Polymer Nanocomposites

About 1 g of powder PVC was dissolved in 30 mL of the solvent of Tetrahydrofurane THF. A measured amount of cadmium sulfide was dissolved in 10 mL of THF and added into the polymer solution under continuous stirring for 1 h. The solution was then left to rest; the heaviest particles got deposited under at the bottom of the container. The upper part of this solution, containing the crystallites of smaller sizes, was recovered for the deposition of PVC/CdS thin film on the glass. Two-step preliminary to the deposition of PVC/CdS nanocomposites films, were the cleaning of substrates and the choice of the deposit technique. The deposition technique used for the preparation of composite films, is the technique of centrifugation (spin-coating). PVC/CdS nanocomposite was deposited onto glass substrates, before deposition the glass was cleaned for 10 min approximately with acetone, methanol then double distilled water to eliminate the traces, greases, and impurities onto the glass surface to

ameliorate the film adhesion. After that the film was dried to remove moisture. The drying operation was carried out by dry the films to a temperature close to its glass transition temperature (10 minutes at 60 ° C). This operation allows evaporation of total traces of solvent still present in the polyvinyl chloride.

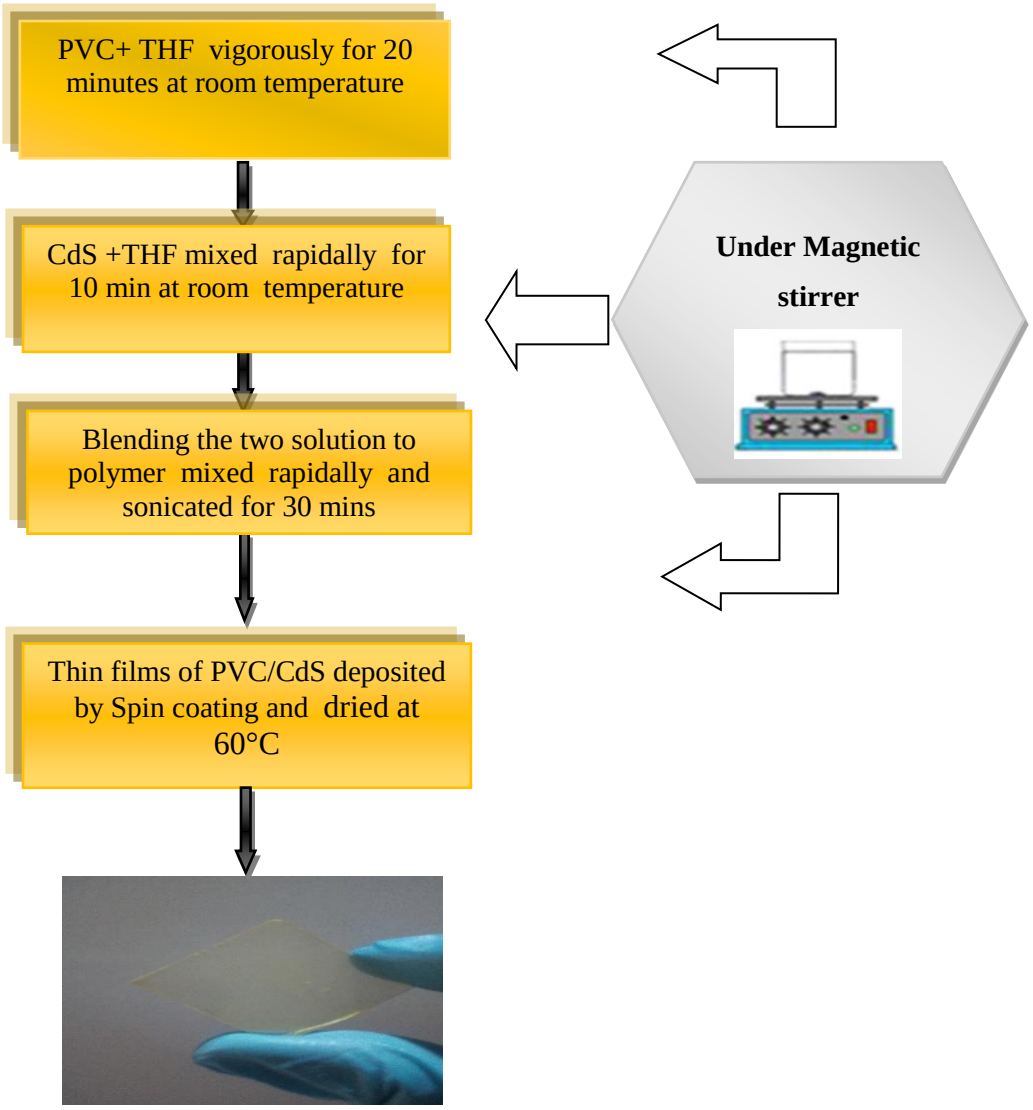

One of the obtained samples

Fig III.2: Synthesis of CdS/PVC nanocomposites.

III. 2.3 Photocatalytic procedure

The obtained materials were studied for their photocatalytic properties. Methylene blue ($C_{16}H_{18}ClN_3S$, $Co = 1 \times 10^{-5}$ mol L^{-1}) which is a standard dye commonly used in the photocatalytic studies was used. The tests were carried out in a glass reactor under ultra violet radiation.

The reactor with the test sample was set on a table with a magnetic stirrer in order to ensure the same distribution of the catalyst in the entire volume of the system. The solution was mixed with the test sample without access to light for 30 min to determine dye adsorption on the photocatalyst surface. Then the UV light was on.

The photodegradation of MB dye with UV light source (VL -215.LC,15W), the maximum emission is at 365 nm was used to evaluate the visible light photocatalytic activity of the PVC/CdS nanocomposites and pure PVC.A cylindrical glass vessel containing an aqueous MB solution (175ml) with an initial concentration of 10^{-5}mg/ml. Then, the thin films PVC/CdS nanocomposites of 5/2.5 cm on the side was posed into the petri dish, which contains the MB solutions (10ml). After that, the system was subjected to visible light emitted by a 300 W iodine tungsten lamp (Philips Co). The distance between the surface of the suspension and the light source was about 20 cm. During irradiation, the samples were taken out every 30 min from the reactor. The clarified solution was analyzed by a 723 UV–Vis spectrometer (UV-1800 Shimadzu LC 2010-HT).

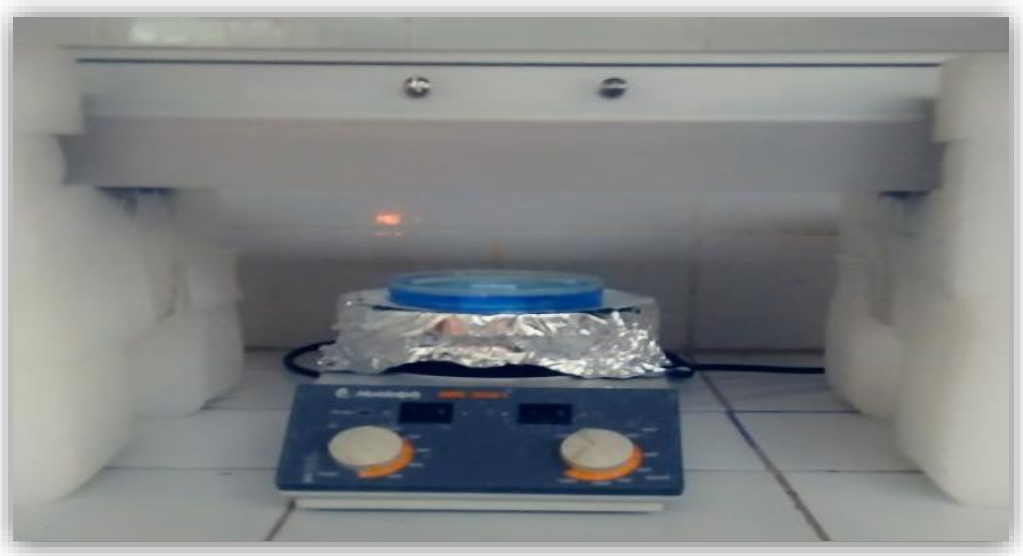

Fig III.3: Photo of the photocatalytic test under UV light source.

III.3. Results and discussion

III.3.1 Structural study

III.3.1.1 X-ray diffraction (XRD) analysis

Fig. III.4 shows the XRD patterns of PVC and PVC/CdS thin films. From the X-ray diffraction spectra, the pure PVC shows an amorphous structure. However, with the addition of CdS nanoparticles into the PVC matrix, the crystalline nature of the nanocomposite has been obtained. The pattern exhibits prominent broad peak centered at 24.83°; 26.50° and 28.20° corresponding to the hexagonal phase of CdS with diffraction planes (100), (002) and (101) respectivelywith JCPDS(N°) data, with preferential orientation along the (002) plane. From these results, it can be concluded that CdS crystallites are incorporated in the polymer matrix. Additionally, it can be seen that the diffraction peaks are considerably broad indicating the fine size of NPs. This broadening may be due to the inhomogeneous strain present in the films [97].

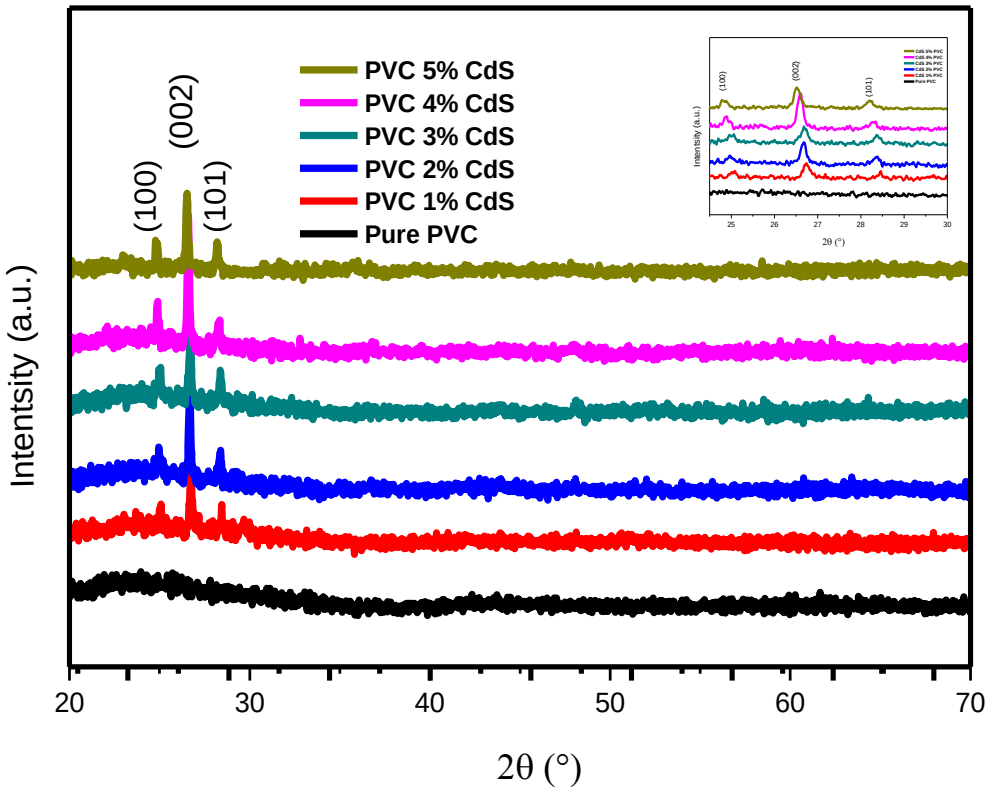

Fig III.4:X-ray diffraction patterns of pure PVC and PVC/CdS nanocomposites thin films.

III.3.1.2 The grains size

The crystallite size has been calculated by using Debye Scherrer's formula [98], and the computed values are reported in Table 1:

$$D = (0.9\lambda)/(\beta cos\,(\theta)) \qquad \text{(III. 1)}$$

Where β is the full width at half maxima (FWHM) of the peaks, θ is the diffraction angle, λ is the X-ray wavelength (1.5405 Å).

When CdS solution of different loading (1-5%) was added, there was change in size of CdS nanoparticles. We believe high loading (5%) of CdS has strong interaction with PVC than low loading (1%). That is why the particle size changes from 56.91-59.14 nm of the high intensity peak at $2\theta = 26.50°$ (002) (**tableIII.1)**.

TableIII. 1 : Structural parameters of PVC/CdS nanocomposites thin films.

Samples	2θ(°)	β(°)	D (nm)
PVC 1% CdS	26,73	0,14	56,91
PVC 2% CdS	24,97	0,47	
	26,68	0,12	69,14
	28,34	0,24	
PVC 3% CdS	25,01	0,24	
	26,67	0,14	59,26
	28,37	0,24	
PVC 4% CdS	24,91	0,16	
	26,61	0,14	59,25
	28,26	0,24	
PVC 5% CdS	24,84	0,16	
	26,49	0,12	69,11
	28,20	0,16	

III.3.1.2 Fourier transform infrared analysis

Fig III.5 displays the Transmission Infrared spectra (FTIR) of the PVC pure and PVC/CdS nanocomposite films with different loading (1-5%) of CdS over the range 4000- 400 cm^{-1}.There are four main peak regions in their FTIR spectra: 760, 905, 1423 and 1560 cm^{-1} [99].Two broad peak centered at 760 and 905 cm^{-1} was observed for all thin films and is assigned to C-Cl and C-C stretching PVC vibration bands, respectively.The intensity of these bands are found to be lower as the CdS content increases in the films[100] .

The small and weak peaks around at ~1423 and 1560cm^{-1} are due to the C-H and C=C stretch in PVC [101,102].

It is confirmed from FTIR that the absorption bands of PVC surface gradually decrease in intensity with increasing CdS nanoparticle content.

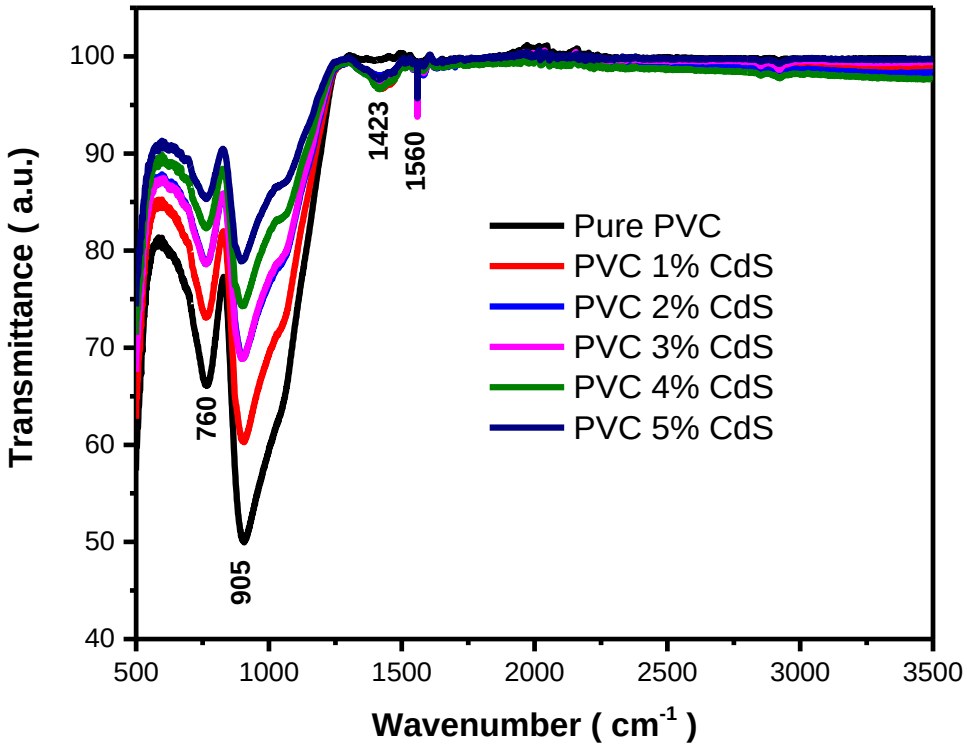

Fig III.5:FTIR spectra of Pure PVC and PVC/CdS nanocomposites thin films.

III.3.1.3Raman spectroscopy analysis

The Raman spectra of pure PVC and PVC/CdS nanocomposites are showing in fig **III.6**. The spectrum of pure PVC display a strong peak at 1597cm^{-1} ascribed to C=C bonds stretching vibrations, and peak at 1351 cm^{-1}, which corresponds to C− H bonds bending vibrations [103,104]. Additionally, the Raman spectrum of PVC/CdS nanocomposites display two peaks of CdShexagonal phase at around 354 cm^{-1} and 630 cm^{-1} corresponds to 1 LO and 2 LO, respectively, and other peaks at about 680 cm^{-1}, 1090 cm^{-1}, and 1317 cm^{-1} assigned respectively to C-Cl, C-C, and C-H stretching vibrations of PVC [105]. The Raman analysis affirmed that our thin films comprised of PVC and CdS elements. Thus, we conclude that the analysis of Raman and XRD are in agreement.

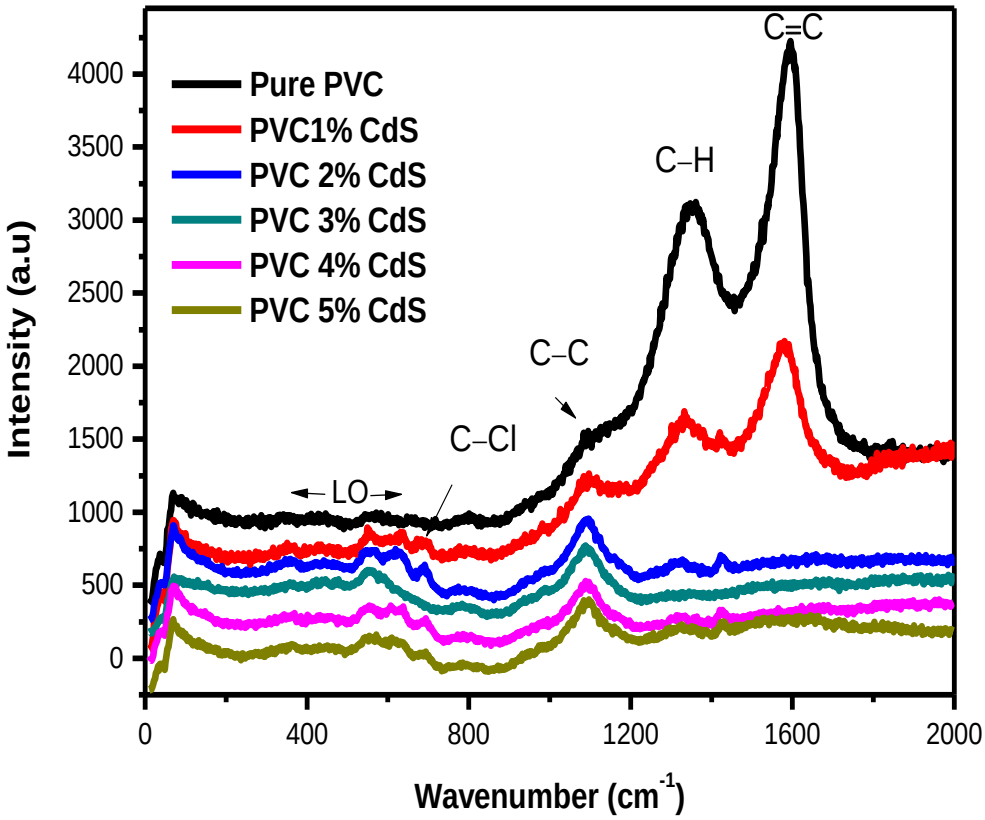

Fig III.6: Raman spectra of Pure PVC and PVC/CdS nanocomposites thin films.

III.3.2 Morphological study

III.3.2.1 Scanning electron microscopy (SEM) analysis

SEM is an efficient and versatile instrument to analyse themicrostructure and surface morphology of polymer nanocomposites.

The morphology of PVC/CdS thin films were investigated using SEM. It is important to declare that the SEM image of PVC film has not performed because of its low electrical conductivity that induces the charging effect. Figure 3(a)-(d) shown some typical PVC/CdS SEM images. As for the PVC/CdS nanocomposites, a large number of nanocrystals of CdS on the surface could be seen clearly (Fig.III.7), which led to the surface of the particles becoming rough. In PVC 3% CdS, the particles of CdS are agglomerated and have almost uniformdispersion in the PVC matrix .The agglomeration increases with the increase of CdS nanoparticles. It is maximum for 5 % CdS nanoparticles in PVC. It is found that at higher CdSconcentration,the density of particles is increase, as well as tiny clusters in spherical shapes are linked together in some rich areas in CdS within the polymers .On the other side, when the CdS lower concentration, some CdS nanoparticles are loosely distributed but some aggregated clusters of varying size can also be found.

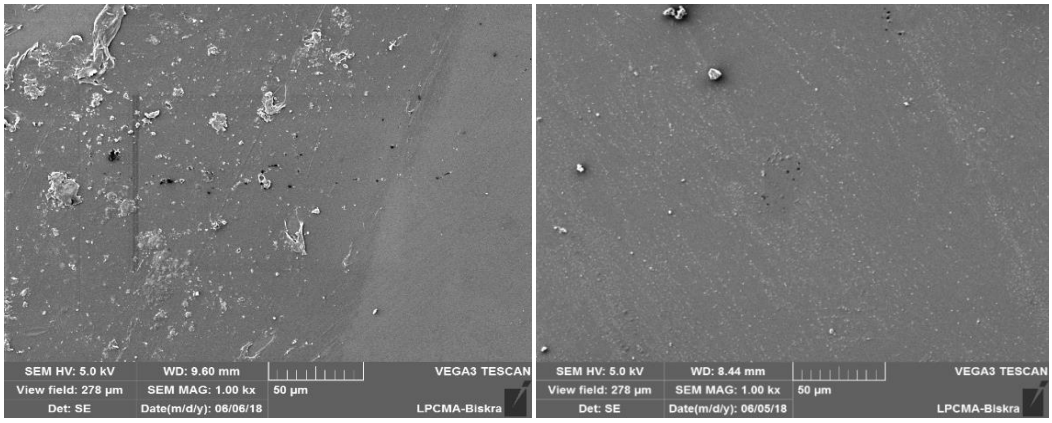

(a) **(b)**

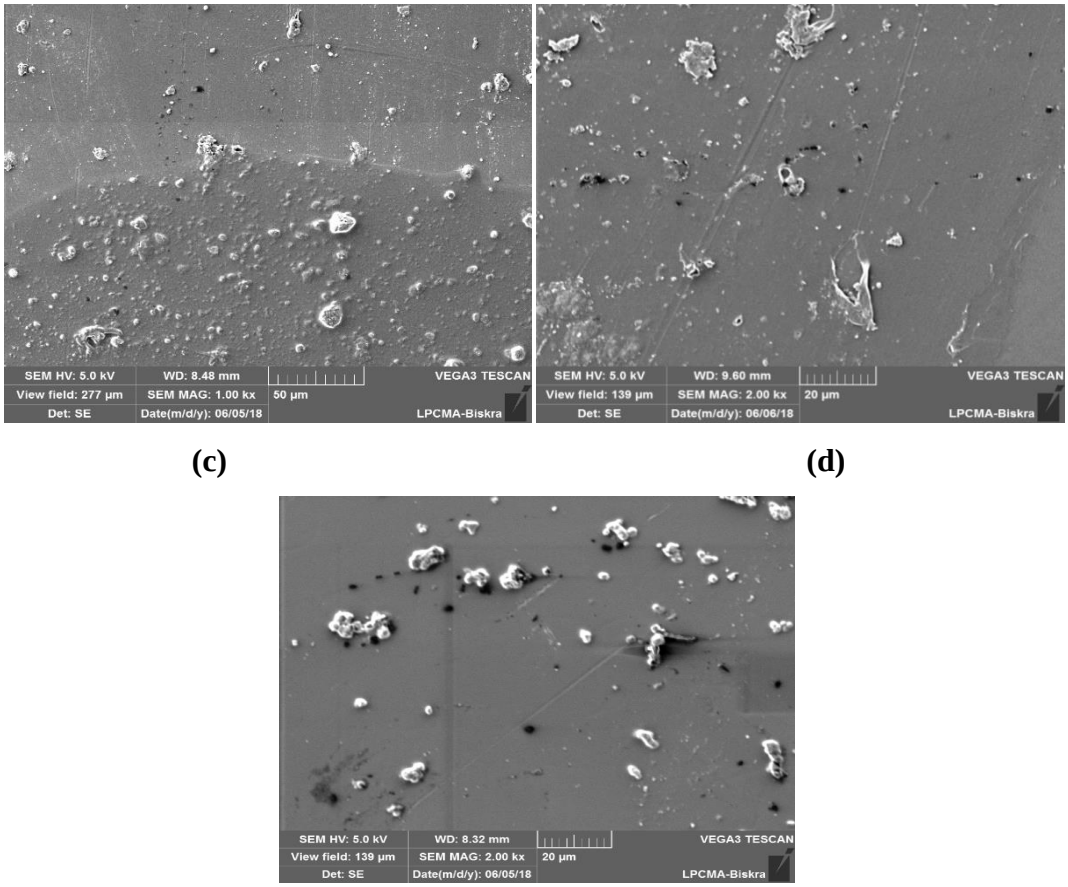

(c) **(d)**

(e)

Fig III.7:SEM images of PVC thin films as a function of CdSnanoparticles content (a)PVC 1% CdS ; (b) PVC 2% CdS ; (c) PVC 3% CdS ; (d) PVC 4% CdS ; (e) PVC5% CdS .

Figure **III.8** displays SEM image of PVC 5% CdS with different scale (10 µm, 1 µm and 100 nm), it is noted that the CdS nanoparticles fill certain pores on the surface of the PVC**.**We observe that the size of CdS is mostly nanometric.It is also observed from the SEM microstructure of PVC/CdS that the polymer nanocomposite has numerous almost spherically shaped rings with a limited number of pores of small size.

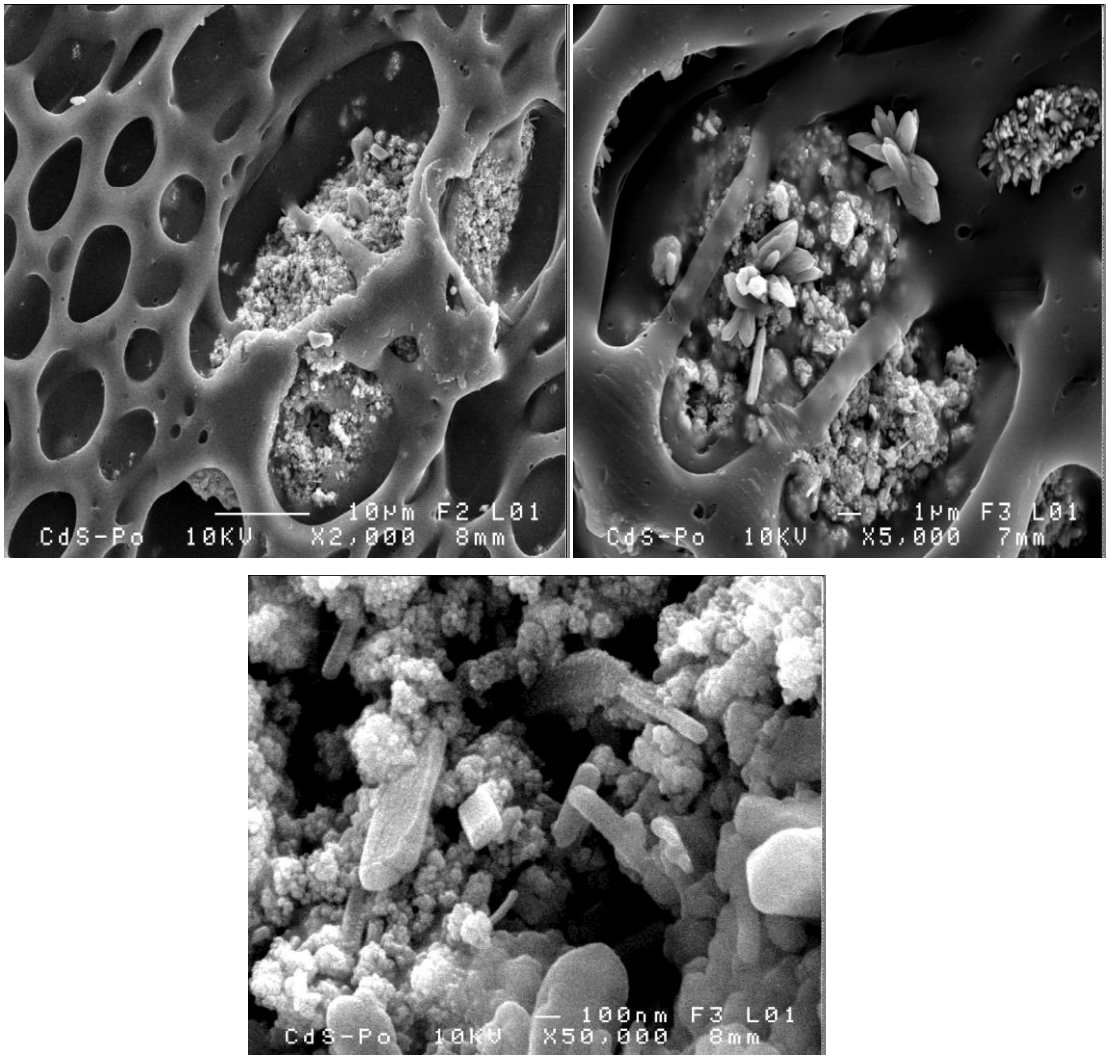

Fig III.8:SEM image of PVC 5% CdS thin film.

III.3.3 Optical study

III.3.3.1 UV–Vis analysis

We were using the UV–vis spectra to indicate how the films are transparent in the visible region and to calculate their thickness using the envelope method [106], band gap energy and disorder. The UV–vis spectra of the PVC/CdS nanocomposite films were shown in Fig **III.9**.In the range 200 nm to 800 nm, the pure PVC is fully transparent and has a steep absorption edge at 300 nm.

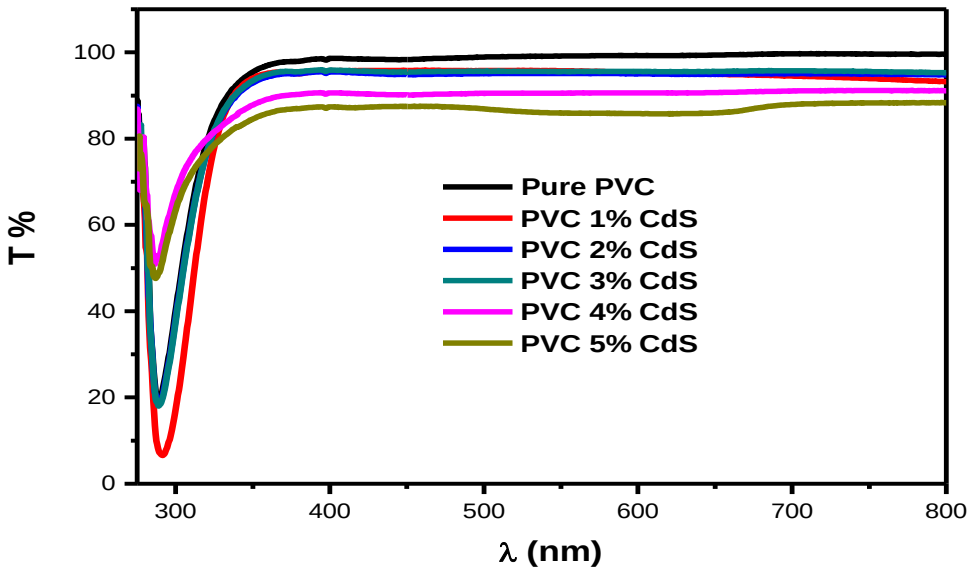

Fig III.9: Optical transmission spectra in the UV–Visible region of Pure PVC andPVC/CdS nanocomposites thin films.

III.3.3.2 Optical Gap

The optical band gap of PVC/CdS nanocomposites has been determined by plotting $(\alpha h\nu)^2$ as a function of the incident energy ($h\upsilon$) which are linear over a wide range of photon energies indicating the direct type of transitions. The intercepts of these plots (straight lines) on the energy axis give the energy bandgap [107], Fig **III.10:**.The estimated values of Eg listed in Table 2, was obtained by the extrapolation of the straight line to $\alpha = 0$. As CdS content increases, the Eg value decreases from 4.07 to 3.85 eV.These band gap value differences of PVC/CdS nanocomposite reflecting the presence of CdS crystallites in the PVC matrix and confirm the results obtained previously.

Table III.2: Thicknesses and gap energy (Eg) of PVC/CdS nanocomposites thin films.

Samples	Thicknesses (nm)	E_g (eV)
Pure PVC	260	4.07
PVC 1% CdS	260	4.04

PVC 2% CdS	225.09	4.02
PVC 3% CdS	233	4.00
PVC 4% CdS	221.34	3.92
PVC 5% CdS	239.52	3.85

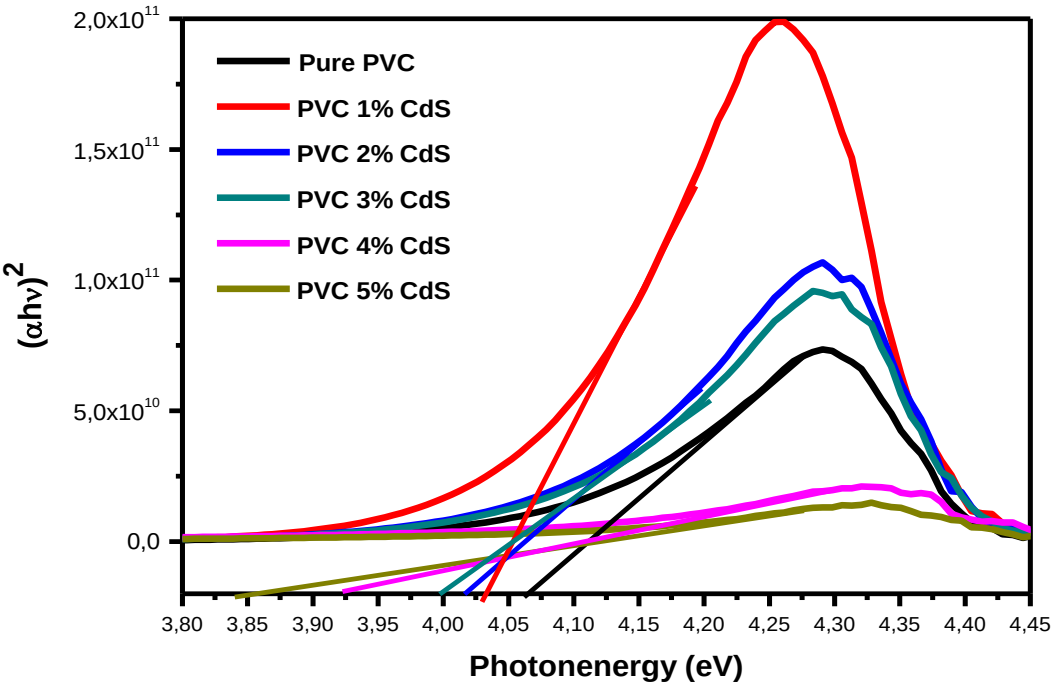

Fig III.10: The plot $(\alpha h\upsilon)^2$ versus incident energy ($h\upsilon$).

III.3.3.3 Photoluminescence analysis

Photoluminescence spectra of the samples have been recorded at an excitation wavelength of 320 nm and shown in Fig. III:11.The spectra of PVC shows the non-emission peak. However, in the PVC/CdS nanocomposite spectra, the yellow emission band has been observed at 560.52 nm (2.97 eV) correspondent to the interstitial cadmium defect states [108]. In CdS nanoparticles, the defects types that contribute to the PL emission are interstitial cadmium, interstitial sulfur, cadmium vacancy and sulfur vacancy [109]. Furthermore, from Figure 7 it can be seen that the PL intensity decreases as a function of CdScontent which can be explained

by the reduction of the electron-hole recombination rate, and this enhances the photocatalytic efficiency.

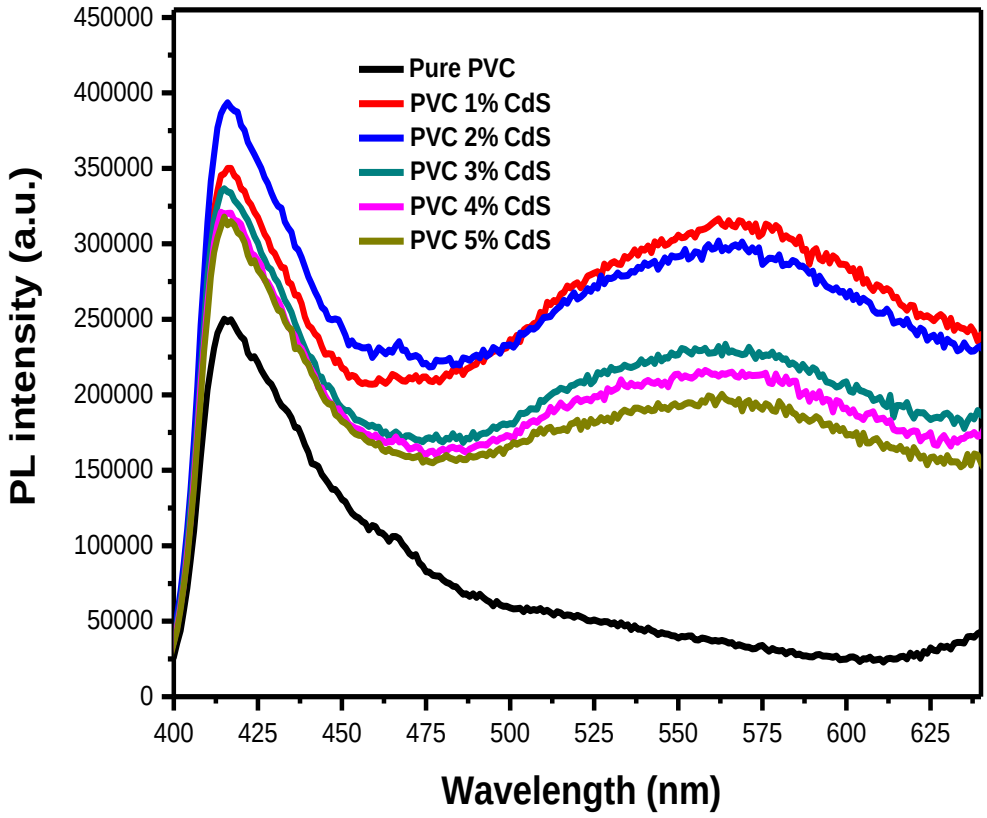

Fig III.11:PL spectra of PVC and PVC doped CdSnanoparticles.

III.3.4 Photocatalytic tests

Figure **III.12** showing the decrease of the absorption spectra of methylene blue solution at 663,5 nm, catalyzed by pure PVC and PVC/CdS nanocomposites under the UV light irradiation with the wavelength of during 3 h. First of all ,we perform the direct photolysis of MB and the obtained result was considered negligible as only less than 5% of degradation was achieved after 4 h of UV irradiation.So,The decrease indicates that both pure PVC and PVC/CdS nanocomposites exhibit UV light photocatalytic activity.

The PVC/CdS nanocomposites show much higher photocatalytic activity due to the more efficient decolorization of MB over CdS nanoparticles. As the CdS content on the

nanocomposites surface increases, the photocatalytic activity of PVC/CdS nanocomposites enlarge. PVC 5% CdS demonstrates the highest photocatalytic activity, displays the greatest photocatalytic activity as there is almost no absorption of the methylene blue solution after two hours. The concentration of MB solution was obtained by a calibration curve. Photocatalytic degradation was calculated based on equation (2) [110]:

$$DE(\%) = \left[\frac{C_0 - C}{C_0}\right] * \ 100 \qquad \text{(III.2)}$$

Where, DE (%) is the $Degradation\ efficiency$, the symbols of C_0 and C are the concentration of MB solutions before and after photoirradiation, respectively. The degradation rate of both MB solutions under UV irradiation for 3 h, are illustrated in Figures 8(a), (b) and (c)

Fig. **III.13** shows the efficiency of decomposition of the dyes (MB) under UV light. It has been clearly shown from the graph that a remarkable decolorization was facilitated by the CdS mainly under UV irradiation. Photodecomposition efficiency is attributed directly to the extent of the source of light absorbed by the catalyst. As shown in Figures III.13 (b), the rates constants increase as a function of the exposition time to UV. However, PVC5%CdS films display the most improved photocatalytic performance. As can be observed in Figure III.13 (c), the Dye degradation increase as a function of reaction time under UV light irradiation, which indicates the producing photogenerated electrons (e^-) and holes (h+). So the separation of e^- and h^+ in the PVC/CdS nanocomposite can be effectively enhanced, and more e^- and h^+ can be involved in the photocatalytic reactions [111]. Through this, the process of photocatalytic efficiency of samples can be explained with the direct bandgap energy of PVC/CdS nanocomposite which decreased from 4,07 eV to 3,85 eV as the CdS content was increased from 0 to 5 %. According to PL the CdS doping decreased the recombination electron holes which leade to the exhibit higher photocatalytic efficiency.

(a) **(b)**

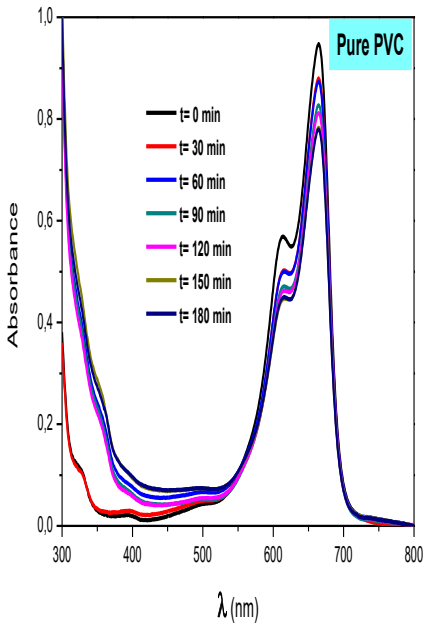
Pure PVC
t= 0 min
t= 30 min
t= 60 min
t= 90 min
t= 120 min
t= 150 min
t= 180 min
Absorbance
λ (nm)

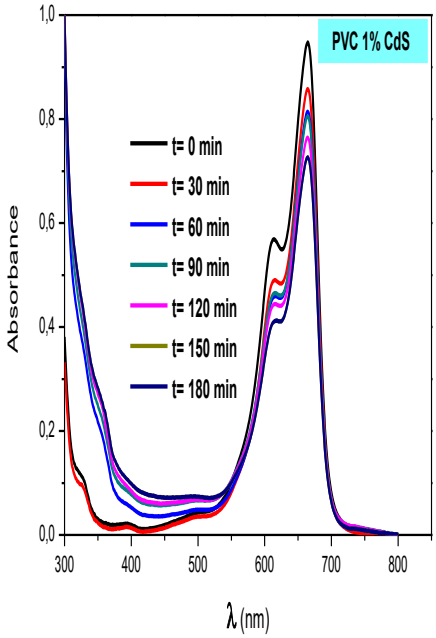
PVC 1% CdS
t= 0 min
t= 30 min
t= 60 min
t= 90 min
t= 120 min
t= 150 min
t= 180 min
Absorbance
λ (nm)

(c) **(d)**

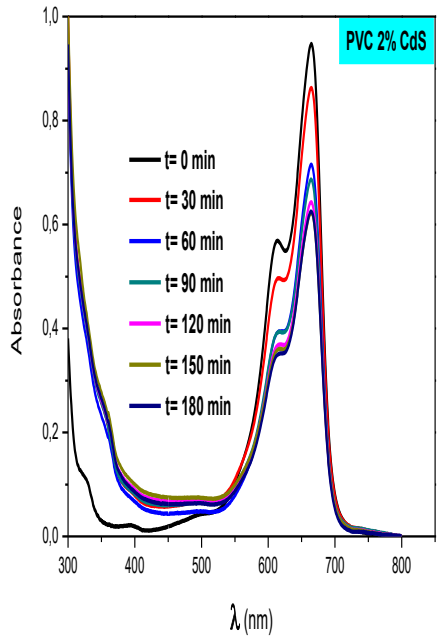

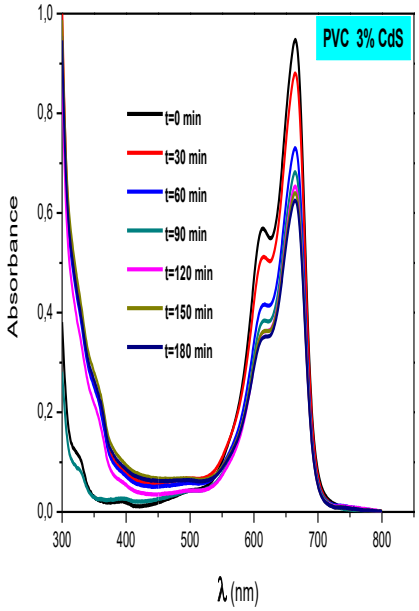

(e) **(f)**

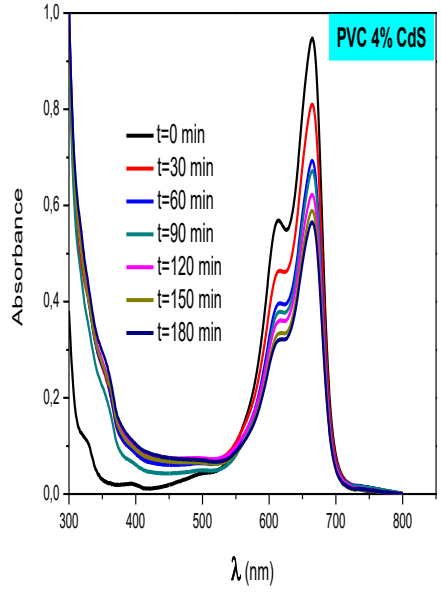

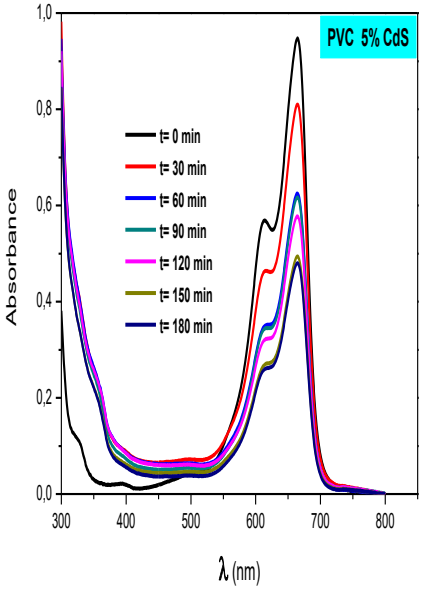

Fig III.12: Absorption spectra of MB dye at UV light irradiation with the wavelength of during 3 h using Pure PVC and PVC/CdS nanocomposites photocatalyst; (a) Pure PVC; (b) PVC 1% CdS ; (c) PVC 2% CdS ; (d) PVC 3% CdS ; (e) PVC 4% CdS ; (f) PVC 5% CdS .

(a) (b)

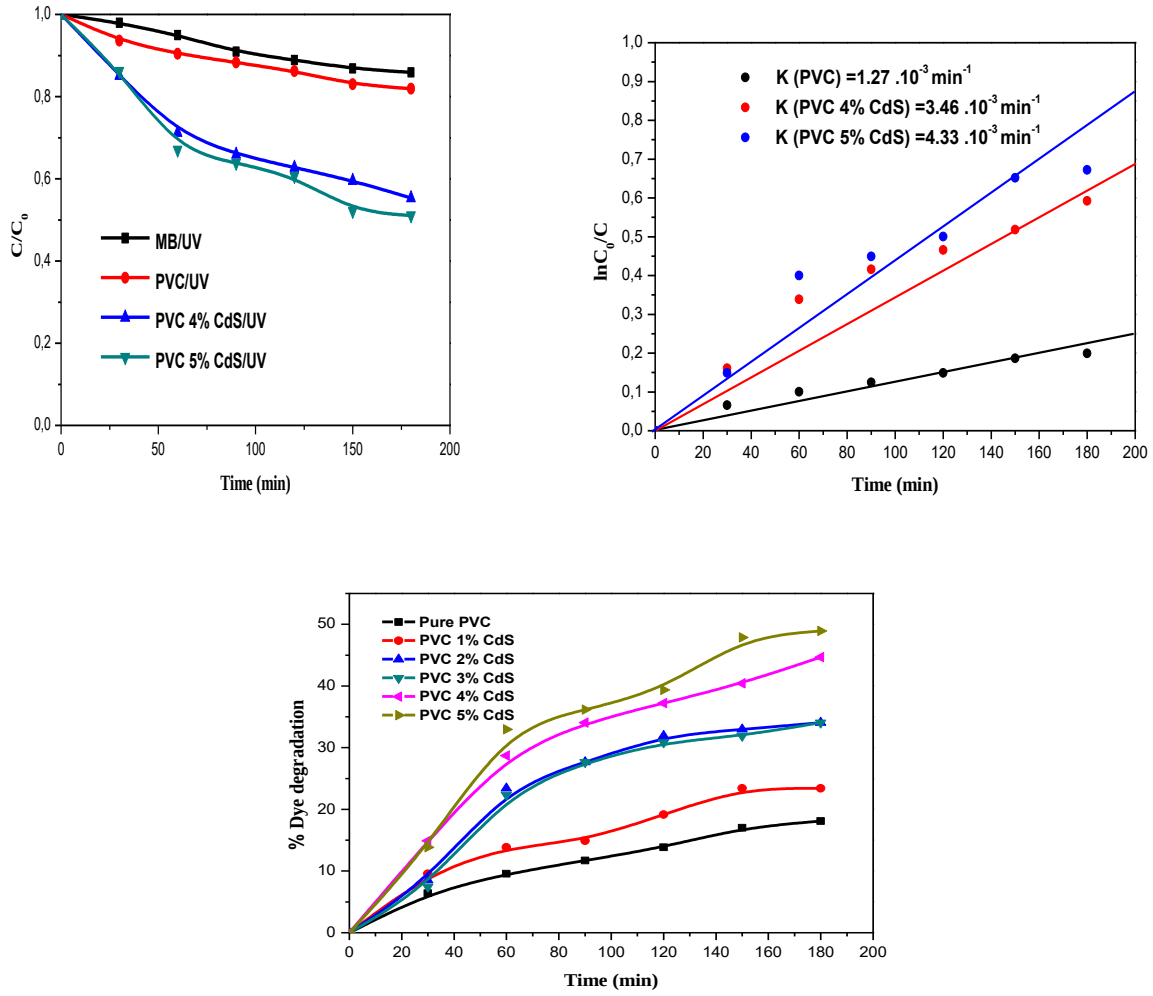

(C)

Fig III.13: Decomposition of the dyes (MB) under UV light(a) C/Co vs time (b) ln C/Co vs time (c) % dye degration vs time.

III.3.5 Photocatalytic Degradation Mechanism

Photocatalytic degradation of CdS/PVC nanocomposites film is initiated by degradation of CdS NPs .Since the degradation of PVC starts indirectly through oxidative radicals generated on CdS [138].

In general ,when CdS is irradiated by UV light ,a photoelectron moves from valence band to the conduction band of the semi conductor.This photon has the energy (hυ) equal to or greater than the band gap.The semi conductor absorbs this radiation and one electron can be excited from the doping donor level to Cb of the semi conductor and forms cationic radicals (eq**III** .3).

$$CdS + h\upsilon\ (E \geq E_g) \longrightarrow CdS^*\ (e_{cb}^- + h_{vb}^+) \qquad (\textbf{III}.3)$$

The photogenerated holes (h_{vb}^+) react with water molecules to produces the hydroxyl radicals •OH. While the electrons in (CB) conduction band meanwhile reacts with O2 and generate superoxide radicals anions $O_2^{\bullet -}$(eq(5)). The oxygen molecules adsorbed on the semi conductor surface acelerates oxidation process and also prevent any further e- / holes recombination by trapping electrons.

$$h_{vb}^+ + H_2O \longrightarrow {}^{\bullet}OH \qquad (\textbf{III}.4)$$

$$e_{cb}^- + O_2 \longrightarrow O_2^{\bullet -} \qquad (\textbf{III}.5)$$

These reactive species like H2O2, $O_2^{\bullet -}$ and •OH radicals produced ,for ultimately help to degrade target pollutants present around it (eq(6)).

$$O_2^{\bullet -} + H_2O \longrightarrow O_2^{\bullet}H + OH^- \qquad (\textbf{III}.6)$$

$$2O_2^{\bullet}H \longrightarrow H_2O_2 + O_2 \qquad (\textbf{III}.7)$$

$$H_2O_2 + h\upsilon \longrightarrow 2{}^{\bullet}OH \qquad (\textbf{III}.8)$$

Photocatalytic degradation of PVC is only excited by UV light due to presence of C-C and C-H bonds in polyvinyl chloride. It is proposed that in PVC/CdS nanocomposites, on CdS nanostructures - MB dye generates holes in ground state which takes part in degradation of PVC matrix also with •OH and $O_2^{\bullet}H$.These oxygenated species are initiators of PVC degradation by attacking the polymeric chain [139].

$$-(CH_2CHCl)-^{*} + {}^{\bullet}OH \longrightarrow -(\,{}^{\bullet}CHCHCl)- + H_2O \quad (\textbf{III}.9)$$

$$-(CH_2CHCl)-^{*} + {}^{\bullet}O_2H \longrightarrow -(\,{}^{\bullet}CHCHCl)- + H_2O_2 \quad (\textbf{III}.10)$$

The oxygen molecules (O_2)have an important central role in the degradation reactions of PVC matrix. Oncethe carbon-centered radicals included in the PVC polymer chain, their successive reactions lead to the chain cleavage with the O_2 incorporation and CO2 evolution.

$$-(\,{}^{\bullet}CHCHCl)- + O_2 \longrightarrow -(CH(OO^{\bullet})CHCl)- \quad (\textbf{III}.11)$$

$$-(CH(OO^{\bullet})CHCl)- + -(CH_2CHCl) \longrightarrow -(CH(OOH)CHCl)- + -(\,{}^{\bullet}CHCHCl)- \quad (\textbf{III}.12)$$

$$-(CH(OOH)CHCl)- + h\upsilon \longrightarrow -(CH(O^{\bullet})CHCl)- + {}^{\bullet}OH \quad (\textbf{III}.13)$$

$${}^{\bullet}OH + \text{MB Dye} \longrightarrow CO_2 + H_2O \quad (\textbf{III}.14)$$

Fig III.14: Schematic diagram for the photocatalytic degradation of CdS/PVC nanocomposites.

III.4. Conclusion

In summary, CdS nanoparticles were doped in the PVC matrix to formed the nanocomposites films PVC/CdS were achieved by a sol–gel method. The result of XRD and Raman revealed that CdS nanoparticles changes their crystalline pure PVC and indicate the dispersion of CdS nanoparticles. The transmission spectra demonstratedthat the films PVC/CdS are transparent in the visible region and the optical band gap decrease from 4.07 eV to 3.85 eV. Also, the analysis of SEM confirmed that the higher density of particles represents the agglomeration of CdS nanoparticles in the PVC polymer. The application of PVC/CdS nanocomposites of their photocatalysis efficiency is evaluable and consideration. Moreover, this films can be used as an excellent photocatalysis for potential application in control of environment friendly photodegradable polymer material

Chapitre IV

Preparation and characterization of Ag :MgO/PVC nanocomposites

IV.1 Introduction

Nanocomposites embedded in polymer matrix have gained a lot of interest and thus a numerous research work has been devoted to it. Single polymer matrix is one of the most attractive classes of materials in the world, due to their interested properties and applications.Nowadays, nanocomposites offer new technology and business opportunities for all sectors of industry, in addition to being environmental friendly. Polymer nanocomposites offer advanced in new technology in various uses and has no environmental benign effects. Moreover, the effective properties of polymer nanocomposites rely on the nature of the components, the shape of the particles, the size and arrangement of the inclusions, the concentration, the volume fraction of the components, extent of dispersion of nanoparticles and interfacial bonding in the polymer matrix.

However, thermoplastic nanocomposites doped with nanoparticles seem to be the new approach in the nanocomposites studies wich have significant interest within the previous few decades because, combining the attractive functionalities of organic polymers and inorganic nanoparticles have been expected to display synergistically improved properties.Moreover, the effective properties of polymer nanocomposites are depend upon the properties of constituents ,particles shape ,size and arrangement of inclusions ,concentration, the volume fraction of components, interfacial bonding and dispersion of the nanoparticles in the polymer matrix.Generally, the resultant nanocomposites display enhanced optical, mechanical, magnetic and optoelectronic properties.Inorganic particles as fillers can improve mechanical, thermal, electronic, magnetic, redox properties, density and refractive index of polymer matrix[114,115,116]. Generally, Inorganic particles in polymer matrix improve density, mechanical, thermal, electronic, magnetic, and redox properties of nanocomposites.

Among oxides, MgO nanoparticles is a well known refractory oxide, which has potential advantages with wide bandgap around 7.8 eV. MgO is a promising inorganic material crystallizes in NaCl type structure and widely used in many applications have various prospects in applications due to their abundant source of raw materials, high thermal stability, low biological toxicity, and biodegradability such as sensor, antimicrobial, optical coatings, water

treatment, catalysis, adsorbents, and additives in fuel, etc. This is mainly due to its superior surface reactivity, wide bandgap, chemical, and thermal stability. Nanostructured metal oxides have uniqueproperties like high thermal stability, high chemical sta-bility, biocompatibility, non-toxicity, and high surfacereaction activity [117,118], here magnesium oxide (MgO) ischosen since it is having a wide applications in thechemical industry as a scrubber for air pollutant gasses,electric insulating material filler, optoelectronics, refrac-tory materials, and as a catalyst support . Sawaiet al. [120] have reported that the MgO has a good bacte-ricidal performance in aqueous environments due to theformation of oxide anions at its surface.
Combination or doping with metallic elements is considered an effective method. The insertion of silver into the crystal lattice of MgO has received great attention for making the anibacterial activity and the catalyst active undervisible light. Additionally,Kakhki et al. reported photocatalytic degradation of toxicorganic dyes under various light radiations . The incorporation of Ag into the MgO structure changes optical absorption towards regions of lower energy, extending the photocatalytic activity towards the visible region of the elec-tromagnetic spectrum. [121].

Polymers are prevalent and dominant materials profitingfrom their low cost and simple processability [14].Polymer like PVC has attainted tremendous attention in many auspects of life, so it is considered as versatile, beneficial and economical commodity polymers. PVC can be used for indoor construction purposes like sash windows and door shutters due to its easy modification and low cost. PVC can also be used in flooring and water hoses. Besides that PVC can be utilized for different Industrial applications and Anti bacterial properties [122]. Polyvinyl chloride (PVC) is used as an insulating material in the construction of power cables, this is due to its good properties, such as easy processing, low cost, excellent mechanical properties, higher rigidity than other general thermoplastic materials and good insulating properties. The advantage of PVC is that it breaks down easily and does not produce dioxins under natural conditions. This wide range of applications of PVC can beeven more extended by incorporation of filler into PVC matrix.

Currently, the search for efficient, cheap,and green treatment processes for wastewater is a challenge around the world.Also,Bacteria resistance to antibiotics is one of the biggest challenges facing human health today. In this chapter, an attempt has been made to synthesized

Ag doped MgO nanoparticles and Ag doped MgO/PVC nanocomposites and investigate their photocatalytic and antibacterial effects . we report the structural, optical, and morphological properties of Ag :MgO/PVC nanocomposites film.It was also understood how they propagate within the solid matrix for the development of efficient photodegradable and antibacterial properties .

IV.2 Experimental Section

IV.2.1 Synthesis of Magnesium oxide (MgO) nanoparticles

A sol-gel technique was employed to synthesize MgO NPs. Mg $(NO_3)_2.6H_2O$ was taken as a precursor of magnesium and treated with C_2H_5OH. The solution was stirred for 24h until white gel was obtained. After that the mixture was filtered, washed with distilled water and ethanol several times and dried at 100 ° C for 24h. The obtained powder was annealed at 950° C for 36h. Finally the powder was grinded and used for further analysis. The annealing phase results in formation of desired product.

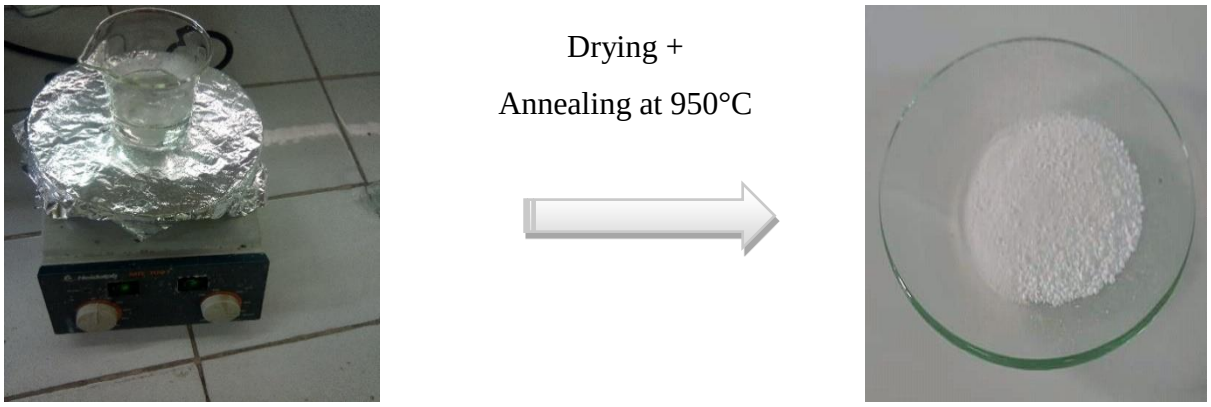

Fig IV.1: Sol gel synthesis of MgO nanoparticules.

IV.2.2 Preparation of Ag doped Magnesium oxide nanoparticles

Same sol-gel technique was employed to synthesize Ag-doped MgO NPs. In brief, In 20ml di-ionized (DI) water 0.019 mol $Mg(NO_3)_2 \cdot 6H_2O$ and X mol (X = 0.001, 0.002, 0.003) of $AgNO_3$ was mixed followed by addition of 0.02 mol of $C_6H_8O_7 \cdot H_2O$ under constant stirring for 2h. Subsequently the mixture was kept on a water bath at 80 °C until a wet gel formed. After that

wet gel was dried at 150 °C to form a fluffy precursor. Finally, the precursor was grinded and calcined at 600 °C in presence of air for 2 h at a heating rate of 2 °C/min.

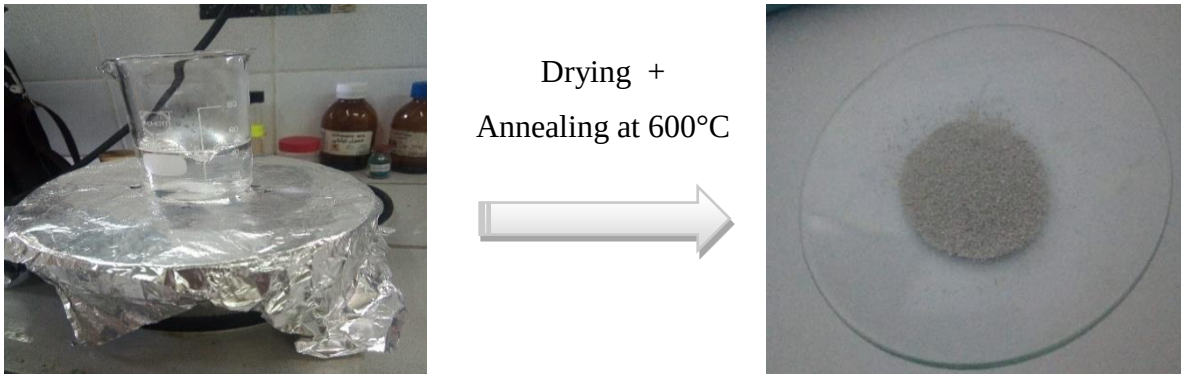

Fig IV.2: Sol gel synthesis of Ag:MgO nanoparticules.

IV .2.3 Ag : MgO/PVC Nanocomposites Preparation of Polymer Nanocomposites:

Ag: MgO/PVC nanocomposites was fabricated by adding 1g of PVC powder in 20ml THF for 30 minutes and a clear transparent viscous solution was obtained. A selected amount of Ag: MgO (depends upon loading taken) was added in 10ml of THF and mixed to PVC solution under constant stirring for 1h. The weight of Ag: MgO added to polymer solution depends upon the different percentage by weight 3%, 7%, 10% Ag:MgO/PVC. After that the solution was allowed to rest which resulted in deposition of heavier particles to get settle at the bottom and the smallest crystallites in the upper part were recovered and deposited as Ag:MgO/PVC nanocomposite thin film on the surface of the glass. Before depositing the film the glass was cleaned and washed by using DI water, methanol and acetone in order to remove the unwanted things (grease and other impurities). Spin coating or centrifugation technique was used to deposit Ag:MgO/PVC nanocomposite on glass substrate. After deposition the thin film was completely dried in order to remove traces of solvents. As synthesized film was having uniform distribution of Ag: MgO NPs.

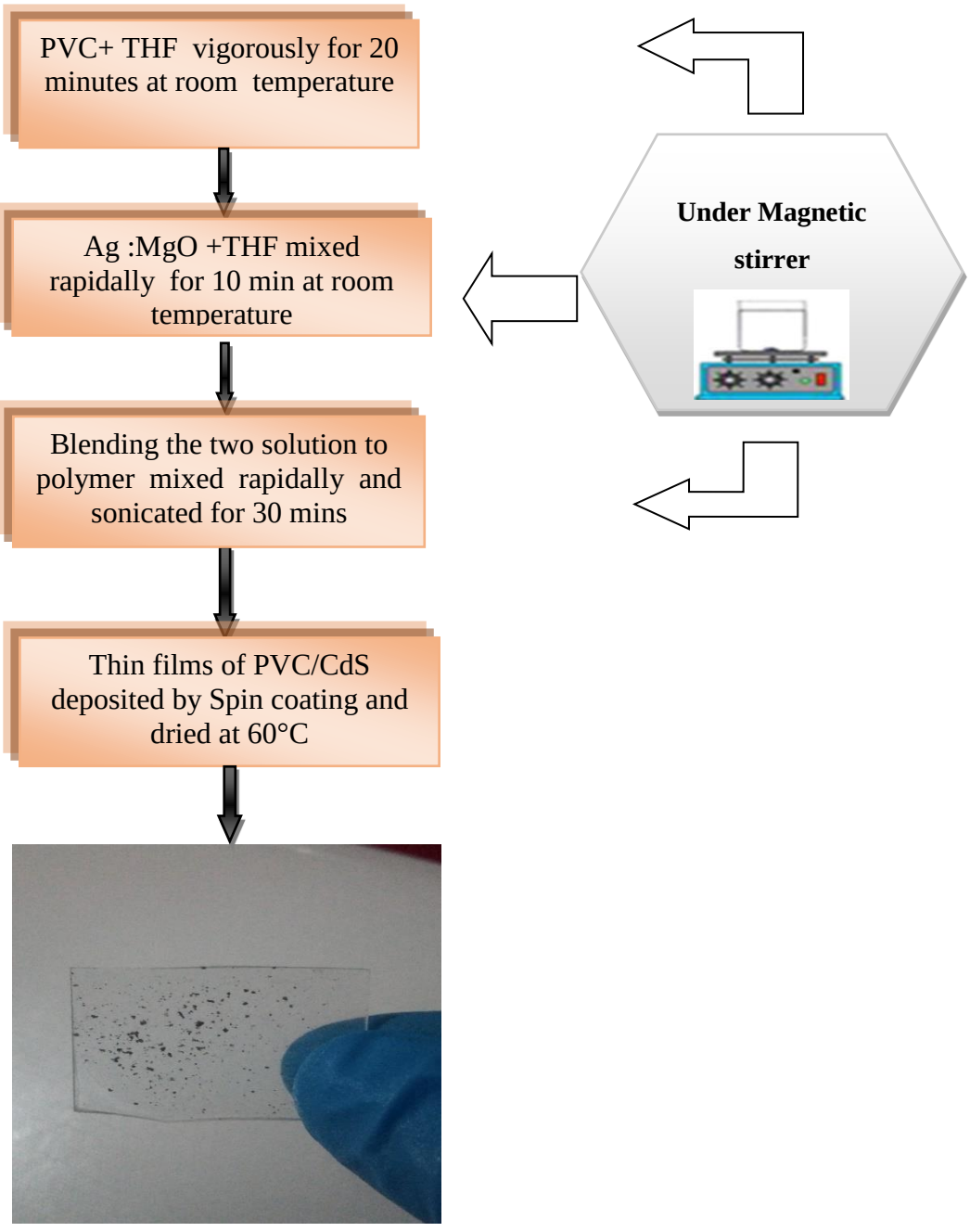

One of the obtained transparent samples

Fig IV.3: Synthesis of Ag:MgO/PVC nanocomposites.

IV .2.5 Antibacterial activity protocol

In this assay, the antimicrobial effect of the prepared films was acheived by the broth dilution method. Bacterial test suspensions were used in the exponential phase which has an OD of 0.08 to 0.10 and then the concentration of the suspension was adjusted. The test was performed by directly contacting the sterilized films (5x15 mm^2) with 5ml of bacterial suspension at 37°C for 24 hours. Two bacterial strains were tested: E. coli, and S. aureus. After 24 hours, their bacterial survival was determined by measuring the optical density (O.D.) of the suspension at 600 nm. The tests were performed at least three times using both E. coli and S. aureus, and the reported data represent average values. All experiments were performed in triplicate.

Fig IV.4: The photograph images of preparation of the bacterial suspension.

IV .2.6 Photocatalytic procedure

The photodegradation of MB dye with UV light source (VL -215.LC,15W), the maximum emission is at 365 nm was used to evaluate the visible light photocatalytic activity of the PVC/CdS nanocomposites and pure PVC. A cylindrical glass vessel containing an aqueous MB solution (175ml) with an initial concentration of 10^{-5} mg/ml. Then, the thin films Ag:MgO/PVCnanocomposites of 5/2.5 cm on the side was posed into the petri dish, which contains the MB solutions (10ml). After that, the system was subjected to visible light emitted by a 300 W iodine tungsten lamp (Philips Co). The distance between the surface of the suspension and the light source was about 20 cm. During irradiation, the samples were taken out every 30 min from the reactor. The clarified solution was analyzed by a 723 UV–Vis spectrometer (UV-1800 Shimadzu LC 2010-HT).

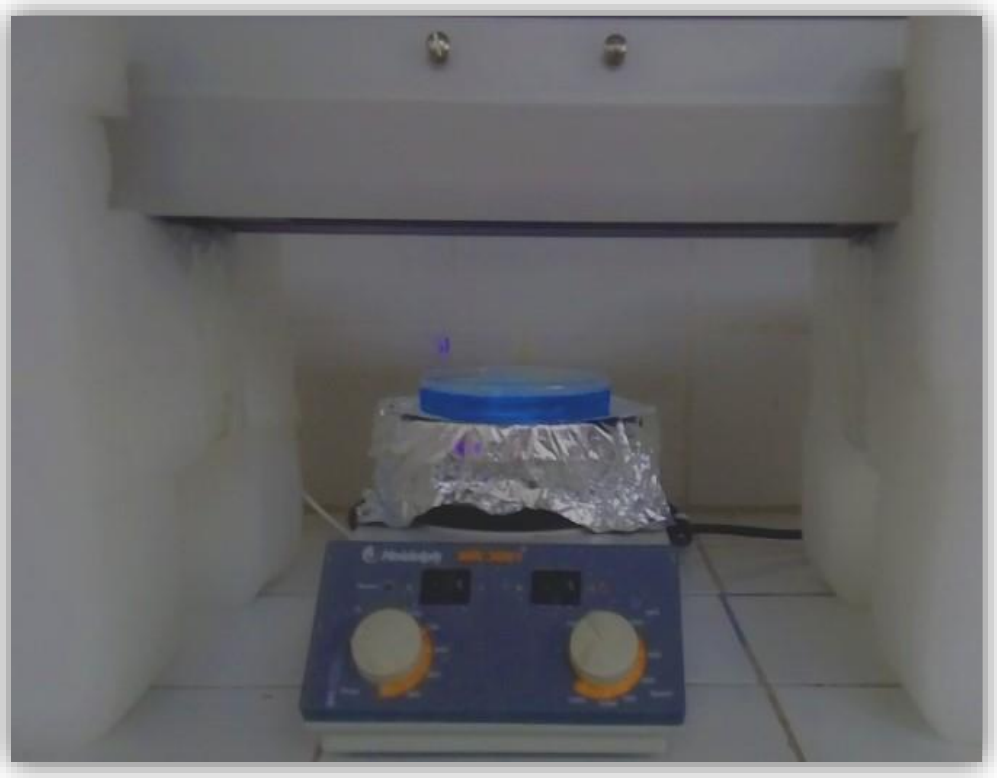

Fig IV.5: Photo of the photocatalytic test under UV light source.

IV.3. Results and discussion

IV.3.1 Structural study

IV.3.1.1 X-ray diffraction (XRD) analysis

Fig IV.6 Fig 1 shows the XRD patterns of pure PVC, MgO/PVC and Ag:MgO/PVC nanocomposites film of different concentration (3, 7 and 10) wt% of Ag doped MgO nanopowder under study. From, XRD of pure PVC film, polymer chain have disordered structure indicating amorphous nature [123]. The MgO/PVC nanocomposites film exhibits lower characteristic peaks as compared to the Ag:MgO/PVC nanocomposites, which appear the peak at 2θ angle 43.04° corresponding to the reflection of (200) correspond to the cubic phase of MgO (JCPDS card N° 45-0946). The XRD pattern of 3% Ag:MgO/PVC reveals MgO crystalline phase and no prominent peak for Ag. However when the amount of Ag:MgO is higher(7%,10%), a notable intense peak is observed at 2θ = 38.11° that arises due to diffraction of metallic Ag [121,124].

The appearance of these three additional peaks at 44.5°, 64.72° and 77.65° corresponds to the (200) ,(220) and (311) planes of metallic Ag, authenticates presence of metallic Ag as second phase crystal planes in the polymer matrix, which indicates the successful insertion of elemental silver on MgO/PVC nanocomposites [125].

From table 1 it can be inferred that intensity and area of Ag:Mg0/PVC under the peaks at 2θ = 39.3° and 43.04° shifts to right when Ag:MgO loading is increased as compared with that of MgO/PVC, this decrease in lattice parameters reflects formation of mixed phase of Ag:MgO. So it can be inferred that there is change in crystal structure due to varying of Ag:MgO dopant ratio. The interplaner distance (d) of MgO/PVC and Ag:MgO/PVC were determined using Bragg's law. The change in the interplaner distance (d) from 2.29 for MgO/PVC (0 % Ag) to 2.36 for highest loading of Ag:MgO (10 at.% Ag:MgO) clearly indicates the increase in the lattice size upon doping, which demonstrating a possible extension of MgO lattice due to substitution of larger Ag+ ions (1.26Å) with the Mg2+ (0.66Å) ions in the lattice. In this process oxygen vacancies are also generated to favour the

structure reorganization and keep an overall neutral charge after Mg2+ in MgO crystal is

replaced by Ag+ [126]. Additionally to these observations, after doping with Ag, the peak of (111) has a high intensity value. Compared to the JCPDS card N° 45-0946, MgO present a texture along the (111) plane.

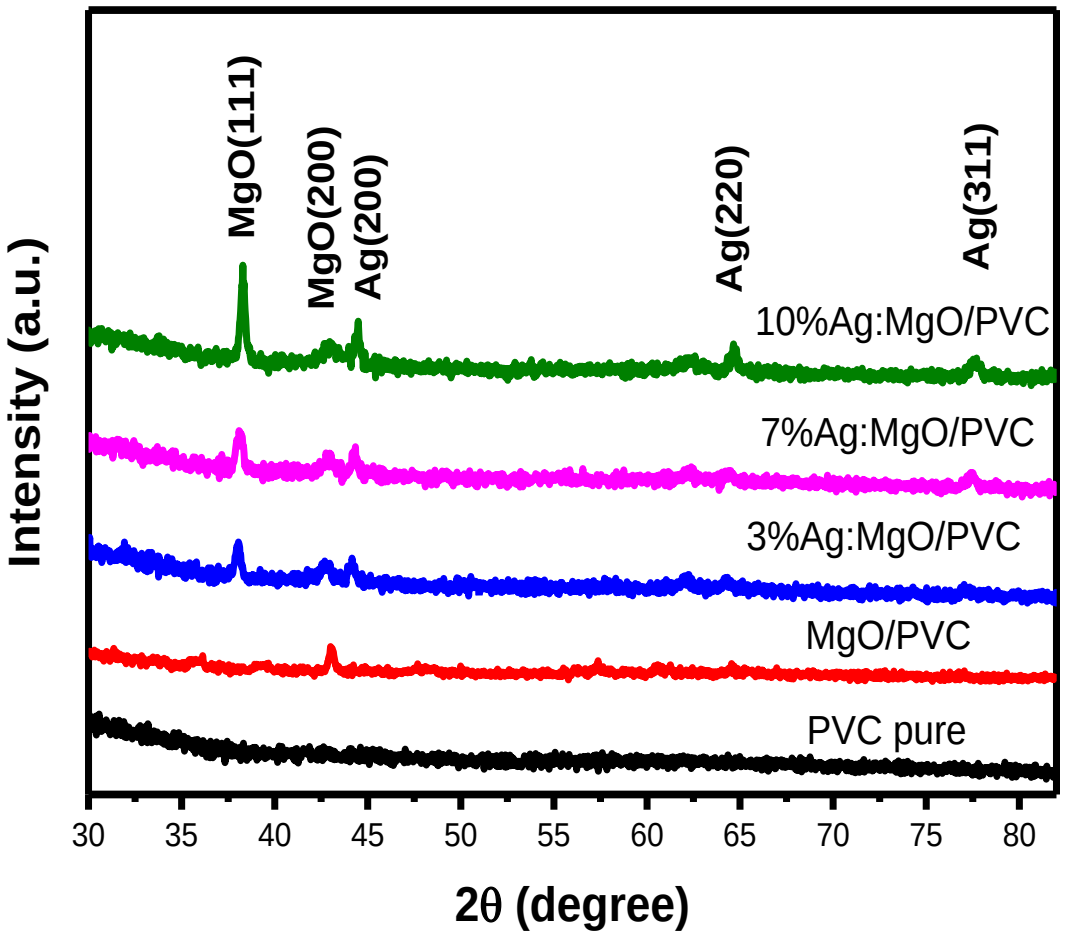

Fig IV.6: X-ray diffraction spectra of Pure PVC , MgO/PVC and Ag :MgO/PVC nanocomposites thin films.

IV .3.1.2 The grains size

Debye Scherer's formula was used to calculate size of crystals , and the values calculated are recorded in **Table 1** [127]::

$$D = (0.9\,\lambda)/(\beta\,cos\,\theta) \qquad (\textbf{IV}.1)$$

Where β = FWHM, θ is the diffraction angle, λ is the X-ray wavelength (1.5405 Å). As the dopant Ag: MgO increases the for Ag:MgO/PVC samples the crystallite size (D) also increases. On the other hand, a lower amount of Ag :MgO is not very effective in the crystal structure.

Also, the D of Ag:MgO doped with 10% in the PVC matrix is approximately similar to that of MgO/PVC. This proves that Ag ions are not incorporated into MgO. This can be attributed to the larger ionic radius of Ag^{+} compared to Mg^{2+}.

TableIV.1. : Structural parameters MgO/PVC and Ag :MgO/PVC nanocomposites thin films.

Samples	2θ(°)	(hkl)	FWMH(°)	d	D (nm)
MgO/PVC	43,08	(200)	0,27	2,10	31,5
3%Ag :MgO/PVC	38,03	(111)	0,4	2,35	22,29
	42,72	(200)	0,35	2,05	
	44,17	(200)	0,4	2,05	
7% Ag :MgO/PVC	38,16	(111)	0,35	2,35	23,77
	42,94	(200)	0,48	2,04	
	44,3	(200)	0,4	2,04	
	77,35	(311)	0,31	1,23	
10% Ag :MgO/PVC	38,3	(111)	0,28	2,36	29,68
	42,94	(200)	0,48	2,04	
	44,43	(200)	0,3	2,04	
	64,72	(220)	0,3	1,44	
	77,65	(311)	0,3	1,23	

IV .3.1.3 FTIR Analysis

The FTIR spectra of pure PVC, PVC/MgO and PVC/MgO-Ag nanocomposits films were recorded in the range 4000–400 cm−1are shown in Fig IV.7 . Sharp peak were recorded in the all films at756 and 904 cm-1. This was attributed to the PVC Bond.

The transmittance band shifted its position towards lower frequency due to increasing content of Ag:MgO nanoparticle .This confirmed the incorporation of Ag doped MgO into the polymer matrix ,due to interaction between Ag doped MgO and C-Cl, C-H bonds of PVC [128].

The spectrum of MgO/PVC nanocomposites film appears three distinct band is observed in the wave number 615, 1324,1434 cm−1, indicating the bending vibrations of Mg–O–Mg, C-H and C=C ,respectively[129] .

The spectrum of the Ag: MgO / PVC nanocomposite film displayed at the low frequencies of 485 cm-1 and 2360 cm-1 were assigned to to the typical stretching mode of the Ag-O bond and the CH2 bending vibration mode[130].

These results indicate that Ag:MgO/PVC nanocomposites resemble with the weak interaction between the polymer matrix and nanofiller particles.

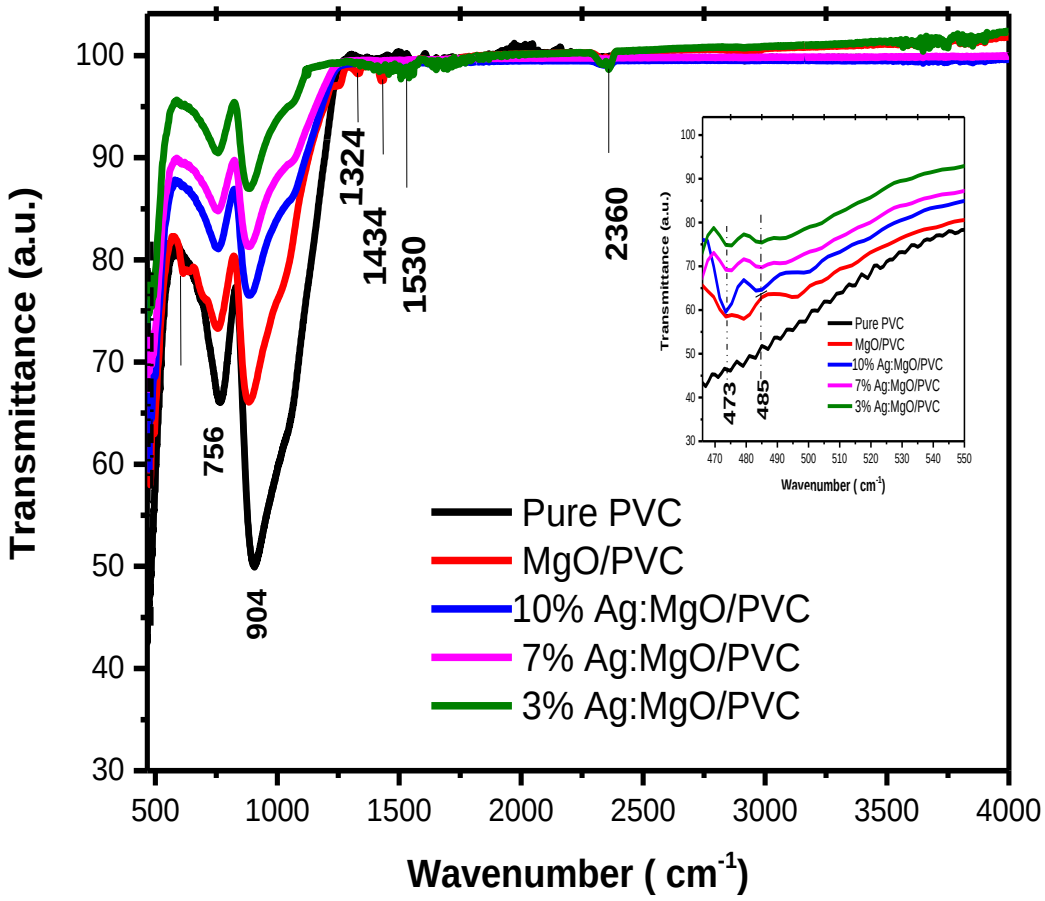

Fig IV.7: FTIR spectrum of PVC, PVC/MgO and Ag :MgO/PVC nanocomposits .

IV.3.2 Optical study

IV.3.2.1 UV–Vis Spectroscopic Analysis

UV–Vis Spectroscopy was employed for determining the optical properties of ion enacted inorganic and its polymeric nanocomposites.

The UV-VIS absorbance spectra in the region 200–800 nm for doped and undoped films are shown in Figure IV.8 , the pure PVC is completely fully transparent (90%) and has a steep absorption edge at 300 nm. The absorption of the films gets decrease with the increase in Ag :

MgO amounts concentration as shown in Fig. 3. The absorption region(300-400nm) is probably due to electron transition from valence band to the conduction band. For Ag:MgO/PVC composite films this absorption band is quite prominent and wider than PVC pure and MgO/PVC. There is a slight shift in UV absorption intensity in Ag:MgO/PVC films. To obtain effective UV absorption the concentration of metal ions needs to be optimized as there is change in absorption with addition of Ag:MgO NPs in PVC matrix [130].

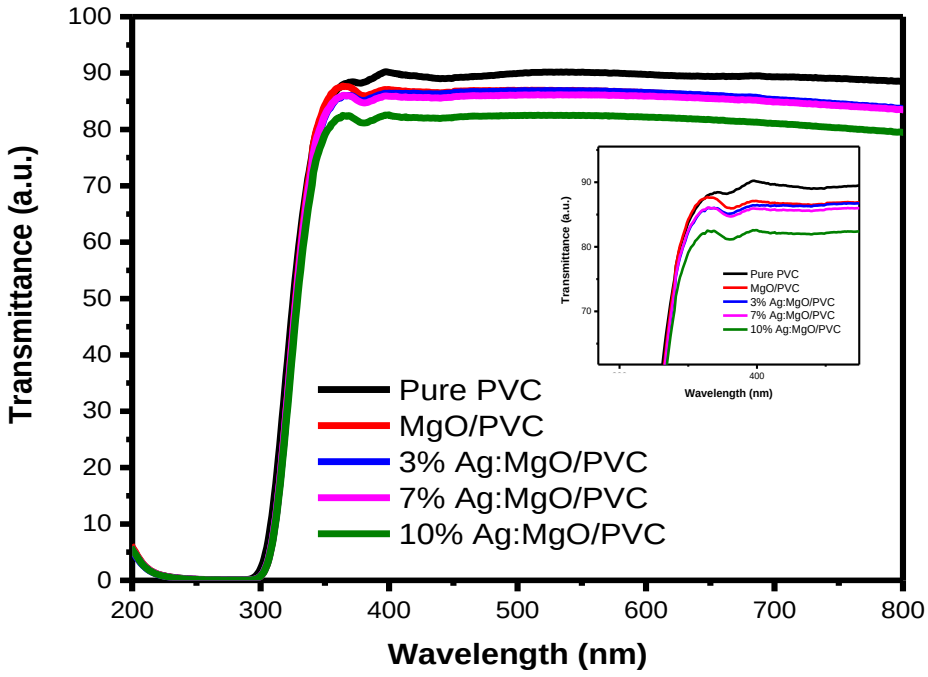

Fig IV.8: Optical transmission spectra in the UV–Visible region of Pure PVC , MgO/PVC and Ag :MgO/PVC nanocomposites thin films .

IV.3.2.2 Determination of Optical Band

Tauc' plot method was employed to determine the optical band gap of PVC, MgO /PVC and Ag:MgO/PVC nanocomposites films. Using the classical Tauc approach, the band gap (Eg) was calculated from the plot of $(\alpha h\nu)^{1/2}$ vs. photon energy ($h\nu$), Figure **4** shows direct optical band gap for neat PVC, MgO/PVC and Ag:MgO/PVC nanocomposites. The optical band gap for PVC was found ~4.1 eV. Incorporation of Ag-doped MgO has great influence on direct

transition in nanocomposites as optical band gap gets decreased with increase in concentration of Ag-doped MgO nanoparticles. This is credited to formation of new local levels in the bottom of conduction band which aid in electron transport from valence band through local levels and then to conduction band [131]. These results revealed that the incorporation of PVC served as accepter for Ag:MgO which reduced the band gap (~3.69eV) for 10% Ag:MgO/PVC nancomposite with red shift confirming p-type conductivity.

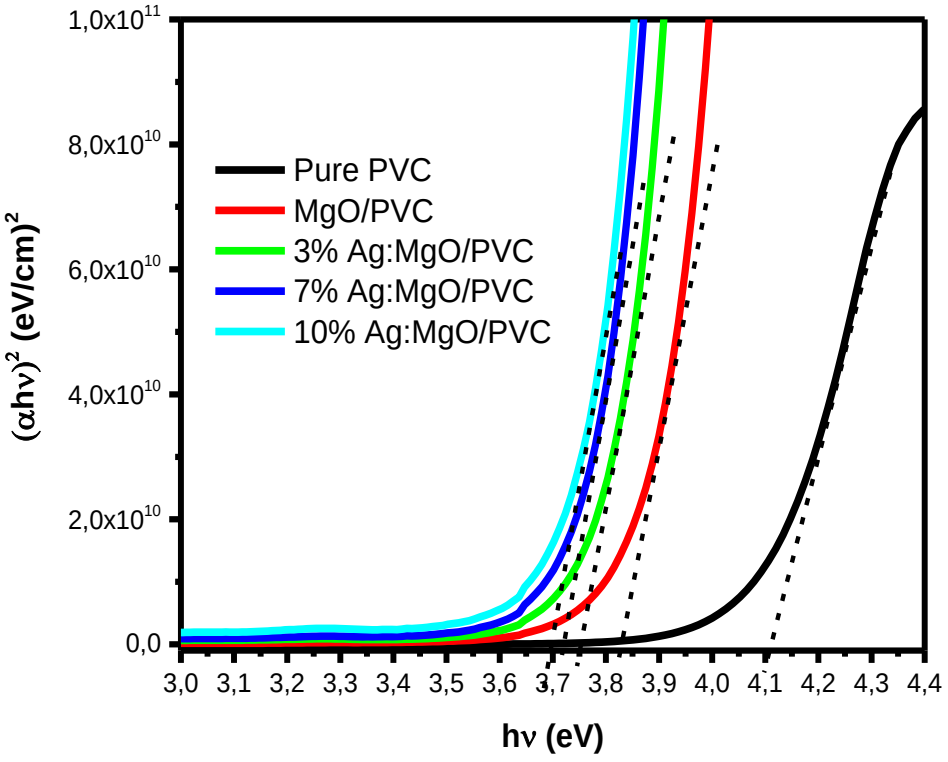

Fig IV.9: The plot $(\alpha h\upsilon)^2$ versus incident energy ($h\upsilon$).

IV.3.3 Morphological study

3.2.1 Atomic Force Microscopy (AFM) analysis

AFM is one of the important analyses for surface characterization. To investigate the topography and roughness of the thin films, AFM 3-D micrographs were recorded. This

measurement technique presents digital images allow the quantitative measurements of roughness average, the root mean square and diameter of pores [134] and are estimated and tabulated below.

The change in surface morphology and roughness due to incorporation of Ag doped MgO nanoparticles in PVC membranes is characterized. The mean roughness (Ra) and root mean square roughness (Rq) parameters were measured for these thin films and are displayed in Table 1. Both parameters increased with increase in the Ag :MgO doping weight percentage. It can be seen from Table 1 that mean roughness (Ra) is varied between$1.933 \leq Ra \leq 35.592$ and the root-mean squared roughness (Rq) is varied between $4.117 \leq Rq \leq 644.643$ .It is clear that the RMS increased with Ag :MgO content, indicating that PVC/MgO-Ag nanocomposites films have a rougher surface than PVC/MgO nanocomposites. This is an acceptable concurrence with XRD results proposing a debasement of crystallinity and a huge change in MgO/PVC nanocomposites film microstructure .Appropriately, 7% and 10% Ag:MgO/PVC nanocomposites film has the most elevated permeable, which prompts a huge explicit surface region. Thusly, this permeable structure film most promising methods to improve the photocatalyst activity and make the recycling safety.

Samples	Avg. Diameter of pores (nm)	Roughness average (nm)	Root mean square (nm)
Pure PVC	36-360	1.93	4.12
PVC/MgO	31-500	34.07	42.30
PVC/MgO-Ag3%	25-500	28 .49	34.76
PVC/MgO-Ag7%	12.5-375	31.33	37.29
PVC/MgO-Ag10%	31-375	35.59	44.64

TableIV.2: Measurements of roughness average, the root mean square and diameter of pores of samples prepared .

Fig IV.10 shows the two-dimensional and three-dimensional AFM images of the surface topography of PVC pure, MgO/PVC and Ag: MgO/PVC nanocomposits films of different concentrations. It can be seen that the number, diameter of the pores augment with increasing the Ag :MgO nanoparticles. may be due to the formation of agglomerates of nanosheets on the membrane surface during the phase inversion process.This is due to increase in the aggregation of tiny particles at some points that contributed in the increase in the roughness parameters [132].As shown by AFM micrographs and their line profiles,7% ,10% Ag : MgO/PVC nanocomposites films have high porous structure as compared to MgO/PVC. This indicates that Ag doping leads to an increased porosity and as a result leads to a large specific surface area.

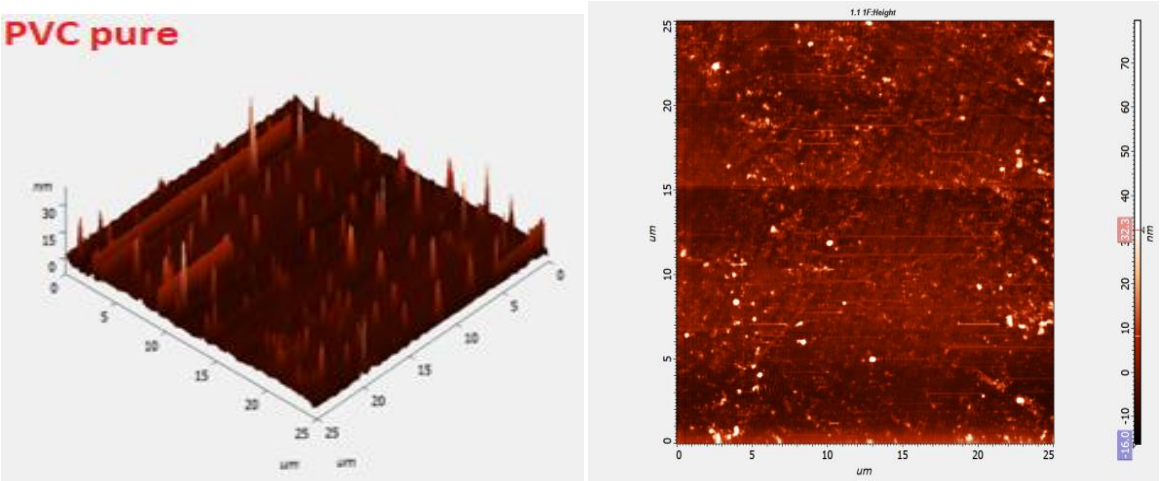

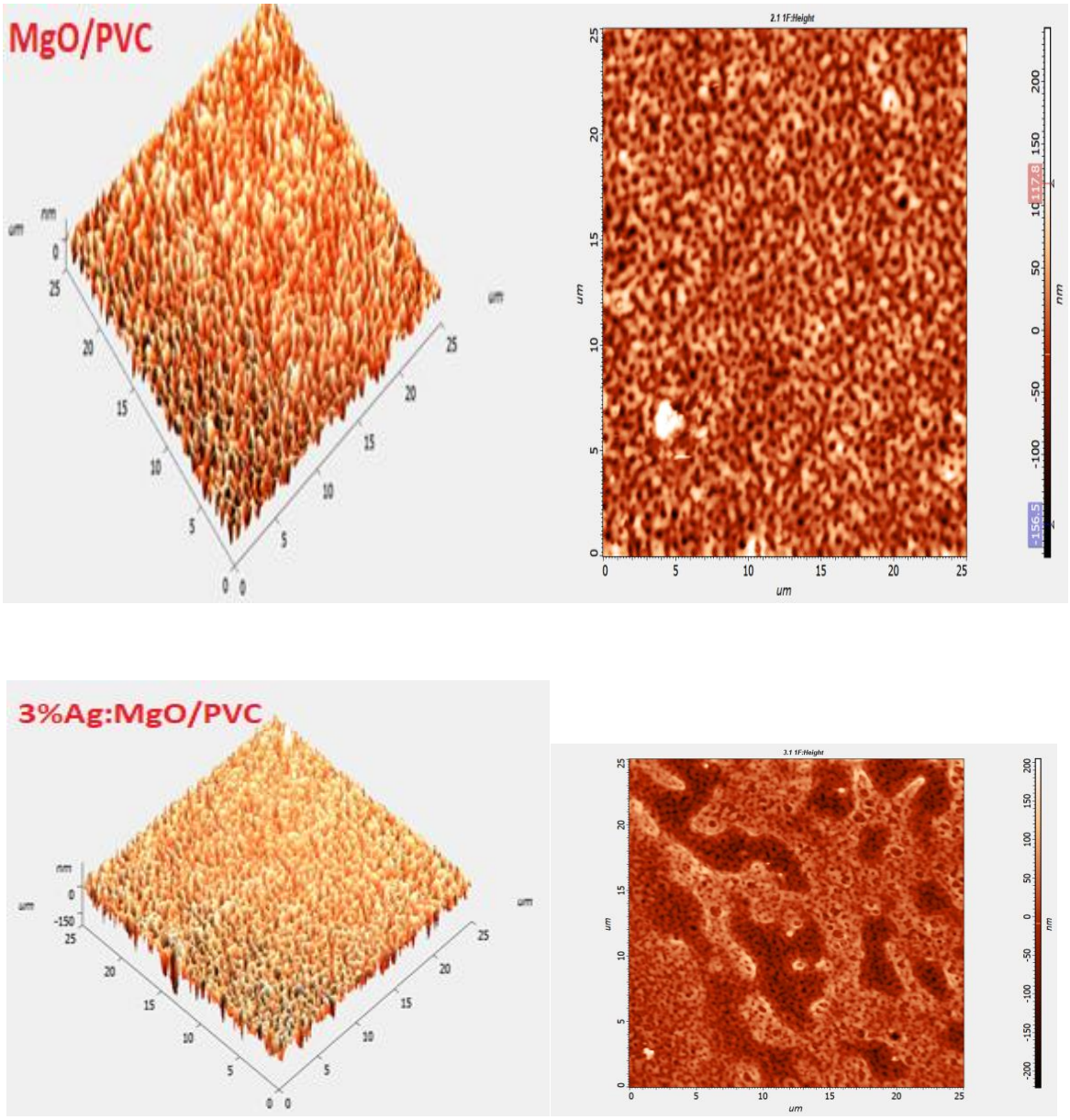

Fig IV.10:AFM for pure PVC, PVC/MgO and Ag :MgO/PVC nanocomposits.

IV.4Antibacterial activity tests

Fig IV.11 showing the antibacterial activity of the Pure PVC ,MgO/PVC and Ag:MgO/PVC nanocomposites were investigated against clinically pathogenic microorganisms of Staphylococcus aureus ATCC 25923(Gram-positive bacteria) and Escherichia coli ATCC 25922 (Gram-negative bacteria).

PVC polymeric material exhibited low antibacterial activity when compared with both standard antibacterial drugs. Introduction of Ag doped MgO nanoparticles to the polymeric matrix has increased the antibacterial activity, in particular against bacteria Escherichia coli and S.aureus. The bacterial growth kinetics(E.coli) has decreased through the addition of 3% Ag:MgO nanoparticles to the matrix polymer PVC (representing a 40 % reduction from the control) and further slight decreased by the addition of additional nanoparticles (representing an 5% , 10% and 5% reduction from the control for the MgO and (7% , 10%) Ag:MgO concentration, respectively .

As for the bacterial growth kinetics (S.aureus) decreased for the MgO/PVC nanocomposites (representing inhibition of about 10% from the control).With a concentration of 3% and 7% the bacterial growth kinetics (S.aureus) decreased rapidly about 35% and 30% respectively, only 10%Ag:MgO/PVC represent low inhibition 5% from the control.

However, the Ag-doped MgO samples exhibit better antibacterial activities compared to pure MgO.Surprisingly, 3% Ag: MgO/PVC shows the best antibacterial activity.It is assumed that the more formed Ag nanoparticles will occupy the defect sites on the surface of MgO particles and thus hinder preventing the adsorption of oxygen to produce ROS.thus the adsorption of oxygen to generate ROS[133].

The results of this present study indicated that this nanocomposite polymer have very effective antibacterial properties and there is a direct relationship between the concentration of nanoparticlesinto the polymer and the rate of elimination of bacteria, and the antibacterial effect is a bactericidal effect.Where the smaller nanoparticle ,the grater the effect of antibacterial[134].

Our result have important implications we have shown that embedding PVC used to manufacture endotracheal tubes with Ag:MgO nanoparticles drastically lessens the adherence of bacteria. It is envisioned that this simple and inexpensive approach could lead to a reduction in nosocomial infections, longer medical device lifetimes, and decreased antibiotic usage and reliance .all of this events could lead to decreased antibiotic resistance and patient infection rate in the clinical setting.

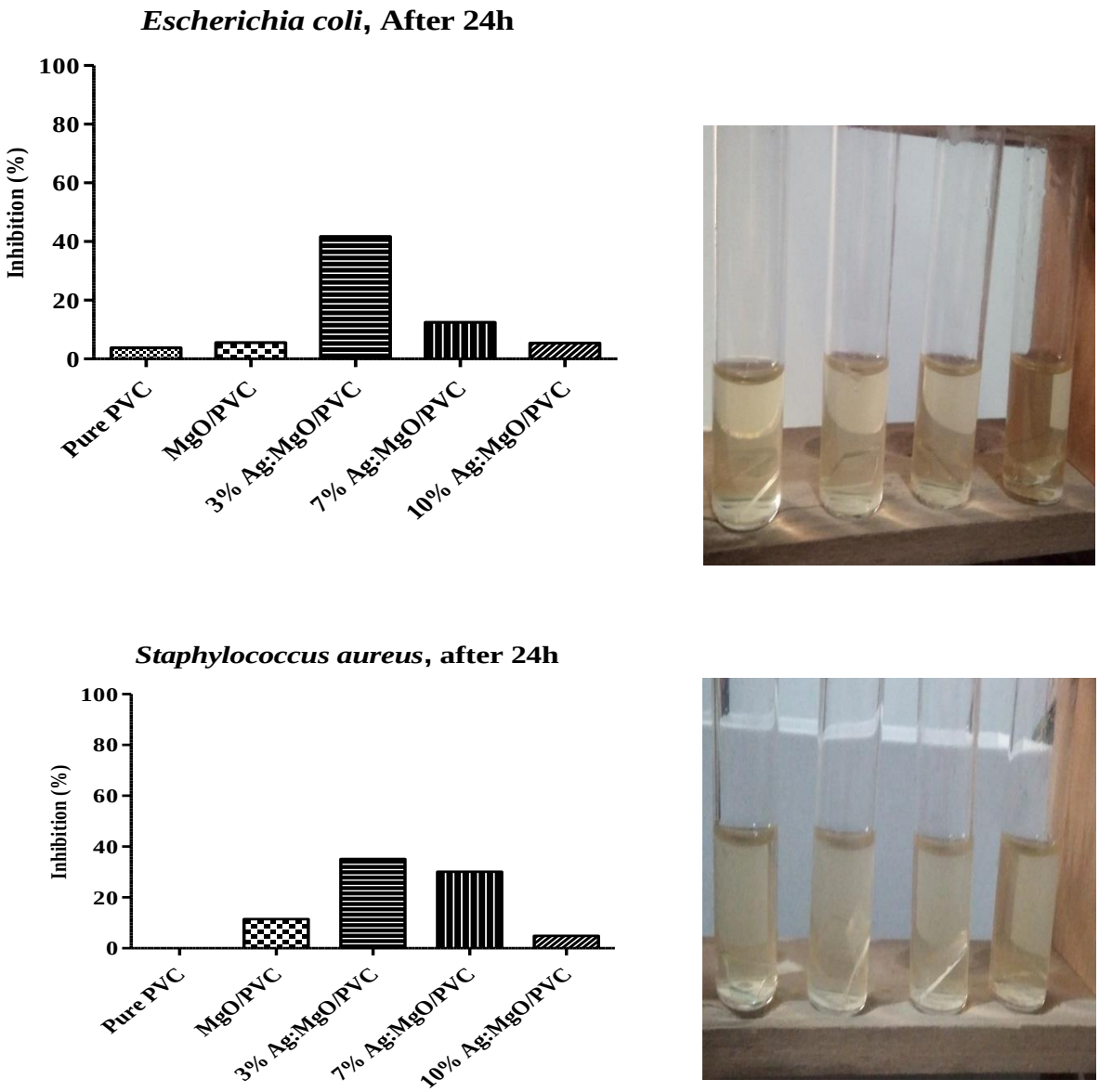

Fig IV.11: Antibacterial activity of Ag :MgO/PVC nanocompositesin absence and in presence of 3% , 7% and 10% Ag :MgO nanoparticles.

IV.5 Photocatalytic tests

The photocatalytic degradation of methylene blue by PVC pure,MgO/PVC and Ag:MgO/PVC nanocomposites are shown in the Figure (IV.12). The methylene blue degradation efficiency increases continuously with increases of time.After two hours of test period, the methylene blue

degradation is found to be 17%, 32% ,35%,46% and 52% for PVC ,MgO/PVC and Ag :MgO/PVC with concentrations 3%,7%,10% respectively .Comparing pure PVC and Ag:MgO/PVC the highest activity is observed for the 10% Ag :MgO /PVC nanocomposites can be assigned to the most efficient charge separation.On the first hand, the presence of a proper content of silver can reduce electron -hole recombination and increase the photocatalytic activity. On the other hand, the introduced of Ag doped MgO onto the PVC matrix increases the rate of electron transfer to dissolved oxygen.

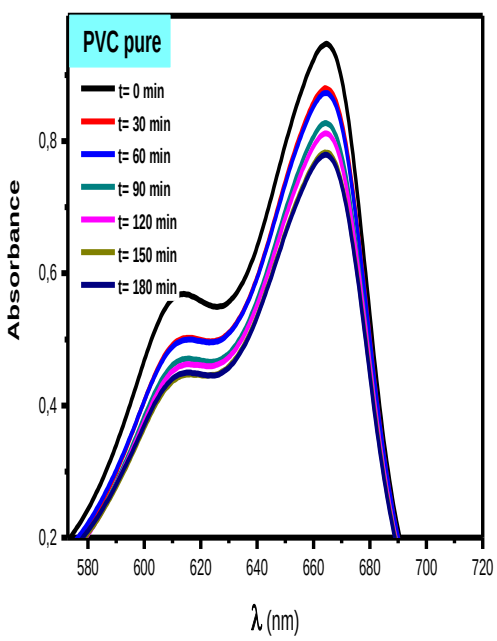

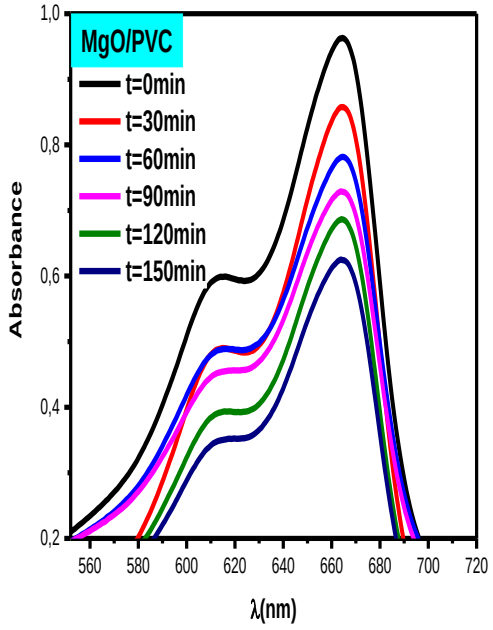

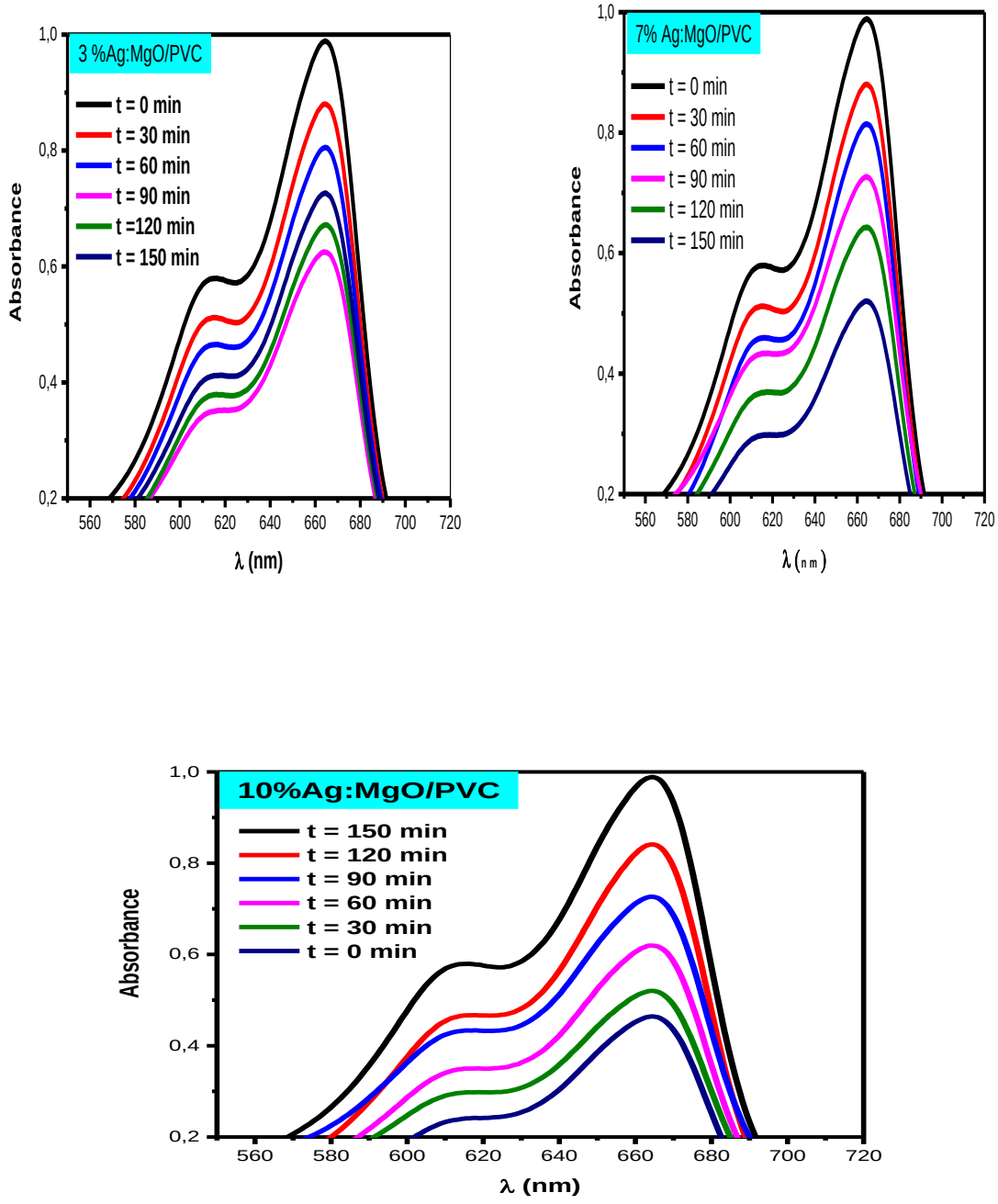

Fig IV.12: (a) Photocatalytic degradation and **(b)** the plots ln (C_0/C) versus time; **(c)** degradation rate of MB dye under UV light irradiation of PVC ; MgO/PVC and Ag:MgO/PVC nanocomposites thin films.

Figure IV.13 shows the kinetic plot between ln(C/C0) and irradiation time " t " for the photodegradation of methylene blue as a function of irradiation time for pure PVC ,MgO/PVC and Ag doped MgO/PVCnanocomposites at different concentrations and a linear relationship is observed.The rate constant (k) was calculated from the slopes of PVC,MgO/PVC,(3%,7%,10%) Ag :MgO/PVC nanocomposites and it was found to be 1.64 × 10-3 min^{-1}, 3.31 × 10^{-3} min^{-1}, 3.50 × 10^{-3} min^{-1} ,4.24 × 10-3 min^{-1}, 6.25 × 10-3 min^{-1} , respectively.This shows that Ag :MgO/PVC has enhanced photo catalytic degradation than pure PVC.

MgO /PVC has only a small effect on the MgO particle surface to reduce photocatalytic activity. In the case of Ag doped MgO, the photo catalytic activity increases due to the doping level has increased. This may be due to the highest porous structure, which provides more active sites for the adsorption of pollutant molecules. The diminution of the band gap (Eg) by the addition of Ag doped MgO in PVC matrix allow the absorption of more UV light energy and higher generation of electron-hole pairs [135]. This promotes the •OH and $O_2^{\bullet-}$ concentrations and thus improves the effectiveness of the photocatalyst. As a result, more electrons and holes can contribute in the photoreaction and so rise the removal of organic molecules [136].

(a) (b)

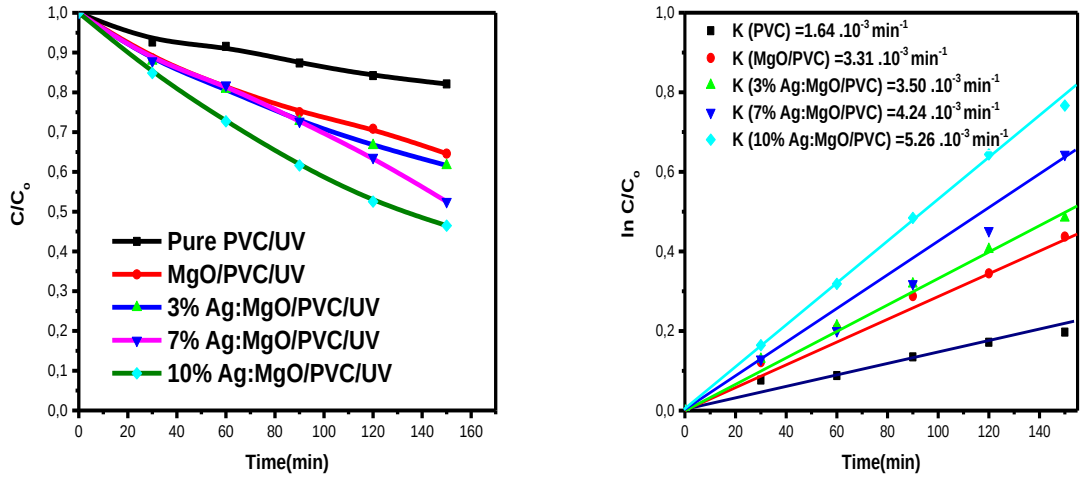

Fig IV.13: Decomposition of the dyes (MB) under UV light (a) C/Co vs time (b) ln C/Co vs time (c) % dye degration vs time.

IV.6 Photodegradation Mechanism

Photocatalytic mechanism of Ag:MgO/PVC nanocomposites is the same as the previous mechanism of CdS/PVC nanocomposites is mentioned in chapter III [112 , 113].

General Conclusion

Semiconductor nanostructure based polymer nanocomposites have attracted considerable focus in the present because of their potential applications due to the interesting physics and chemistry involved. Polymers provide good environmental stability to the incorporated nanostructures and also they act as capping and reducing agents. The critical parameters which decide the effect of nano particles on the properties of composites are size, shape, aspect ratio and particle-matrix interactions. Elongated semiconductor nanostructures like CdS and MgO are of special interest as they exhibit completely different electrical, optical and thermal properties when compared to their bulk counterpart.

The present work discusses the synthesis and characterization of CdS/PVC and Ag:MgO/PVC nanocomposites. CdS and Ag:MgO nanoparticles were synthesized by hydrothermal, sol gel methods , respectively. CdS/PVC and Ag:MgO/PVC composite thin films were synthesized by spin coating technique. The concentration of CdS/PVC was varied from 1% to 5% where as Ag:MgO/PVCwith concentration of 3%,7% and 10% in order to improve the structural, optical and morphological properties. The films nanocomposites are characterizedby XRD, SEM, AFM, FTIR, Raman and Optical studies. The antibacterialandphotocatalytic activitiesof the samples are tested.

The structural studies of CdS/PVC and Ag:MgO/PVC nanocomposites were done by XRD , Raman and Ftir. In the XRD of all samples , the intensity of structural peak of the polymers got intensified showing the improvement of polymer chains arrangement when doped with CdS and Ag:MgO. XRDand Raman of CdS/PVC confirms the formation of CdS nanoparticles with hexagonal phase in the PVC matrix. The structural studies (XRD & Ftir) of Ag:MgO/PVC nanocomposites indicates some additional diffraction peaks combined with the Face Centered Cubic (FCC) phase of metallic Ag,so the Ag :MgO/PVC samples are composed of metallic Ag and MgO phases. The crystallite size of CdS/PVC, Ag:MgO/PVC nanocomposites increased with the increase in CdS and Ag:MgO nanoparticles in the matrix, up to certain concentration.From the FTIR spectra a broad peak was observed at 904 cm-1, the intensity of the peak was decreased with the increase in Ag:MgO content due to interaction between Agdoped MgO and O–H bond of PVC .These results indicate that Ag:MgO/PVC nanocomposites resemble with the weak interaction between the polymer matrix and nanofiller particles.

General Conclusion

The morphological properties of the samples were investigated using SEM and AFM analysis. From SEM analysis, good dispersion of CdS in the lower concentrations compared to that of higher concentrations of CdS in the polymer matrices . This may be due to agglomeration of CdS nanoparticles in the matrix after a certain concentration. Also, it is observed that dispersed CdS nanoparticles create considerable change in morphology of the pure PVC . This is because the CdS nanocrystals fill the pores on the surface of the PVC. According to atomic force microscopy images (AFM), 10% Ag:MgO/PVC nanocomposites films have high porous structure as compared to undoped MgO/PVC. This indicates that Ag:MgO doping leads to an increased porosity and as a result leads to a large specific surface area.This is due to increase in the aggregation of tiny particles at some points that contributed in the increase in the roughness parameters .

The optical properties of pure polymers and their composites were studied using UV-Vis absorption spectroscopy and Photoluminescence studies.UV-Vis spectrum of all samples shows a transmission between 80 and 95% in the visible region .The band gap value of prepared CdS/PVC nanocomposites decreases with increase inconcentration of dopants between 4.07eV for 3.85 eV.Good decrease in band gap was observed in Ag:MgO/PVC samples to 3.69 eV .Photoluminescence analysis is carried out at room temperature with an excitation wavelength of 325 nm for the samples of CdS/PVC.The PL emission spectra indicate the interstitial cadmium defect states.

The photocatalytic study shows a good potential of PVC/CdSnanocomposites films for MB degradation under UV light irradiation.The higher concentration of CdS in the matrix produce 46% of colour degradation in methylene blue dye .In addition, Ag:MgO/PVC nanocomposite spheres exhibit a high efficiency and recyclability in catalysis, and an excellent antibacterial performance against Salmonella and Escherichia coli as well.Comparing pure PVC and MgO/PVC the highest activity is observed for the 10% Ag :MgO /PVC nanocomposites can be assigned to the most efficient charge separation.The antibacterial activity of Ag:MgO/PVC increases with decrease of the size of Ag:MgO nanoparticles.

References

[1] Yang Li, Eric Chun Yeung Liu, Nigel Pickett, Peter J. Skabara, Siobhan S. Cummins, Stephen Ryley, Andrew J. Sutherlandc and Paul O'Brien ; Synthesis and characterization of CdS quantum dots in polystyrene microbeads; J Mater Chem 15(2015) 1238-1243.http://dx.doi.org/10.1039/b412317d

[2] Ahmed A. El-Sayed, Ahmed M. Khalil, Mahmoud El-Shahat, Nahid Y. Khaireldin &. Samira T. Rabi ; Antimicrobial activity of PVC-pyrazolone-silver nanocomposites; J Macromol Sci A .53 (2016) 346-353.

[3] Ning Chen, Chaoying Wan, Yong Zhang, Yinxi Zhang ; Effect of nano-$CaCO_3$ on mechanical properties of PVC and PVC/Blendex blend ; J Polymer Testing. 23 (2004) 169–174.Doi : 10.1016/S0142-9418(03)00076-X

[4] T. Trindade,P. Obrien,N.L. Pickett ;Nanocrystalline Semiconductors: Synthesis, Properties and Perspectives; J Chem. Mater.13(2001)3843-3858.

[5] Bingcai Pan,Yingmei Xie,Shujuan ZhangLu ,and Weiming Zhang ;Visible Light Photocatalytic Degradation of RhB by Polymer-CdS Nanocomposites: Role of the Host Functional Groups ; JournalACS Appl. Mater. Interfaces2012, 4, 8, 3938–3943

[6] Yuncheng Caia, Dan Wua, Xiwei Zhua, Wei Wanga, Fatang Tana, Jianguo Chena, Xueliang Qiaoa,Xiaolin Qiu ; Sol-gel preparation of Ag-doped MgO nanoparticles with high efficiency forbacterial inactivation ; Journal Ceramics International .43 (2017) 1066–1072

[7] Y.H. Leung, A. Ng, X. Xu, Z. Shen, L.A. Gethings, M.T. Wong, C. Chan, M.Y. Guo,Y.H.Ng, A.B. Djurišić ; Mechanisms of antibacterial activity of MgO: non-ROS mediated toxicity of MgO nanoparticles towards Escherichia coli ; Journal Small NANO MICRO .10 (2014)1171–1183 .

[8] K. V. Gothelf, Handbook of Nanomaterials Properties, Science 338 (2012) 1159-1160.

[9] G.Murali, Thesis of doctorat ,University of TIRUPATI-517 502,India(2013)

[10] http://en.wikipedia.org/wiki/Nanotechnology

[11] Guozhong Cao,Nanostructures & Nanomaterials Synthesis, Properties & Applications, University of Washington, USA(2011)

[12] Glenn Clayton ;Nanoscience and Nanotechnology , 316 pages , ISBN-13 : 978-1788820769

References

[13] Stefan Spange ,Silke Grund ;Nanostructured Organic–Inorganic Composite Materials by Twin Polymerization of Hybrid Monomers; J Adv. Mater. 21(2009)2111–2116. https://doi.org/10.1002/adma.200802797

[14] Eldho Elias ;Development of Biodegradable Polymer Nanocomposites for Various Applications ; Mahatma Gandhi University, Kottayam, Kerala India February 2019

[15] Elizabeth Francis ; Design and development of based on POLY VINYL CHLORIDE System ; Doctoral thesis ; India ; 2018

[16] P. DEVENDRAN ;Synthesis and characterization of cadmium sulfide nanoparticles using signal source precursor for photocatalytic applications; Doctoral thesis ; UNIVERSITY OF MADRASin ;India, 2015

[17] Yong Ding and Zhong Lin Wang ; Structure Analysis of Nanowires and Nanobelts by Transmission Electron Microscopy; J. Phys. Chem. B2004,108,12280-12291

[18] Gul Amin;ZnO and CuO Nanostructures: Low Temperature Growth , Characterization, their Optoelectronic and Sensing Applications;Linköping University;2012

[19] Kittel, C. ," Introduction to Solid State Physics." (2005).

[20] Ganesh Skandan and Amit Singhal ,Perspectives on the Science and Technology of Nanoparticle Synthesis. Nanomaterials handbook / [edited by] Yuri Gogotsi.

[21] YURY GOGOTSI ;Nanomaterials Handbook ; International Standard Book Number-13: 978-0-8493-2308-9 (Hardcover),2006

[22] G.Cao, 2nd edition, World scientific series in nanoscience and nanotechnology (2004) p-433, ISBN-13:978-1860944802.

[23] Guozhong Cao;Nanostructures & nanomaterials Synthesis, Properties G;Z: Applications; University of Washington; USA ISBN 1-86094-4159 ISBN 1-86094-480-9

[24] Salem, S.S., Fouda, A; Green Synthesis of Metallic Nanoparticles and Their Prospective Biotechnological Applications: an Overview. Biol Trace Elem Res (2020). https://doi.org/10.1007/s12011-020-02138-3

[25] Cristina Buzea , Ivan I Pacheco , Kevin Robbie ; Nanomaterials and nanoparticles: Sources and toxicity ;Queen’s University;Canada .

[26] SADAO ADACHI ; Properties of Semiconductor Alloys: Group-IV, III–V and II–VI Semiconductors; Gunma University; Gunma ; Japan(1950)

References

[27] Abdul Majid Maryam Bibi; Cadmium based II-VI Semiconducting Nanomaterials Synthesis Routes and Strategies; Series editor Carlos P. Bergmann, Porto Alegre, Brazil , University of Gujrat Gujrat, Pakistan https://doi.org/10.1007/978-3-319-68753-7

[28] M.MalekiaSh.MirdamadiaR.GhasemzadehaM.Sasani Ghamsarib; Preparation and characterization of cadmium sulfide nanorods by novel solvothermal method; Journal Materials Letters ; Volume 62, Issues 12–13, 30 April 2008, Pages 1993-1995 https://doi.org/10.1016/j.matlet.2007.10.062

[29] Crystallographic structures of CdS Rittner ES and schulman JH, J. Phys. chem., 1943:47;537.

[30] Haider, Adawiya J., Ali M. Mousa, et. Al., Journal of Semiconductor Technology and Science 8(4) (2008).

[31] Mohammad Moslem Imani, Mohsen Safaei ; Optimized Synthesis of Magnesium Oxide Nanoparticles asBactericidal Agents ; Hindawi Journal of Nanotechnology.(2019) https://doi.org/10.1155/2019/6063832

[32] cristalography MgOVenkateswaran U, Chandrasekhar M and Chandrasekhar HR, Phys. Rev. B, 1984:30;3316.

[33] Suzuki T, Yagi T, Akimoto S, Kowamura T, Tayoda S, Endo S, J. Appl. Phys., 1983:54;748-751.

[34] Gao, S. Z., Wang, J. S., & Gao, X. W. (2013). Modeling and advanced control method of PVC polymerization process. Journal of Process Control, 23(5), 664-681.

[34] Bao, Y.Z., et al; Preparation and characterization of poly(viny1 ch1oride)llayered double hydroxides nanocomposite via in situ suspension polymerization; J. Appl. Polym. Sci. 102(2), 1471 -1477,2006.

[35] Nalwa, H. S. (2003) ; Handbook of Organic-Inorganic Hybrid Materials and Nanocomposites.American Scientific Publishers

[36] Augier, L., et al. Influence of the wood fiber filler on the internal recycling of poly(viny1 chloride)-based composites, Polym. Degrad. Stab. 92(7), 1 169-1 176,2007.

[37] Roy, M., Nelson, J. K., MacCrone, R. K., Schadler, L. S., Reed, C. W., & Keefe, R. (2005); Polymer nanocomposite dielectrics-the role of the interface;J IEEE Transactions on Dielectrics and Electrical Insulation. 12(4), 629-643.

References

[38] Jiang, H. & Kamdem, D.P. Effects of copper amine treatment on mechanical properties of PVCIwood-flour composites, J. Vinyl Add. Tech. 10(2), 70-78,2004.

[39] Journal Materials (Basel). 2015 Jun; 8(6): 3377–3427. doi: 10.3390/ma8063377

[40] Serena Coiai,1 Elisa PassagliaAndrea Pucci, and Giacomo Ruggeri ; Nanocomposites Based on Thermoplastic Polymers and Functional Nanofiller for Sensor Applications

[41] Thermal and Electrical Properties of Nanocomposites, Including Material Processing, Roman KOCHETOVMaster of Electrical Engineering, Lappeenranta University of Technology, FinlandMaster ofTechnique and Technology,Saint-Petersburg State Electrotechnical University‘LETI’, Russia,2012

[42] W Zheng, XH Lu, SC Wong, J Appl Polym Sci 91 (2004) 2781

[43]. H Fukushima. LT Drzal, Proceedings of the 14th international conference on composite materials (ICCM-14), San Diego (2003) 532

[44] W Zheng, SC Wong, Compos Sci Technol 63 (2003) 225

[45] PG Collins, P Avouris, Scient Am 283 (2000) 62

[46]. RA Vaia, EP Giannelis, Macromolecules 30 (1997) 7990

[47]. RA Vaia, EP Giannelis, Macromolecules 30 (1997) 8000

[48] Althues, H.; Henle, J.; Kaskel, S. Chem. Soc. Rev. 2007; 36:1454

[49]. Okada, A.; Usuki, A. Mater. Sci. Eng. C. 1995; 3: 109.

[51] Zhou, X.D., Gu, H.C; J. Mater. Sci. Lett. 21(2002) 577.

[52] P Musto, Polymer .45 (2004) 1697

[53] OSMANIA ; Synthesis and Characterization of Nanocomposites: Photocatalysis and Solid Polymer ElectrolyteApplications; UNIVERSITYHyderabad,-Indian ,2014

[54] S. C. Tjong and Y.-W. Mai ; Handbook of Physical properties and applications of polymer nanocomposites ; ISBN 978-1-84569-672-6 (2010)

[55] Surekha Shrimantrao Jogdand, Effect of Polymer, Ligand and Synthetic Route on Magnetic Behaviour of Cobalt Oxide, Cobalt Ferrite and Cobalt Metal Nanoparticles,Thesis doctorial, Savitribai Phule Pune University,Pune-411007

[56] Ghazaleh Allaedini Siti Masrinda Tasirin Payam Aminayi ;Magnetic properties of cobalt ferrite synthesized by hydrothermalmethod ;J Int Nano Lett (2015) 5:183–186DOI 10.1007/s40089-015-0153-8

[57] LARRY L. HENCH* and JON K. WEST, The Sol-Gel Process, Chem. Rev, 1990, 90, 33-72

[58] John D. MACKENZIE,APPLICATIONS OF THE SOL-GEL PROCESS , Journal of Non-Crystalline Solids 100 (1988) 162-168 North-Holland, Amsterdam

[59] F. C. Krebs, Fabrication and processing of polymer solar cells : A review of printing and coating techniques, Solar Energy Materials Solar Cells, 2009, p 394-412.

[60] THOMAS CARON, « Développement de capteurs chimiques d'explosifs basés sur la détection par fluorescence», THESE DE DOCTORAT, Nationale Supérieure de Chimie de Montpellier, 2010.

[61] Claudine PORCEL ,« Etude de la construction de films de polyélectrolytes par nébulisation», doctoral thesis , Université LOUIS PASTEUR,2006

[62] S. E. Dann, Reactions and characterization of solids, Royal Society of Chemistry, USA (2002).

[63] B. D. Cullity, S. R. Stock, Elements of X-ray Diffraction, Prentice Hall, 3rd edition (2001)

[64] A. I. Gusev, A. A. Rempel, Nanocrystalline Materials, (2004), Cambridge International Science Publishing

[65] R. M. Silverstein, F. X. Webster, Spectroscopic Identification of Organic Compounds, 6th edition, John Wiley and Sons Inc. (1998)

[66] V.Saptari, Fourier-Transform Spectroscopy Instrumentation Engg. (2003) SPIE- The International Society for Optical Engineering, Washington, USA.

[67] F. Huth, A. Govyadinov, S. Amarie, W. Nuansing, F. Keilmann, R. Hillenbrand, Nano Lett. 2012, 12, 3973−3978.

[68] M. Cardona, R. Merlin, Light scattering in solids I-X (Topics in Applied Physics), edited by Springer, Berlin (1983-2007).

[69] N. Esser and J. Geurts, Optical Characterization of Epitaxial Semiconductor Layers, Edited by G. Bauer and W. Richter, Springer, Berlin, 129-202 (1996).

[70] . J. Geurts, Prog. Crys. Grow. And Charact., 32, 185-224 (1996).

[71] S. Entani, S. Sakai, Y. Matsumoto, H. Naramoto, T. Hao, Y. Maeda, J. Phys. Chem. C 2010, 114, 20042–20048.

[72] L. E. Brus, J. Chem. Phys., 79 (1983) 5566

[73]. S. K. Kulkarni, Nanotechnology-Principles and Practices, Capital books (2007).

[74] T. H. Gfroerer, "Photoluminescence in Analysis of Surfaces and Interfaces", Encyclopedia of Analytical Chemistry, Edt. R. A. Meyers, John Wiley & Sons Ltd. (2000) 9209

[75] F. Williams, Theoretical Basis for Solid-State Luminescence, Academic Press, New York, (1966)

[76] Quddos, A; Samtio, N.H.; Syed, A.M. j. Phys. Cof. Ser. 2013, 439, 012011.

[77] Leonard, D.N.; Chandler, G.W.; Seraphin, S. Characterization of Materials : John Wiley and Sons 2012

[78] D. Shindo, T. Oikawa; Analytical Electron Microscopy for Material Science; Springer-Verlag Tokyo (2002)

[79] J. I. Goldstain, D. E. Newbury, P. Echlin, D. C. Joy, C. Fiori, E. Lifshin; Scanning Electron Microscopy and X-ray Microanalysis; Plenum Press; NewYork (1981)

[80] Fabiula Danielli Bastos , Carlos Henrique Scuracchio, Polímeros .24 (6) (2014)

[81] N. Yao, Z. L. Wang; Handbook of Microscopy for Nanotechnology (2005).

[82] S. O. Vansteenkiste, M. C. Davies, C. J. Roberts, S. J. B. Tenter and P. M. Williams, Prog. Surf. Sci. 1998, 57, 95

[83] N. B. Holland and R. E. Marchant; J. Biomed. Mater. Res. 2000, 51, 307

[84] Francis Opoku, Ephraim M. Kiarii, Penny P. Govender and Messai Adenew Mamo; Metal Oxide Polymer Nanocomposites in Water Treatments;University of Johannesburg, Johannesburg, South Africa

[85] S. Malato,P. Fernández-Ibáñez, M. Maldonado, J. Blanco, and W. Gernjak; Decontamination and disinfection of water by solar photocatalysis: recent overview and trends;J Catalysis Today 147, pp. 1-59(2009)

[86] Violeta Melinte , Lenuta Stroea and Andreea L. Chibac-Scutaru ; Polymer Nanocomposites for Photocatalytic Applications;J Catalysts.9(2019) doi:10.3390/catal9120986

[87] Huang, J.-H., Ibrahem, M. A. and Chu, C.-W; Interfacial engineering affects the photocatalytic activity of poly (3-hexylthiophene)-modified TiO2; RSC Advances. 3(2013)

[88] Qadir, D., Mukhtar, H. and Keong, L. K ; Mixed matrix membranes for water purification applications ; Separation & Purification Reviews 46, pp. 62-80(2017)

[89] Serena Coiai, Elisa Passaglia , Andrea Pucci , Giacomo Ruggeri ;Nanocomposites Based on Thermoplastic Polymers and Functional Nanofiller for Sensor Applications. J materials .8(2015) 3377-3427. http://dx.doi. 10.3390/ma8063377

[90] V. Mathur, K. Sharma ; Small Angle X-Ray Scattering Analysis of PS/CdS, PVC/CdS & PMMA/CdSPolymeric Nanocomposites; JSSNT 12(2014) 420-422. 0.1380/ejssnt.2014.420

[91] M.A. RamazAnov,Y.Babayev; Preparation and Structure Nanocomposites based on Zinc Sulfide in Polyvinylchloride; Journal of Non -Oxide Glasses 10 (2018)1-6.

[92] Ahmed A. El-Sayed, Ahmed M. Khalil, Mahmoud El-Shahat, Nahid Y. Khaireldin &. Samira T. Rabi ; Antimicrobial activity of PVC-pyrazolone-silver nanocomposites; J Macromol Sci A . 53 (2016) 346-353.

[93] Jorge M.Meichtry,Christophe Colbeau-Justin,GracielaCusto,Marta I.Litter ;TiO2-photocatalytic transformation of Cr (VI) in the presence of EDTA: Comparison of different commercial photocatalysts and studies by Time Resolved Microwave Conductivity. J Appl Catal B-Environ .144 (2014) 189-195.

[94] P. Devendran, T. Alagesan, K. Pandian ; Single pot microwave synthesis of CdS nanoparticles in ionic liquid and their photocatalytic application; Asian J Chem. 25(2013) S79 – S82

[95] Changjun Yang,Chuqing Gong,Tianyou Peng,Kejian Deng,Ling Zan ; High photocatalytic degradation activity of the polyvinyl chloride (PVC) – vitamin C (VC)–TiO2 nano-composite film.J Hazard Mater .178(2010) 152-156. https://doi.org/10.1016/j.jhazmat.2010.01.056

[96] Desong Wang,Cai Bao,Qingzhi Luo,Rong Yin,Xueyan Lib,Jing An, Zexuan Xu ; Improved visible-light photocatalytic activity and anti-photocorrosion of CdS nanoparticles surface-modified by conjugated derivatives from polyvinyl chloride;J Environ Chem Eng. 3(2015) 1578-1585. https://doi.org/10.1016/j.jece.2015.05.013

[97] A.Khorsand Zaka,W.H.Abd. Majid,M.E.Abrishami,RaminYousefi ; X-ray analysis of ZnO nanoparticles by Williamson–Hall and size–strain plot methods ;Solid State Sci 13(2011)251- 256.https://doi.org/10.1016/j.solidstatesciences.2010.11.024

[98] Ramneek Kaur ,S.K.Tripathi ; Study of conductivity switching mechanism of CdSe/PVP nanocomposite for memory device application. J Microelectron Eng 133(2015) 59-65.https://doi.org/10.1016/j.mee.2014.11.010

[99] V.S.Solodovnichenko,V.Polyboyarov,A.Zhdanok,A.B.Arbuzov, E.S.Zapevalova,Yu.G.Kryazhev,V.A.Likholobov; JProcedia Eng 152 (2016) 747 – 752 https://doi.org/10.1016/j.proeng.2016.07.684

[100] F. Kajzar; Organic Thin Films for Waveguiding Nonlinear Optics. CRC Press (Ed)(1996) pp.829

[101] M. Veronelli, M. Mauro, S. Bresadola ; Polym. Degrad. Stab. 66 (1999) 349.

[102] J.F. Rabek; Mechanisms of Photophysical Processes and Photochemical Reactions in Polymers: Theory and Applications; Wiley; New York (1987) (Chapter 14).

[103] S.P. Pappas, F.H. Winslow (Eds.), Photodegradation and Photostabilization in Coatings, ACS Symposium Series 151, American Chemical Society, Washington, DC, 1981.

[104] Mayank Pandey,Girish M Joshi,Amitava Mukherjee and P Thomas ; Electrical properties and thermal degradationof poly(vinyl chloride)/polyvinylidenefluoride/ZnO polymer nanocomposites ;J Polym Int(2016)

[105] Jagdish K. Vij ; Advances in Liquid Crystals,Advances in Chemical Physics; John Wiley & Sons (Ed) (2009) pp .259-261.

[106] R Swanepoel ; Determination of the thickness and optical constants of amorphous Silicon; J. Phys. E: Sci. Instrum .16(1983) 1214-1222. https://doi.org/10.1088/0022-3735/16/12/023

[107] M. Caglar, Y. caglar, S. Ilican ; The determination of the thickness and optical constants of the ZnO crystalline thin film by using envelope method ; J Optoelectron Adv M .8 (2006)1410 - 1413.

[108] S. Chaure , N.B. Chaure , R.K. Pandey , A.K. Ray ;Stoichiometric effects on Optical properties of cadmium sulphide quantum dots; IET Circuits Devices Syst .1(2007) 215–219.https://doi.org/10.1049/iet-cds:20070048

[109] V. Singh, P.Chauhan ; Structural and optical characterization of CdS nanoparticles prepared by chemical precipitation method ; J Phys Chem Solids. 70 (2009) 1074–1079. https://doi.org/10.1016/j.jpcs.2009.05.024

[110] Desong Wang, Lei Shi , Qingzhi Luo , Xueyan Li , Jing An ; An efficient visible

light photocatalyst prepared from TiO2 and polyvinyl chloride; J Mater Sci. 47(2012) 2136–2145.https://doi.org/10.1007/s10853-011-6014-6

[111] Genkuo Nie, Guozhu Li, Li Wang, Xiangwen Zhang ; Nanocomposites of polymer brush and inorganicnanoparticles: preparation, characterization and application. Polym Chem 4 (2016) 753–769 .https://doi.org/10.1039/C5PY01333J

[138] Changjun Yang, Kejian Deng, Tianyou Peng, Ling Zan; Enhanced Solid-Phase Photocatalytic Degradation Activity of a Poly(vinyl chloride)-TiO2 Nanocomposite Film with Bismuth Oxyiodide ; J Chem. Eng. Technol. 2011, 34, 886–892.

[139] Changjun Yang, Chuqing Gong, Tianyou Peng, Kejian Deng, Ling Zan ; High photocatalytic degradation activity of the polyvinyl chloride (PVC)–vitamin C (VC)–TiO2 nano-composite film ; Journal of Hazardous Materials. 178 (2010) 152–156.

[112] In-Yup Jeon and Jong-Beom Baek ; Nanocomposites Derived from Polymers and Inorganic Nanoparticles ; Journal of Materials.3(2010) 3654-3674 https://doi.org/10.3390/ma3063654

[113] Saheli Roy,Suneel Kumar Srivastava,Vikas Mittal ;Facile noncovalent assembly of MWCNT-LDH and CNF-LDHas reinforcing hybrid fillers in thermoplastic polyurethane/nitrilebutadiene rubber blends ; J Polym Res (2016) 23: 36 DOI 10.1007/s10965-016-0926-4

[114] Sunil Meti, Udaya K. Bhat, M. Rizwanur Rahman; Colossal dielectric permittivity of Nylon-6 matrix-based composites with nano-TiO2 fillers; Applied Physics A (2020) 126:264 https://doi.org/10.1007/s00339-020-3445-4

[115] Shalini Agarwal, Vibhav K. Saraswat ; Structural and optical characterization of ZnO doped PC/PS blendnanocomposites; Journal Optical Materials (2015) http://dx.doi.org/10.1016/j.optmat.2015.01.024

[116] G. Balakrishnan, R. Velavan, Khalid Mujasam Batoo, Emad H. Raslan; Microstructure Optical and Photocatalytic Properties of MgO Nanoparticles (2020) 10.1016/j.rinp.2020.103013

[117] Zhen-Xing Tang , and Bin-Feng Lv ; MgO nanoparticles as antibacterial agent: preparartion and activity ; Brazilian Journal of Chemical Engineering . 31(2014) : 591 - 601

[118] Yuncheng Cai, Dan Wu, Xiwei Zhu, Wei Wang,Fatang Tan, Jianguo Chen, Xueliang Qiao, XiaolinQiu ; Sol-gel preparation of Ag-doped MgO nanoparticles with high

efficiency for bacterial inactivation ; Journal Ceramics International 10.1016/j.ceramint.2016.10.041

[119] Upasana Gulati,U. Chinna Rajesh, Diwan S. Rawatb and Jeffrey M. Zaleski ; Development of Magnesium Oxide-Silver Hybrid Nanocatalysts for Synergistic Carbon Dioxide Activation to Afford Esters and Heterocycles at Ambient Pressure ; J. N ame (2012) 1-3 .https://doi.org/10.1039/C9GC04040D

[120] O¨zlem Altıntas Yıldırım, Husnu Emrah Unalan, and Caner Durucan ; Highly Efficient Room Temperature Synthesis of Silver-Doped Zinc Oxide(ZnO:Ag) Nanoparticles: Structural, Optical, and Photocatalytic Properties ; J. Am. Ceram. Soc.96(3) 766–773 (2013) .doi : 10.1111/jace.12218

[121] S.M. Hosseini, I. Abdolhosseini Sarsari⇑, P. Kameli, H. Salamati ; Effect of Ag doping on structural, optical, and photocatalytic propertiesof ZnO nanoparticles ; Journal of Alloys and Compounds 640 (2015) 408–415 10.1016/j.jallcom.2015.03.136

[121] Dorel Feldman ; Poly(vinyl chloride) Nanocomposites ; Journal of Macromolecular Science, Part A: Pure and Applied Chemistry.51 (2014) 659–667 . https://doi.org/10.1080/10601325.2014.925265

[122] T. J. Chem ; Turkish Journal of Chemistry. 28(2004) 725-729.

[123] Ziwei Deng, Haibao Zhu, Bo Peng, Hong Chen, Yuanfang Sun, Xiaodong Gang, Pujun Jin, and Juanli Wang ; Synthesis of PS/Ag Nanocomposite Spheres with Catalytic and Antibacterial Activities ; J ACS Appl. Mater. Interfaces .4 (2012) 5625−5632 . dx.doi.org/10.1021/am3015313

[124] Xiaofang Zhou ; Ag-doping improving the detection sensitivity of bolometer based on ZnO thin films ;J Vacuum .117 (2015) 47-49

[125] Khuram Shahzad Ahmad , Shaan Bibi Jaffri ; Phytosynthetic Ag doped ZnO nanoparticles: Semiconducting green remediators ; J Open Chem.16(0218) 556–570. https://doi.org/10.1515/chem-2018-0060

[126] M. Z. Kassaee, M. Mohammadkhani, A. Akhavan and R. Mohammadi ; Structural Chemistry. 22(2011) 11–15.

[127] V. V. Vodnik, J. V. Vuković and J. M. Nedeljkovi ; Colloid and Polymer Science .287(2009) 847–851.

[128] R.Kandulna , R.B. Choudhary1 , P. Maji ; Ag-doped ZnO Reinforced Polymeric Ag:ZnO/PMMA Nanocomposites as Electron Transporting Layer for OLED Application ; J Inorg Organomet Polym (2017)
DOI 10.1007/s10904-017-0639-0

[129] A Almontasser1, A Parveen2 and A Azam ; Synthesis, Characterization and antibacterial activity of Magnesium Oxide (MgO) nanoparticles ; J IOP Conf. Ser: Mater. Sci. Eng.577 (2019) 012051.

[130] Ljerka Kratofil Krehula1 ,Ana Papic´, Stjepko Krehula ,Vanja Gilja, Lucija Foglar, Zlata Hrnjak-Murgic´ ; Properties of UV protective films of poly(vinyl-chloride)/TiO2nanocomposites for food packaging ;J Polym. Bull.(2016)

[131] K B Bhavith , Anju K Nair, Hanna Mariya, Jiya Jose, Anshida Mayeen, Kala M S, Abhijit Saha,d Sabu Thomas, Oluwatobi S Oluwafemi, and Nandakumar Kalarikka ; In-situ Dose dependent Gamma ray Irradiated Synthesis of PMMA-Ag nanocomposites films for multifunctional applications ; New Journal of Chemistry (2018). DOI: 10.1039/C8NJ02684J

[132] N. Siddiqui, A. Bhardwaj, A. Shaikh, A. Jain and S. K. Verma; Oriental Journal of Chemistry. 30 (2014) 1777–1783.

[133] Saravanan Natarajan Jyoti Kumari D. Shanthana Lakshmi Ankita Mathur M. Bhuvaneshwari Abhinav Parashar Mrudula Pulimi N. Chandrasekaran Amitava Mukherjee ; Differences in antibacterial activity of PMMA/TiO2/Ag nanocomposite on individual dominant bacterial isolates from packaged drinking water and their consortium under UVC and dark conditions ; J Applied Surface Science (2015)

[134] Nadia Baniasadi, Ashraf Kariminik , Sayed Mohamad Reza Khoshroo ; Synthesis of MgO Nanoparticles and Their Antibacterial Properties on Three Food Poisoning Causing Bacteria ;Iran J Med Microbiol.(2019) ;13(5): 380-391

[135] K. Mageshwari, Sawanta S. Mali, R. Sathyamoorthy, Pramod S. Patil ; Template-free synthesis of MgO nanoparticles for effective photocatalytic applications ; Journal Powder Technology. 249 (2013) 456–462.

[136] Y. Li, W. Zhang, J. Niu, Y. Chen ; Surface-coating-dependent dissolution aggregation and reactive oxygen species (ROS) generation of silver nanoparticles under different irradiation conditions ; J Environ. Sci. Technol. 47 (2013) 10293-10301.

[138] Sungmin Cho, Wonyong Choi ; Solid-phase photocatalytic degradation of PVC–TiO2 polymer composites ; Journal of Photochemistry and Photobiology A: Chemistry. 143 (2001) 221–228

Abstract

The interdisciplinary nature of polymer nanocomposite advanced in the materials, electronics, healthcare, manufacturing, and energy sectors. Polymers provide good environmental stability to the incorporated nanostructures and also they act as capping and reducing agents.

CdS and Ag:MgO nanoparticles were synthesized by hydrothermal, sol-gel methods, respectively. CdS/PVC and Ag:MgO/PVC nanocomposites have been prepared by spin coating technique. The prepared samples are characterized by XRD, FTIR, Raman, SEM, AFM, PL, and UV analysis. The antibacterial and photocatalytic activities of the prepared samples are examined.

The structural properties of the CdS/PVC nanocomposites have been studied using X-ray diffraction, FTIR and Raman methods. The CdS/PVC have been observed in hexagonal wurtzite structure nature.The structural studies of Ag:MgO/PVC nanocomposites are composed of metallic Ag and MgO phases and indicate that all the samples nanocomposites resemble the interaction between the polymer matrix and nanofiller particles.

The surface morphology of the prepared nanocomposites has been observed by using SEM and AFM. The scanning electron microscope and atomic force microscopy images show that almost the particles are uniformly distributed in the polymer matrix with agglomeration of nanoparticles in the matrix after a certain concentration. .

The optical properties have been examined using UV-Vis spectroscopy and Photoluminescence studies.The addition of CdS ,Ag:MgO nanoparticles in PVC polymer shifts the absorption edge wavelength towards the longer wavelength which reduces the band gap value lower than that of the pure PVC .The band gap values for the samples nanocomposites have been calculated to lie in the range of 4.1eV to 3.69eV.

The antibacterial activity of Ag:MgO/PVC nanocomposites are tested against the bacterial strains Staphylococcus aureusand Escherichia coli. The Ag :MgO addition is enhanced the inhibition than pure PVC.

The degradation of methylene blue dye by the pure PVC, CdS/PVC, and Ag:MgO/PVC nanocomposites are carried out by a specially designed photocatalytic reactor. The percentage of methylene blue dye degradation by the pure PVC, CdS/PVC and Ag:MgO nanocomposites

17%, 46%, and 52% respectively.The degradation efficiency of Ag:MgO/PVC is found better than the other samples.

Key words : Nanocomposites; CdS; MgO; PVC; XRD and photocatalysis

ملخص

تعمل الطبيعة متعددة التخصصات لمركبات البوليمر النانوية على التقدم في قطاعات المواد والإلكترونيات والصحة والتصنيع والطاقة. توفر البوليمرات استقرارًا بيئيًا جيدًا للبنى النانوية المدمجة ، كما أنها تعمل كعوامل للتغطية والحد.

تم تصنيع الجسيمات النانوية CdS, MgO: Ag بواسطة hydrothermal، sol gel methodsعلى التوالي.

تم تحضير المركبات النانويةCdS / PVC و MgO: Ag / PVC بواسطة تقنية spin coating. تتميز العينات المعدة بتحليل XRD و FTIR و Raman و SEM و AFM و PL و UV. يتم فحص الأنشطة المضادة للبكتيريا والتحفيز الضوئي للعينات المحضرة.

تمت دراسة الخصائص الهيكلية للمركبات النانوية CdS / PVC باستخدام طرق حيود الأشعة السينية وطرق FTIR و Raman. لوحظ وجود CdS / PVC في طبيعة بنية wurtzite سداسية الشكل. تتكون الدراسات الهيكلية لـ Ag: MgO / PVC nanocomposites من أطوار Ag و MgO وتشير إلى أن جميع العينات متناهية الصغر مع وجود التفاعل بين مصفوفة البوليمر وجزيئات النانو.

وقد لوحظ التشكل السطحي للمركبات النانوية المحضرة باستخدام SEM و AFM. يُظهر المجهر الإلكتروني الماسح والصور المجهرية للقوة الذرية أن الجسيمات تقريبًا موزعة بشكل موحد في مصفوفة البوليمر مع تكتل الجسيمات النانوية في المصفوفة بعد تركيز معين. .

تم فحص الخواص البصرية باستخدام التحليل الطيفي للأشعة المرئية وفوق البنفسجية ودراسات اللمعان الضوئي PL، وإضافة جزيئات CdS و Ag: MgO النانوية في بوليمر PVC يغير طول موجة الامتصاص نحو الطول الموجي الأطول مما يقلل من قيمة فجوة النطاق أقل من قيمة PVC النقي. تم حساب قيم فجوة النطاق للعينات المركبات النانوية لتقع في النطاق من 4.1 فولت إلى 3.69 فولت.

يتم اختبار النشاط المضاد للبكتيريا لـ Ag: MgO / PVC النانوي ضد السلالات البكتيرية Staphylococcus aureus و Escherichia coli. إن إضافة Ag: MgO تعزز التثبيط أكثر من PVC النقي.

يتم إجراء تحلل صبغة الميثيلين الزرقاء بواسطة مادة PVC النقية ، CdS / PVC ، و Ag: MgO / PVC بواسطة مفاعل تحفيز ضوئي مصمم خصيصًا. تم العثور على النسبة المئوية لتحلل صبغة الميثيلين الزرقاء بواسطة مركبات PVC النقية ، CdS / PVC و Ag: MgO nanocomposites، 17%، 46%و 52%على التوالي. تم العثور على كفاءة تحلل MgO: Ag / PVC أفضل من العينات الأخرى.

الكلمات المفتاحية: المركبات النانوية. CdS ؛ MgO ؛ PVC ؛ DRX والتحفيز الضوئي

Résumé

La nature interdisciplinaire du nanocomposite polymère fait progresser les secteurs des matériaux, de l'électronique, de la santé, de la fabrication et de l'énergie. Les polymères fournissent une bonne stabilité environnementale aux nanostructures incorporées et agissent également comme agents de coiffage et de réduction.

Les nanoparticules CdS et Ag: MgO ont été synthétisées par des méthodes hydrothermales, sol gel, respectivement. Les nanocomposites CdS / PVC et Ag: MgO / PVC ont été préparés par technique de revêtement par centrifugation. Les échantillons préparés sont caractérisés par analyse XRD, FTIR, Raman, SEM, AFM, PL et UV. Les activités antibactériennes et photocatalytiques des échantillons préparés sont examinées.

Les propriétés structurales des nanocomposites CdS / PVC ont été étudiées à l'aide des méthodes de diffraction des rayons X, FTIR et Raman. Les CdS / PVC ont été observés dans la nature de la structure hexagonale wurtzite.Les études structurales des nanocomposites Ag: MgO / PVC sont composés de phases métalliques Ag et MgO et indiquent que tous les échantillons de nanocomposites ressemblent à l'interaction entre la matrice polymère et les particules de nanofiller.

La morphologie de surface des nanocomposites préparés a été observée en utilisant SEM et AFM. Les images au microscope électronique à balayage et en microscopie à force atomique montrent que presque les particules sont uniformément réparties dans la matrice polymère avec agglomération de nanoparticules dans la matrice après une certaine concentration. .

Les propriétés optiques ont été examinées à l'aide de la spectroscopie UV-Vis et des études de photoluminescence.L'ajout de nanoparticules CdS, Ag: MgO dans le polymère de PVC décale la longueur d'onde du bord d'absorption vers la longueur d'onde plus longue, ce qui réduit la valeur de la bande interdite inférieure à celle du PVC pur. Les valeurs de la bande interdite pour les échantillons de nanocomposites ont été calculées comme étant comprises entre 4,1 eV et 3,69 eV.

L'activité antibactérienne des nanocomposites Ag: MgO / PVC est testée contre les souches bactériennes Staphylococcus aureus et Escherichia coli. L'ajout d'Ag: MgO améliore l'inhibition par rapport au PVC pur.

La dégradation du colorant bleu de méthylène par les nanocomposites PVC pur, CdS / PVC et Ag: MgO / PVC est réalisée par un réacteur photocatalytique spécialement conçu. Le pourcentage de dégradation du colorant bleu de méthylène par les nanocomposites PVC pur, CdS / PVC et Ag: MgO 17%, 46% et 52% respectivement. L'efficacité de dégradation de Ag: MgO / PVC est meilleure que les autres échantillons.

Mots clés : Nanocomposites ; CdS ;MgO;PVC;DRX et photkufkuyfgshkdoqfsljk ;b :ksd